TH-AM-A1 THE EFFECT OF MAGNESIUM AND CALCIUM ON THE MGATPASE ACTIVITY OF MYOSIN IN RELATION TO THE L_2 LIGHT CHAIN. Suzanne M. Pemrick, Mount Sinai School of Medicine of the City University of New York, New York, New York 10029

The MgATPase activity of rabbit skeletal and bovine cardiac myosin is activated by micromolar concentrations of calcium. This activation is not abolished nor shifted to higher concentrations of calcium when the free magnesium concentration is increased to 1 mM. To date it has not been possible to link this response directly to the L_2 light chain. In the presence of pure F-actin the MgATPase activity of both myosins is activated maximally at very low concentrations of free magnesium. Increasing the free calcium concentration from 10^{-7} to 5×10^{-5} M results in a 20 to 30 % inhibition at 2×10^{-5} M (see also R.D. Bremel and A. Weber, Biochimica et Biophysica Acta 376 (1975) 366). Increasing the magnesium concentration to 1 mM inhibits the actin-activated MgATPase activity and the specific response at 20 μM calcium. DTNB-treated skeletal myosin containing 1 mole L_2/mole and various subfragment 1 populations containing 0.5 moles L_2/mole (papain digestion) or 0.0 moles L_2/mole (chymotryptic digestion with and without an $(NH_4)_2SO_4$ precipitation step) were analyzed for the above phenomena. The magnesium inhibition of the actin-activated MgATPase requires the full complement of the L_2 light chain. The calcium-dependent inhibition at 2×10^{-5} M free calcium which is observed at low concentrations of free magnesium is reduced substantially in all L_2 deficient proteins. All preparations possessed comparable K^+/EDTA-ATPase activities and were capable of forming a calcium-sensitive complex with actin in the presence of troponin and tropomyosin. (S.M.P. is a Fellow of the New York Heart Association. Also supported by USPHS, NIH grants HL-13191 and HL-18801)

TH-AM-A2 PHYSICAL CHARACTERIZATION OF THE REGULATORY LIGHT CHAINS OF SOME INVERTEBRATE MYOSINS. W. F. Stafford, III and A. G. Szent-Gyorgyi. Department of Biology, Brandeis University, Waltham, Massachusetts.

Sedimentation velocity, analytical gel filtration and diffusion measurements were used to estimate the geometry of the light chains of Aequipecten irradians, Mercenaria mercenaria, Spisula solidissima, and Loligo pealei. The frictional coefficient measured by these techniques was compared to the calculated value for an equivalent hydrated sphere of the same molecular weight. The data of I. D. Kuntz and W.Kauzmann(Adv. Prot. Chem., 28, 239-345(1974) were used to estimate hydration from the amino acid composition. The frictional ratio was calculated and axial ratios, a:b:c, were estimated from both Perrin's equation and numerical solutions for the general ellipsoid of E. W. Small and I.Isenberg (personal communication) and gave a length ranging from 100-140A depending on the ellipsoidal model chosen. The regulatory light chain appears to be nearly as long as the S1 portion of myosin and possibly forms multiple interacting links with it. The asymmetric geometry may play an important role in the regulatory process.

Circular dichroic spectra of the light chains were analyzed according to the method of N. Greenfield and G. D. Fasman (Biochem., 8, 4108 (1969) to estimate the amounts of alpha, beta, and random structure. The amount of alpha-helix varied from 19-47% and the amount of beta structure, from 8-30% depending on the species from which the light chain was obtained.

All species had about 50% random structure.

This work was supported by a Fellowship from The Muscular Dystrophy Association, Inc. and a grant from Public Health Service (AM-15963).

TH-AM-A3 PROTON MAGNETIC RESONANCE STUDY OF TROPONIN-C. B.A. Levine[1], D.Mercola,*[2] and J.M. Thornton[3] 1. Inorganic Chemistry Laboratory, Oxford; 2. Agricultural Research Council Unit, Zoology Dept., Oxford; 3. Laboratory of Molecular Biophysics, Zoology Dept., Oxford, England.

The binding of H^+ or Ca^{2+} to rabbit skeletal muscle troponin-C induces a large conformational change as detected by proton magnetic resonance spectroscopy. Successive additions of Ca^{2+} to the metal-free protein leads to four distinguishable transitions or sets of transitions which may correspond to the four binding sites of troponin-C. Spectra of the native form of troponin-C are indicative of a tightly folded protein conformation with little conformational change under different pH conditions. In contrast an overall conformational change of the Ca^{2+}-free protein to a more compact form occurs with increasing pH. This conformation differs from that of the Ca^{2+}-bound species. The pH titration of the Ca^{2+}-free form appears to involve at least a two proton cooperativity in that the effective titration curve for histidine - 125 shows a transition which is not that for one proton binding at a single site. Several spectral assignments have been made to help the identification of the four calcium binding sites and thereby elucidate the nature of the conformational changes induced by Ca^{+2}.

TH-AM-A4 SPECTRAL DISCRIMINATION BETWEEN THE TWO HIGH AFFINITY CA^{++} BINDING SITES OF TROPONIN C. P.C. Leavis, B. Nagy, and S.S. Lehrer, Dept. Muscle Research, Boston Biomedical Research Institute, Boston, Mass. 02114.

Previous studies of the spectral effects of Ca^{2+} binding to troponin C (TnC) have employed Ca-EDTA or Ca-EGTA buffer systems. To determine stoichiometry, we have performed direct Ca^{2+} and Tb^{3+} titrations on metal-free TnC in the absence and presence of 6M urea. Titrations of native TnC show that fluorescence and CD changes require two moles of Ca^{2+} or Tb^{3+} per mole TnC. The fluorescence of bound Tb^{3+} (λ_{ex}=280 nm) is 300-fold higher than the free ion due to energy transfer from Tyr. CD and difference absorption spectral changes produced by Tb^{3+} are similar to those reported for Ca^{2+}. CD changes at 222 nm and in the 260 nm region indicate increased α-helix and increased asymmetry of Phe respectively. Difference spectra suggest that Phe residues are shifted to a less polar milieu. Tb^{3+} binds more strongly than Ca^{2+} to the two high affinity sites from competitive binding studies. In 6M urea the spectral changes are complete by the binding of one mole of Ca^{2+} per mole of TnC, in contrast to the two required in the native state. Tb^{3+}-induced changes in 6M urea, however, saturate at a ratio of 2:1, although the sites appear to have slightly different affinities. Tb^{3+} preferentially displaces the single bound Ca^{2+}. Studies of Tb^{3+} binding to the cyanogen bromide peptide, CB9, which includes one Ca^{2+}-binding site containing Tyr 109, show fluorescence and CD changes qualitatively similar to whole TnC at a mole ratio of 1. These results present evidence that this site is responsible for the reported spectral changes. Supported by an MDAA fellowship to P.C.L. and by grants from NIH (AM 11677) and NSF (GB 24316 and GB 38380).

TH-AM-A5 IN VITRO CONFORMATIONAL BEHAVIOR OF BOVINE CARDIAC REGULATORY PROTEINS. Tsung-I Lin and Joseph Y. Cassim, C.V.R.I., University of California, San Francisco, California 94143 and Department of Biophysics, The Ohio State University, Columbus, Ohio 43210.

Recent X-ray diffraction studies of striated muscle by several laboratories have provided evidence for an appreciable spatial displacement of tropomyosin in response to a signal from troponin during calcium ion (Ca^{++}) activation. In view of the distances involved a reasonable model for the transmition of such a signal would be a delocalization of a Ca^{++} induced conformation change in one or both of the regulatory proteins. However, previous circular dichroic studies of cardiac regulatory proteins in this laboratory have failed to find evidence for such a conformation change for the in vitro interaction of Ca^{++} and troponin (Biophys. J. 15, 36a(1975). To determine if perhaps tropomyosin was essential to the induction of such a conformation change by Ca^{++} similar studies have now been done with the troponin-tropomyosin complex. We find that (1) the complexing of the two regulatory proteins does not result in conformation changes (as determined by circular dichroism) of either protein and (2) the conformational response of the complex to Ca^{++} interaction is very similar to the one previously observed for the troponin alone. In view of these results we suggest the following possibilities: (1) actin and the ordered structure of the thin filament may be essential to the induction and propagation of the proposed conformation change, (2) the Ca^{++} regulatory mechanisms of cardiac and striated muscle may be different, and (3) a delocalized conformation model for the propagation of Ca^{++} induced signal may not be valid (Supported by Central Ohio Heart Association grant #73-41).

TH-AM-A6 CA^{2+}-INDUCED CONFORMATIONAL CHANGES IN A CYANOGEN BROMIDE FRAGMENT OF TROPONIN C THAT CONTAINS ONE OF THE BINDING SITES. B. Nagy, J.D. Potter and J. Gergely, Dept. Muscle Research, Boston Biomedical Research Institute; Dept. Neurology, Mass. Gen. Hospital; and Dept. Neurology and Biological Chemistry, Harvard Med. School, Boston, Mass.,02114.

Ca^{2+}-binding to two sites of TnC in the native state, or to one in 6M urea, produces the same increase in α helical regions, viz. $\Delta[\theta]_{222}$ = 5,200 deg cm^2 $dmole^{-1}$ mean residue weight. Phe sidechain circular dichroic (CD) and difference spectra, and the change in reactivity of the single cys-98 residue suggest that one of the segments undergoing such coil-helix transition involves residues 94-103 of the amino acid sequence (Nagy et al., Biophys. J. 15, 35a, 1975; Potter, ibid, 36a; Collins et al., FEBS Lett. 36, 268, 1973). On Ca^{2+} binding a chromophoric marker, 3-nitro-4-hydroxyacetophenone, attached to cys-98 shows a red shift (indicating transfer to a more hydrophobic environment) and becomes optically active, in accord with the above suggestion. A cyanogen bromide fragment, CB-9 (Collins et al., l.c.) including residues 84-134, contains Ca^{2+} binding site III with 3 phe, 1 tyr and the cys residue. It binds Ca^{2+} with $K \sim 10^5 M^{-1}$ as judged by the Ca^{2+} dependence of the tyr fluorescence. On Ca^{2+} binding the cys-98 reactivity with Nbs decreases. Ca^{2+} binding produces $\Delta[\theta]_{222}$ = 4800 suggesting that about 13% of the fragment of CB-9 (about 7 residues) is involved. They include phe (red shift in difference spectrum, increase in phe CD bands), and tyr (fluorescence increases). The chromophoric marker attached to cys-98 in CB-9 also shows a red shift and becomes optically active on Ca^{2+}-binding. Three conclusions emerged from these studies: a) the Ca^{2+}-binding site is preserved in the fragmented CB-9; 2) shifts in the environment of the residues (chemical reactivity, absorption, and CD spectra) occur within a limited domain; 3) conformational changes in one region affect other regions of TnC. (Supported by grants from NIH, NSF and MDAA)

TH-AM-A7 THE EFFECTS OF TROPONIN AND ITS SUBUNITS ON THE CALCIUM ION ACTIVATED TENSION IN MECHANICALLY DISRUPTED MUSCLE CELLS. W.G.L. Kerrick, D.A. Malencik, P.E. Hoar,* S. Pocinwong,* R. Coby,*, Sylvia Lucas,* and E.H. Fischer.* Department of Physiology and Biophysics and Department of Biochemistry, University of Washington, Seattle, Washington 98195.

Ca^{2+}-activated isometric tension was recorded from functionally skinned rabbit skeletal and cardiac and scallop muscle fibers (sarcolemma mechanically disrupted) which were immersed into test solutions containing 1 mM Mg^{2+}, 1 x 10^{-7}M H^+, 70 mM K^+, 7 mM EGTA, 2 mM MgATP, 1 x 10^{-6} → 2.5 x 10^{-4} M Ca^{2+}, 5 x 10^{-5} M of appropriate rabbit protein (troponin, TNI, TNB, TNC, or TNT), imidazole propionate (used to adjust the ionic strength to .15), and propionate as the major anion. Troponin, TNC and TNT do not affect Ca^{2+}-activated tension. TNI and TNB will reversibly inhibit the Ca^{2+}-activated tension in white, red and cardiac muscle. The time course of phosphorylated vs. non-phosphorylated TNI inhibition is exponential and ten times faster in white than in red or cardiac rabbit muscle. When inhibition is complete, it cannot be reversed unless the fiber is soaked in a solution containing TNC. None of the troponin subunits affect the Ca^{2+}-activated tension relationship in mechanically skinned fibers of the scallop which is consistent with the known myosin Ca^{2+} control of these muscles. In contrast, rabbit troponin increases the Ca^{2+}-sensitivity of the scallop fibers ten-fold such that the relationship between % Ca^{2+}-activated tension and % Ca^{2+} binding to troponin is the same for identical Ca^{2+} test solutions. These data indicate that the troponin Ca^{2+} control of actomyosin can override the myosin Ca^{2+} control of the scallop.

Supported by PHS grants GM00260, HL13517, NS05082, GM53362, 5RO11AM79, and grants from the Muscular Dystrophy Association of America.

TH-AM-A8 REVERSIBLE ACTIVATION OF TENSION IN THE ABSENCE OF CALCIUM IN RAT HEART. G. McClellan*, N-P. Lai*, and S. Winegrad, Physiology Dept., University of Pennsylvania School of Medicine, Phila., Penna. 19174

Papillary muscles and trabeculae from rat ventricle have been "chemically skinned" by soaking the tissues in 10mM EGTA overnight. Such preparations reproducibly begin to develop tension at pCa of 7.1 and achieve maximum tension at pCa of 5.0 in the presence of a standard contraction solution (140mM KCl, 4mM MgATP). The supernatant from a suspension of rat heart ventricle which has been homogenized in relaxing solution with 3mM EGTA and 4mM MgATP contains a cardiotonic substance. The activity remains in the supernatant even after centrifugation at 89,000 g for 1 hr. Skinned fibers suspended in the supernatant buffered at a pCa of 9.0 produce as much as 30-40% of the tension produced in pCa of 5.0 and relax almost completely when the supernatant is replaced by a standard relaxing solution. The active component of the homogenate can be destroyed by heat. It passes through dialysis tubing and retains considerable activity even when the homogenized tissue has been diluted 2500X as long as ATP is present but not in its absence. These observations are consistent with enzymatic synthesis from ATP of a compound which activates the contractile proteins at high pCa.

TH-AM-A9 EFFECTS OF pH ON THE SENSITIVITY OF THE MYOFILAMENTS TO CALCIUM AND ON THE RELEASE OF CALCIUM FROM THE SARCOPLASMIC RETICULUM IN SKINNED CELLS OF CARDIAC AND SKELETAL MUSCLE. A.Fabiato and F.Fabiato,*Cardiovascular Research, Harvard Medical School, Boston.

Single skinned cardiac cells were obtained by homogenization and micro-dissection of rat ventricle. The free [Ca^{2+}] was buffered with 4.0mM total EGTA and the pH with Imidazole. Schwarzenbach's constant was used for Ca-EGTA. Curves of tension as a function of the pCa were obtained at pH 6.6, 7.0 and 7.4. The pMg was maintained at 3.5 and the pMgATP at 2.5. Temperature was 22°C. Increase of pH did not modify the maximum tension but produced a shift to the left of the tension-pCa curve which started at a higher pCa for a higher pH. The pCa necessary for 50% of maximum tension was pCa 5.70 at pH 6.6, pCa 6.05 at pH 7.0 and pCa 6.35 at pH 7.4. Qualitatively similar results were obtained on skinned cells of frog cardiac muscle (ventricle) and frog skeletal muscle (semi-tendinosus). However, the effects of the same variations of pH were smaller in skeletal muscle as compared to cardiac muscle.

Phasic contractions by Ca^{2+}-triggered release of Ca^{2+} from the sarcoplasmic reticulum (SR) were induced in skinned cardiac cells from the rat ventricle by a slight decrease of pCa from 7.70 to 7.40 in the presence of 0.05mM total EGTA. The increase of amplitude of the phasic contractions when pH was increased from 6.6 to 7.4 was accounted for by the effect of pH on the sensitivity of the myofilaments to Ca^{2+}. Contractions were induced by caffeine or the ionophore A 23187 at a constant pH of 7.0 after the contractions triggered by Ca^{2+} at variable pH. The amplitude and duration of these contractions were not significantly modified by variations of the pH at which the Ca^{2+}-triggered release of Ca^{2+} was obtained. A sudden increase of pH from 6.6 to 7.4 at a constant pCa of 7.70 with 0.50mM total EGTA did not induce a phasic contraction. In conclusion the increase of pH from 6.6 to 7.4 neither induces a Ca^{2+} -release from the SR nor modifies the Ca^{2+}-triggered release.

TH-AM-A10 THE EFFECTS OF pH ON SUBMAXIMAL AND MAXIMAL CA^{2+}-ACTIVATED TENSION IN SKINNED FROG SKELETAL FIBERS. S.P. Robertson and W.G.L. Kerrick, Department of Physiology and Biophysics, University of Washington, Seattle, Washington 98195.

Single frog semitendinosus muscle fibers were skinned by the method of Natori, 1954. Tension was measured with a photodiode transducer similar to that used by Hellam and Podolsky, 1969. Ca^{2+} concentration was buffered with 7mM EGTA, and pH and ionic strength (.17) were controlled with MES or imidazole. All solutions contained 2mM $MgATP^{2-}$, 90mM K^+, 1mM Mg^{2+}, 15mM creatine phosphate, 15 units per ml creatine phosphokinase; and the major anion was propionate. For each fiber the maximum Ca^{2+}-activated tension was measured at different pHs and normalized to the maximum Ca^{2+}-activated tension developed in the same fiber at pH 7.0. Normalized maximum tensions (NMT) for each pH were averaged. At a given pH the ratio of submaximal Ca^{2+}-activated tension to maximal Ca^{2+}-activated tension was used as a measure of the percent Ca^{2+} activation (%A). All ratios at a specified pCa and pH were averaged. The pCa corresponding to 50% activation and mean NMT values are shown in the table below. All changes in NMT or %A were reversible. The shift in pCa required for 50% activation at each pH can be explained by a single competitive site for Ca^{2+} and H^+ with a pKm for Ca^{2+} equal to 5.73 M and a pKi for H^+ equal to 7.03 M. The decline in maximum tension as pH is decreased as described by a single H^+ binding site with a pKi = 5.68 M. Supported by PHS grants GM00260, AM17081, and NS08384.

pH	7.5	7.0	6.5	6.0	5.5	5.0
pCa for 50% A	5.6	5.4	5.0	4.6	4.2	-
mean NMT	.95	1.0	.83	.73	.54	0

TH-AM-A11 EFFECTS OF Mg^{2+} ON TENSION GENERATION OF MECHANICALLY DISRUPTED BUNDLES OF RAT LEFT VENTRICULAR MUSCLE FIBERS. S.K.B. Donaldson, P.M. Best,* and W.G.L. Kerrick. Departments of Physiology and Biophysics and Physiological Nursing, University of Washington, Seattle, Washington 98195

The sarcolemmas of small bundles of rat left ventricular fibers were disrupted and the intracellular ionic and enzymatic environment of the fibers was controlled by varying bathing solution compositions. Steady state isometric tension generation (T) of the fiber bundles was measured using a photodiode force transducer. Complete $pCa^{2+}(= -\log_{10}Ca^{2+}(M))$ and $pSr^{2+}(Ca^{2+}$analogue) vs. tension relationships were obtained at free Mg^{2+} concentrations of 5×10^{-5}, 10^{-3}, 5×10^{-3}, and 10^{-2}M. Each submaximum Ca^{2+} or Sr^{2+}-activated tension measurement was normalized to the maximum Ca^{2+} or Sr^{2+}-activated tension for that bundle under identical ionic conditions. A computer program was used to solve the complex equilibrium for each bathing solution and the following remained constant: pH = 7.0 (imidazole), EGTA = 7 mM, $MgATP^{2-}$ = 4 mM, μ = 0.15 M, K^+ = 70 mM. Room temperature was 20 + 1°C and major anion was chloride. The midpoint of the pCa^{2+} and pSr^{2+} versus tension relationships were identical at each $[Mg^{2+}]$. As Mg^{2+} was increased from 5×10^{-5}M (50% T at pCa^{2+} or pSr^{2+} = 5.56), the curves shifted such that $10^{1.1}$ times more Ca^{2+} or Sr^{2+} was required for 50% tension generation at $Mg^{2+} = 10 \times 10^{-3}$M ($pCa^{2+}$ or pSr^{2+} = 4.4). Although the steepness of all of the saturation curves indicated evidence of cooperativity the degree of cooperativity did not appear to be significantly affected by Mg^{2+}. These data are consistent with a competitive effect of Mg^{2+} with an inhibitory dissociation constant for Mg^{2+} of $10^{-3.1}$ to $10^{-3.5}$M. Maximum tension increased as Mg^{2+} increased suggesting a noncompetitive effect of Mg^{2+} also.

Research supported by USPHS grants HL17373, AM17081, FR00374 from NIH.

TH-AM-A12 DEVELOPMENT OF DIFFERENCES IN SENSITIVITY TO CA^{2+} IN FAST TWITCH AND SLOW TWITCH SKELETAL MUSCLE FIBERS. Diane J. Secrist, W. Glenn L. Kerrick, Robin Coby,* Phyllis Hoar,* Sylvia Lucas* and Bruce Spaulding.* Using functionally skinned (sarcolemma mechanically disrupted) muscle fibers Ca^{++} sensitivity was determined as the amount of tension produced per submaximal $[Ca^{++}]$. Single fibers were mounted in a tension transducer and immersed in solutions containing 70mM K^+, 1mM Mg^{2+}, 2mM $MgATP^{2-}$ and 7mM EGTA. The ionic strength was adjusted to 1.5 by imidazole, pH = 7, and the major anion was propionate. The pCa's ranged from 8 (relaxing) to 3.6 (maximally contracting). The soleus (slow twitch) muscle of the rabbit embryo showed the same sensitivity to Ca^{++} as did the embryonic and adult magnus adductor (fast twitch) muscle. Ca^{2+} sensitivity in soleus was found to increase with development until, in the adult, the slow fibers were 2.5 times more sensitive than the fast twitch fibers. These results are different from those expected from biochemical measures which show greater Ca^{2+} binding to troponin in fast twitch than in slow twitch muscle. Both types of embryonic and adult fast twitch muscles showed decreased sensitivity to Sr^{2+} when substituted for Ca^{2+}. However, adult slow twitch muscle had approximately the same sensitivity to Sr^{2+} as to Ca^{2+}, i.e. it showed about 10 times greater sensitivity to Sr^{2+} than fast twitch muscle did. Similar measurements made on a 1-day old chick ALD (slow) and PLD (fast) muscles showed the increased sensitivity of adult ALD fully developed immediately after hatching. The Ca^{++} sensitivity of breast muscle (of fast twitch) from adult chicken was intermediate between ALD and PLD. SDS polyacrylamide gel electrophoresis of homogenized rabbit myofibrils showed changes consistent with the developing Ca^{++} sensitivity in slow twitch fibers. Gels of chick ALD and PLD showed differences in the light chain content of myosin at birth. Supported by PHS grants GM00260, HL13517, and AM17081.

TH-AM-A13 TRIVALENT METAL ION-INDUCED POLYMERIZATION OF TROPOMYOSIN. J. R. Bunting, C. C. Ford*, and R. M. Dowben, Biophysics Graduate Program, University of Texas Health Science Center, Dallas, Texas 75235.

In high monovalent salt concentrations, tropomyosin (TM) is known to exist in solution as the monomer. After removal of divalent cation species by treatment with EDTA, we have found solutions of TM in 1 M KCl, pH 5.5 to form highly insoluble polymeric structures upon addition of trivalent lanthanide ions. The effect is found to be biphasic with increasing M^{+3} concentrations. The apparent pK's of dissociation for polymer formation as a function of (M^{+3}), determined by visible light scattering, are centered at 3.8 and 3.4. The M^{+3} effect is not inhibited by the presence of either Ca^{+2} or Mg^{+2} at millimolar concentrations. The apparent pK's correlate linearly with the solution radii of the various M^{+3} ions used for titration, suggesting specific sites on TM which interact with the metal ion. Tb^{+3} emission enhancement of fluorescence is observed to occur upon binding to TM with a pK of dissociation obtained from fluorescence data identical to the higher affinity binding observed from the scattering data. An hypothesis consistent with these findings will be discussed.

TH-AM-B1 EFFECTS OF NYSTATIN ON THE APLYSIA GIANT NEURON. J.M. Russell, D.C. Eaton and M.S. BRODWICK* (Intr. by F.H. Rudenberg), Department of Physiology and Biophysics, University of Texas Medical Branch, Galveston, Texas 77550.

Two different methods were used to study the effects of nystatin on neuron R2 of the Aplysia abdominal ganglion. One was to voltage-clamp the neuron and examine the effects of various concentrations of nystatin on the current-voltage relationship at a fixed time (15 min) after exposure to the agent. Nystatin increased membrane conductance in dose-dependent manner. The dose-response relation (see Figure) was observed to be very steep (slope ≈ 3) with little or no effect below 15 mg/L and an effect too large to measure at concentrations greater than 30 mg/L. Upon return to antibiotic-free solution, the effect on conductance was reversible within 30 min. The second type of experiment involved the use of ion-specific microelectrodes to measure the changes in intracellular ion activities which attended the greatly increased membrane permeability induced by large doses of nystatin (>35 mg/L). These results also indicate that large changes in membrane permeability occur following nystatin treatment and that they involve univalent ions like K, Na and Cl, but not divalent ones such as Mg or Ca. This method can be used to selectively rearrange the internal ionic milieu to study the effect of such a change on transport or electrical properties.

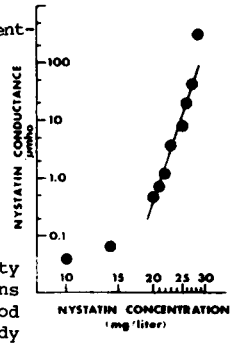

(Supported by NIH grants, NS-11946; NS-12008)

TH-AM-B2 STUDIES OF ETHANOL ON THE SQUID GIANT AXON. D.L. Gilbert, J.V. Henderson, Jr.*, and M. Lowenhaupt,* Lab. Biophysics, NINCDS, Natl Institutes of Health, Bethesda, Maryland, 20014, Dept.Physiology, SUNY Medical School, Buffalo, N.Y. 14214, and Marine Biological Laboratory, Woods Hole, Mass. 02543.

Ethanol-treated squid giant axons have been reported to have lower action potential amplitudes at high temperature and to exhibit spontaneous action potentials at low temperatures (Tasaki, I., Spyropoulos, C.S., In: Johnson, F.H., The Influence of Temperature on Biological Systems, Washington, D.C., Amer. Physiol. Soc., p. 201, 1957). We have restudied this very interesting finding with 24 squid giant axons. Action potential amplitudes decreased at the temperature range between about 15° to 20° C. for space-clamped axons treated with 3% ethanol in sea water. Spontaneous or repetitive activity occurred as reported by Tasaki et al. but only in the temperature range of 1 to 14°C and only in one-fourth of the treated axons. The frequency of the activity decreased when the temperature was lowered. Moore et al. (Moore, J.W., Ulbricht, W., Takata, M., J. Gen. Physiol. 48:279, 1964) reported a tendency for the ethanol treated axon to exhibit shorter action potential durations, which we also observed. The ionic currents measured using the voltage clamp were decreased by 3% ethanol at low temperatures as was previously reported by Moore et al. and Armstrong and Binstock (Armstrong, C.M., Binstock, L., J. Gen. Physiol. 48:265, 1964). We also observed some tendency for the time-to-peak of the early current to decrease in the ethanol treated axons. Since most axons do not exhibit spontaneous activity, it is not surprising that Moore et al. did not observe this tendency. An ethanol effect on the rate constants of the ionic currents might account in part for the spontaneous activity. Action potentials were abolished if the 3% ethanol-treated axons were returned to sea water at low temperatures but not at high temperatures.

TH-AM-B3 'SLOW' INACTIVATION OF SODIUM CONDUCTANCE IN NERVE FOLLOWING REACTION WITH N-ETHYLMALEIMIDE. Peter Shrager, Dept. of Physiology, Univ. of Rochester Medical Center, Rochester, N. Y. 14642.

Addition of 1-3 mM of the sulfhydryl blocking reagent N-ethylmaleimide (NEM) to the external bath of voltage clamped crayfish axons results in a progressive decline in peak early transient currents with no effect on steady state currents. Block of sodium currents is not reversed on washing away unreacted NEM. Short hyperpolarizing prepulses (<50 msec) have little effect, but hyperpolarizing the fiber by 40 mV for 350-850 msec restores early transient currents to 70% of control values. The time-to-peak transient current is not affected by NEM, nor is the time constant of the decay of sodium tail currents, suggesting no effect on the sodium activation system. After exposure to NEM, reversal of the inactivation of Na currents by a hyperpolarizing prepulse proceeds in two phases, with time constants of 1-4 msec (τ_h) and 100-200 msec. The rapid component accounts for only 10-20% of the restoration of Na conductance. The slow component is closely similar to that seen in control fibers depolarized by raising the external K^+ concentration or lowering the holding potential, and reported earlier in squid axons (Adelman and Palti, 1969, J. Gen. Physiol., 54:589). The data have been compared with a number of different kinetic models. Supported by NIH Grants 2 RO1 NS10500 and 5 PO1 NS10981.

TH-AM-B4 CURRENT AND FREQUENCY DEPENDENT BLOCK OF SODIUM CHANNELS BY STRYCHNINE. M.D. Cahalan, Physiology Department, University of Pennsylvania, 19174, and B.I. Shapiro, Biology Department, Harvard University, Cambridge, Massachusetts, 02138

The characteristics of sodium channel block by strychnine have been studied in perfused, voltage-clamped squid axons. Internally applied strychnine (0.1 to 1 mM) or n-methyl strychnine produce a rapid "inactivation" of sodium current for potentials beyond the sodium equilibrium potential. In axons treated with pronase to remove normal sodium inactivation (h), the time course of block by strychnine can be directly observed. The amount of block was compared for several different external and internal sodium concentrations. In general, block by strychnine depends upon the direction of sodium current through the membrane. There is very little block of inward sodium current (< 10%) with high external sodium at the same potentials for which there is considerable block of outward sodium current (> 60%) with low external sodium. This is consistent with the idea that strychnine can be knocked out of open sodium channels by inward sodium movement. The kinetics of sodium tail currents are altered in parallel with block by strychnine. There is a pronounced hook in the tail current, and the channels close more slowly following inactivation induced by strychnine. Strychnine also reduces gating current associated with both activation and closing of sodium channels. In axons with a normal h inactivation process sodium current is frequency dependent with strychnine inside, and recovery from frequency dependent block is slow ($\tau \approx 10$ sec). In pronase-treated axons this frequency dependence disappears, and recovery from strychnine-induced inactivation proceeds with a rapid phase ($\tau \approx 1$ msec) and a slower phase on the order of 100 msec. It appears that strychnine may become trapped in the channel by the gating mechanism, and that the release of strychnine is much slower if the inactivation process is intact. Supported by NIH grant NS 08951.

TH-AM-B5 PHARMACOLOGICAL PROPERTIES OF THE Na CHANNEL OF FROG SKELETAL MUSCLE. D.T. Campbell and B. Hille, Department of Physiology, Yale Medical School, New Haven, Ct. 06510, and Department of Physiology and Biophysics, University of Washington, Seattle, Wa. 98195.

Na currents in frog skeletal muscle fibers studied under voltage clamp conditions are reduced by raising outside H^+ and Ca^{++} concentrations and by external application of saxitoxin (STX). Reduction of peak Na currents caused by H^+ and Ca^{++} is well described by the model developed by Woodhull (J. Gen. Physiol. 61: 687, 1973) for the node of Ranvier. This model attributes the reduction of currents to a voltage shift in the P_{Na} vs E relation and to ionic blockage of the Na channel. The blockage is described as a voltage dependent binding of H^+ or Ca^{++} to a site inside the channel with an apparent dissociation constant given by:

$$K_{diss}(E)=K_{diss}(0)\exp(z\delta FE/RT)$$

where z is the charge on the blocking ion and δ is a number between 0 and 1 expressing the fraction of the membrane potential drop affecting binding. Block by H^+ ions is fit with an apparent $pK_a(0)$ of 5.33 and δ of 0.27; block by Ca^{++} is fit with an apparent $K_{diss}(0)$ of 80 mM and δ of 0.27. These values are like those found in nerve. The shift in the P_{Na} vs E relation as H^+ and Ca^{++} are changed is also like nerve. STX block of Na channels was measured at pH 7.4 in both nerve and muscle. The apparent dissociation constants of STX binding to the Na channel are 0.88 nM in muscle and 1.3 nM in nerve; these values are not significantly different at the p=0.05 level. It is concluded that the Na channels of nerve and muscle are nearly the same. Supported by NIH grants NS 08174, NS 05082, GM 00260 and FR 00374.

TH-AM-B6 A STUDY OF MOLECULAR DYNAMICS IN A NERVE SYSTEM BY RAYLEIGH SPECTROSCOPY. B. Simic-Glavaski, Chemistry Department, Case Western Reserve University, Cleveland, Ohio, 44106.

Rayleigh scattering of light was used to monitor molecular dynamics in a bundle of large nerve fibers disected from a claw of crab Libinia emarginata. Spectra of polarised and depolarised Rayleigh light scattered by axon system were analysed by a laser homodine technique in the frequency range up to 20 kHz. They show a complex form and spectral shapes can be fitted by two Lorentzian lines indicating at least two relaxation processes. Principal quantaties such as molecular translational and re-orientational diffusion constants are determined. The obtained values for translational and re-orientational diffusion constants are $D_t = 4.77 \times 10^{-9} cm^2 s^{-1}$ and $D_r = 7460\ s^{-1}$. When the value of viscosity $\eta = 2$ poise was taken (for lobster membrane available in the literature), and Stokes-Einstein equation was employed; a molecular hydrodinamic diameter was calculated to be 68Å, closely corresponding to a membrane thickness. Both constants and molecular radii are dependent on the applied potential across the membrane. Broadening of spectra of polarised scattered light was observed as a function of scattering angle, showing no-conformational changes of molecules at a given membrane potential. A significant change in molecular translational diffusion constant and size was recorded when the nerve fibers were stained by a fluorescent dye molecules.

TH-AM-B7 EFFECTS OF ION SUBSTITUTION AND SCORPION VENOM ON OPTICAL SCATTERING OF LOBSTER SINGLE AXONS. H.J. Bryant, R. Gruener, R. Kilkson, & W.S. Bickel*, Departments of Physiology and Physics, University of Arizona, Tucson, Arizona 85724

Transient changes in the intensity of light scattered from lobster single axons were measured during the propagation of the action potential (AP) in order to correlate possible conformational changes in the axolemma with membrane excitability. Changes in the scattered light intensity, normalized to resting scattering levels ($\Delta I/I_o$) were averaged from 2000 to 4000 events. At the peak of the AP the optical signal ($\Delta I/I_o$) had a value of $4.8 \pm 0.4 \times 10^{-5}$ ($\bar{X} \pm$ SEM). External cation substitution for sodium and application of scorpion venom to the axon were employed to alter transmembrane voltages and currents during the AP and to perturb the kinetics of the sodium channel. Sodium substitution by guanidine and aminoguanidine resulted in reduction of the AP amplitude by 69% and 50%, respectively. The intensity of the scattered light, however, was not significantly altered. The duration of ($\Delta I/I_o$) in control saline was shorter than the duration of the AP. Guanidine and aminoguanidine substitution prolonged both the AP and ($\Delta I/I_o$) and increased the duration difference between the two signals. Superfusion of the axon with scorpion venom (32 µg/ml) resulted in a prolongation of the falling phase of the AP which correlated with the duration of ($\Delta I/I_o$). If the optical signal reflects two states of the sodium channel, (open-closed), ions with lower permeabilities (guanidine and aminoguanidine) would cause a prolongation of the time-course of the optical signal and the AP because of the longer dwell time in the channel. In addition, if the less permeable ions do not cause significant distortion of the open channel the peak value of ($\Delta I/I_o$) should remain constant. The findings reported are consistent with this model. Supported by NIH Grant 10417-03 to RG, NSF Institutional Grant to the University of Arizona, and NIH Research Fellowship to HJB.

TH-AM-B8 EFFECTS OF CHOLINERGIC COMPOUNDS ON THE TRANSIENT VOLTAGE INDUCED OPTICAL RETARDATION CHANGE OF NERVE AXONS. Peter G. P. Ang and Melvin P. Klein*, Laboratory of Chemical Biodynamics, University of California, Berkeley, California 94720.

The optical retardation of the nerve responds to perturbation of the membrane potential as detected from the signal-averaged changes in light intensity transmitted through the nerve. By applying square voltage pulses (about 50 mV) through two pairs of external electrodes on a small bundle of axons from the walking leg of the lobster, Homarus Americanus, we transiently perturb the membrane potential. One electrode pair is positioned adjacent to the fibers, while the other pair is positioned at the open ends of the nerve, one electrode at each end. This symmetrical electrode and chamber assembly closely resemble the arrangement in the conventional double sucrose gap technique, except here 2% agar is used instead of sucrose to separate the liquid pools. Adding acetylcholine (10 mM) to the solution bathing the nerve in the central chamber strongly reduces the voltage induced birefringence change. Procaine, nicotine, carbamylcholine, hexamethonium, tetraethylammonium and hemicholinium-3 have no significant effect. On the other hand, physostigmine salicylate, an inhibitor of acetylcholinesterase, drastically affect the birefringence signal, while neostigmine, another inhibitor, is less effective. It is known that physostigmine is more lipid soluble. Our findings suggest that a significant part of the retardation change may be associated with a cholinergic system on the membrane.

(Supported by the U.S. Energy Research and Development Administration.)

TH-AM-B9 EXTRINSIC BIREFRINGENCE AND DICHROISM CHANGES IN SQUID GIANT AXONS. W.N. Ross, L.B. Cohen, B.M. Salzberg, A. Grinvald*, and N. Kohn.* Dept. of Physiology, Yale University, New Haven, Conn. 06510.

The absorption of light by dyes bound to giant axons from the squid, Loligo pealii, changes when membrane potential is altered. In experiments where the direction of light propagation is perpendicular to the longitudinal axis of the axon, the absorption changes for several dyes were found to depend upon the plane of polarization of the incident light. The absorption change of a merocyanine dye (dye I, J. Membr. Biol., 19: 1, 1974) was larger with light polarized perpendicular to the longitudinal axis than with light polarized parallel to the axon at wavelengths between 550 and 600 nm. At wavelengths between 450 and 550 nm and between 600 and 630 nm, the converse was found. When the dichroism was plotted, an approximately bell-shaped curve with a peak at 550 nm was obtained. As expected from the dichroism in the absorption change, there was also a dye dependent birefringence change. For depolarizations there was a net decrease in optical retardation at wavelengths longer than 550 nm and an increase at wavelengths shorter than 550 nm. The general shape of the spectrum of the birefringence change was in agreement with the prediction from a Kramers-Kronig transformation of the dichroism spectrum. With a merocyanine-rhodanine dye, 5-[(1-γ-sodium sulfopropyl-4(1H)-quinolylidene)— 2-butenylidene]-3-ethylrhodanine, both the dichroism and birefringence changes were larger and easily detected in a single sweep. These birefringence signals may prove to be useful monitors of membrane potential because wavelengths outside the absorption band can be used.

Supported in part by Public Health Service grants NS-98437 and NS-10489 and NIH Fellowship 1 F22 NS-00927.

TH-AM-B10 NMR STUDIES OF WATER IN THE MN++ DOPED GAR FISH OLFACTORY NERVE. J.L. Pirkle*, R.W. Smithwick*, Y. Matsumoto, J.H. Goldstein*, Depts. of Chemistry and Physiology, Emory University, Atlanta, Ga. 30322

The non-myelinated Gar Fish Olfactory Nerve (GFON) has been shown to have interesting morphological properties including: 1) small uniform C fibers, 80% of which are from 0.20-0.28 um in diameter and 2) a membrane surface to volume ratio about 5400 times that for squid axon of the same diameter (Easton 1971). The present preliminary study of the water of the GFON has utilized a Mn++ doped Gar Ringer bathing solution to separate the resonances of the intracellular and extracellular water fractions. The NMR spectrum of the GFON in such a solution shows a relatively narrow intracellular water peak mounted on a broad (150-200 Hz) extracellular water peak. The two peaks could be separated mathematically by fitting the spectrum to a model equation of the sum of two Lorentzian line shapes (one for each peak). The spectrum was described by over 200 points and the line widths, chemical shifts and areas of the peaks were determined by a non-linear regression fit of the model equation. The statistical error of each parameter was less than 3%. Subsequent studies showed that as the temperature was raised in 3° steps from 0° to 30°C: 1) the line widths of both peaks increased and 2) the chemical shift difference of the two peaks decreased. After each experiment, the GFON was checked to insure action potential propagation. Further work on the exchange rate of water across the axonal membrane is in progress. This work was supported by the Insurance Medical Scientist Scholarship Fund (Provident Life & Accident Ins. Co.) and the National Institutes of Health.

TH-AM-B11 A DIRECT MEASUREMENT OF THE RESISTIVITY OF AQUEOUS CYTOPLASM. Kenneth R. Foster, Jeannette M. Bidinger*, and David O. Carpenter, Armed Forces Radiobiology Research Institute. Bethesda, MD 20014.

The apparent intracellular resistivities of frog sartorius muscle fibers, barnacle giant muscle fibers, and giant neurons from Aplysia were measured using an extension of a single metal microelectrode technique previously described by this laboratory. Each cell was penetrated by the microelectrode, and the impedance was measured as a function of frequency between 100 KHz and 3 MHz. By plotting the data on the complex impedance plane and extrapolating the data to infinite frequency, the substantial effects of electrode polarization were overcome. The high frequency resistance of the electrode is strictly proportional to the resistivity of the solution within a few microns of the electrode tip. For Aplysia giant neurons, barnacle giant muscle fibers, and frog sartorius muscle fibers, the observed cytoplasmic resistivities were 33, 56, and 154 ohm-cm, respectively. The frog sartorius data are in excellent agreement with sarcoplasmic resistivity values derived from cable studies on these cells, and the barnacle results are consistent with sarcoplasmic resistivity measurements of other marine crustacean tissues. The resistivity of Aplysia somatoplasm is about the same as that measured in squid axoplasm, and is much lower than values measured at 100 KHz previously reported by our laboratory. It appears likely that the previous high values reflect a contribution to the total impedance by intracellular membranes which lie in the current path between the metal microelectrode and the indifferent electrode outside the cell. The present observations indicate that there is no significant binding of ions or extraordinarily high cytoplasmic microviscosity, as previously suggested.

TH-AM-B12 FULLY COUPLED TRANSIENT EXCITED STATE MODEL FOR THE SODIUM CHANNEL. E. Jakobsson, Department of Physiology and Biophysics, and Bioengineering Program, University of Illinois, Urbana, Ill. 61801

The behavior of a fully coupled model for the sodium conductance employing a transient excited state as a precursor to the conducting state is examined. The kinetic scheme for the model is given by the diagram at the right, where the rate constant for the A⟶A* transition is a function of voltage and rate of voltage change, while all of the other rate constants are functions of voltage alone. Evidence of varying degrees of rigor is presented in support of the following propositions: 1) the model is capable of simulating all of the anomalies which have been observed between axons and the H-H model with regard to the "h" gates, while retaining the correct features of the H-H model; 2) the model is minimal; no simpler kinetic scheme will fit the array of data which it does; and 3) a transient excited state is necessary to fit the data; no energetically closed kinetic scheme with pure voltage-dependent kinetics is adequate. In addition, a correlation is predicted between the size of the inactivation shift and the tendency to repetitive firing such that the larger the inactivation shift the less tendency to fire repetitively. This correlation has recently been seen experimentally by Dr. J. Connor, working with crab axons.

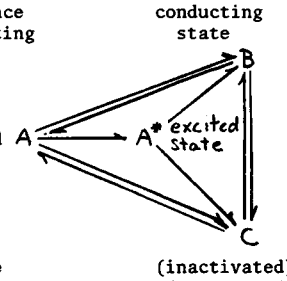

Partially supported by NSF Grant #GB 39946.

TH-AM-B13 IMPULSE PROPAGATION IN THE MYELINATED NERVE FIBER. F.A. Dodge, IBM Research, Yorktown Heights, N.Y. 10598

Two outstanding questions about the design of myelinated fibers have been examined by simulation. By analysis of limiting cases Huxley and Stampfli (J.Physiol. 1949) conjectured that the curve relating conduction velocity (θ) and internodal length (ℓ) should show a broad optimum and Rushton (J.Physiol. 1951) suggested that nodes might be separated more widely than optimal to minimize energy consumption. Direct measurement of current-voltage relations (Dodge and Frankenhauser, J. Physiol. 1958) showed that the density of the sodium and potassium ionic conductances in a frog node are about 10 times greater than in the squid axon, but that the voltage-dependent kinetics are inessentially different. Taking Hardy's (Biophys. J. 1973) standard model I computed θ for various ℓ (Fig.), and both of the above conjectures were confirmed. Rushton's (1951) dimensional analysis indicated that θ should vary directly with fiber diameter (a) in the myelinate fiber, but for the uniform unmyelinated fiber θ goes as $\sqrt{a}$. We may ask at what fiber diameter would these relations cross if the two nerves had the same excitable membrane? If we scale the standard frog fiber to 1/200, at which size the myelin would be a single membrane thick, ionic conductance is nonuniform, the nodes occuping about 25° of the fiber surface. The computed conduction velocity of this nonuniform axon is 25% less than that of the equivalent uniform fiber. We might therefore expect to find myelinated fibers as small as a single wrapping by the Schwan cell.

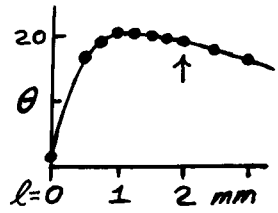

TH-AM-B14 SQUID GIANT AXON AS A MODEL FOR THE EFFECTS OF NEURON GEOMETRY. M.Westerfield*, J.W.Moore, F.Ramón and R.Joyner*, Department of Physiology and Pharmacology, Duke Univ. Med. Ctr., Durham, N.C. 27710

A regional decrease in the internal resistance of squid giant axons, produced by low resistance axial electrodes, has been offered as a model for investigating the effects that geometrical properties of neurons have on the initiation and propagation of action potentials. Electrical measurements made in a normal region of the axon differ from those in a shunted region. For example, with appropiate selection of electrode length and surface resistance, the input resistance ratio between the two axon regions can be made to equal the ratio between axon and soma regions of motorneurons. Furthermore, passing current through the axial electrode shifts the ratio of the input resistances of the two regions between 1.5 and 7, the later value causing failure of propagation into the region of reduced internal resistance. In addition, the following properties of the two regions quantitatively match published values obtained from motorneurons:

1. the rheobase current
2. the threshold as measured at the inflection on the rising phase of the action potential
3. the threshold as measured by direct electrical stimulation, and
4. the rate of rise of the action potential

Comparison of electrical measurements made in one region of the axon to those obtained in a shunted region demonstrates that this squid giant axon preparation quantitatively matches the axon-soma transition properties of vertebrate spinal cord motorneurons.

Supported by NIH Grant # NS03437

TH-AM-C1 ELECTROSTATIC EFFECTS OF CHOLESTEROL ON ALAMETHICIN AND EIM INDUCED CONDUCTANCES IN BLACK LIPID FILMS. Ramon Latorre‡ Osvaldo Alvarez‡ and James E. Hall, Dept. of Physiological and Pharmacological Sciences. The Pritzker School of Medicine, The University of Chicago, The University of Chile, and Dept. of Physiology, Duke University Medical Center, Durham, N. C. 27710.

The mechanisms by which cholesterol alters membrane permeability are of some interest. Szabo (1974) showed for membranes formed from mixtures of glycerol monooleate and cholesterol that increasing cholesterol content decreased cation conductance and increased anion conductance for conductances induced by lipophyllic ions. He attributed this effect mostly to a dipole potential resulting in an increasingly positive membrane interior with increasing cholesterol content. Since voltage-dependent conductances may involve the movement of gating charges across the membrane interior, we wondered if the gating charges might be influenced by the cholesterol dipole potential.

We confirmed Szabo's results using nonactin K^+ and carbonylcyanide m-chlorophenylhydrazone ($CCCp^-$) as lipophyllic probes for phospholipid membranes (bacterial phosphatidyl ethanolamine or soy bean lecithin) with varying cholesterol content. We also tested EIM and alamethicin induced conductances in membrane of the same compositions. We found that the alterations of both EIM and alamethicin conductances are consistent with the dipole potential induced by cholesterol as deduced from lipophyllic ion conductance measurements. The data can be analyzed in a self-consistent, but not unique way, to give a length for the cholesterol induced dipole of about 0.2 the length of the electric field (~ 6Å).

1. Szabo, G. Dual mechanism for the action of cholesterol on membrane permeability Nature. 252:47 (1974).

TH-AM-C2 FLUCTUATION AND RELAXATION OF ANALYSIS OF MONAZOMYCIN CONDUCTANCE CHANNELS IN BLACK LIPID MEMBRANES. L. E. Moore and E. Neher*, Max Planck Institute of Biophysical Chemistry, Goettingen, Germany.

Fluctuation and relaxation analyses were performed on the monazomycin induced conductance of lecithin-cholesterol bilayer membranes. With both methods a slow (sec) and a fast (msec) current component are apparent, however, the amplitude of the slow, voltage dependent process is greater than that of the more rapid step in the relaxation experiment and less in the correlation analysis. The fluctuation analysis showed principally a rapid voltage independent process which appears to be related to the multistate character of the conducting channel. The value of the correlation function at time zero, or the variance of the fluctuation, σ_G^2, in conjunction with the mean conductance, was used to estimate an average unit conductance step of $1.55 \times 10^{-12}\ \Omega^{-1}$. This value was independent of the membrane potential and the monazomycin concentration. A multistate model for channel formation which has a relatively slow, voltage dependent step for the insertion of ionophores into the membrane and a subsequent series of voltage independent aggregation steps to form the conducting channel was used to calculate amplitudes of the correlation function corresponding to the slow and fast processes of the reaction scheme. The fluctuation amplitudes were calculated using the expression $\sigma_C^2 = kT/d^2G/dC^2$ where σ_C^2 is the variance in the concentration of a reaction product, C, and dG is the Gibbs free energy change for the reaction in question. The maximum relative fluctuation for both processes, $\sigma_C^2 = C/N_L$, where N_L is Avogadro's number, is the limiting case for independent fluctuations and is approached for the fast aggregation process. The fluctuation amplitude related to the slower, voltage dependent step is less than the limiting case because the equilibrium of the slow step favors the insertion of ionophores in the membrane. Supported in part by NS-08409 (LEM).

TH-AM-C3 MODIFICATION OF VALINOMYCIN-MEDIATED BILAYER MEMBRANE CONDUCTANCE BY TMB. K.-H. Kuo* and L.J. Bruner, Dept. of Physics, University of California, Riverside, CA. 92502

The compound 4,5,6,7 tetrachloro-2-methylbenzimidazole (TMB), though itself electrically neutral in aqueous solution, markedly modifies the valinomycin-mediated ohmic steady-state conductance of K^+ ions through lipid bilayer membranes. Valinomycin-K^+ conductance is not affected by TMB concentrations below 10^{-7}M, and increases in direct proportion to K^+ concentration. Carrier-mediated conductance then increases to a maximum as the TMB concentration is increased to 10^{-5}M. As the TMB concentration is further increased the val-K^+ conductance drops sharply, and becomes independent of K^+ ion concentration. This transition is accompanied by a change of high field current-voltage characteristics from a superlinear (or weakly sublinear) to a strongly sublinear form. These observations can be correlated by a kinetic model of carrier-mediated conductance[1], from which it may be inferred that membrane current is limited by back diffusion of uncomplexed carrier at high ($\sim 10^{-4}$M) TMB concentration. Additional experiments involving addition of valinomycin to either the membrane-forming solution or to the aqueous phase establish that, in the latter case, addition of 10^{-4}M TMB to the aqueous phase restricts the entry of uncomplexed carrier into the membrane interfaces. Valinomycin present prior to TMB addition is then lost by lateral diffusion to the surrounding torus. Measurement of the associated time-dependent loss of conductance permits determination of the coefficient of lateral membrane diffusion for valinomycin, $D = 5 \times 10^{-6}$cm^2/sec. This result is about two orders of magnitude larger than the corresponding coefficient for transmembrane carrier diffusion, and provides further evidence for the concentration of valinomycin in energy minima at the membrane/solution interfaces. This work was supported by the U.S. Army Research Office.

1. Läuger, P., and Stark, G., Biochim. Biophys. Acta, 211, 458 (1970).

TH-AM-C4 EVIDENCE FOR MULTIPLE OCCUPANCY OF GRAMICIDIN A CHANNELS BY IONS. G. Eisenman, J. Sandblom,* E. Neher,* Dept. of Physiol., UCLA Med. Sch., Los Angeles, Ca. 90024.

Pursuing the interactions between Tl^+ and gramicidin (Neher, BBA 401:540), we find the membrane potential for Tl^+-K^+ mixtures to be described by the Goldman-Hodgkin-Katz equation both for the individual channel and for macroscopically conducting GMO membranes, with P_{Tl}/P_K depending on aqueous ion concentrations in a manner describable by the empirical eq. (1), where c' and c" signify the millimolar concentrations on the two sides of the membrane.

$$\frac{P_{Tl}}{P_K} \cong \frac{1.0 + 2.0\ c'_{Tl}c''_{Tl} + .003\ c'_Kc''_K + .2\ (c'_{Tl}c''_K + c''_{Tl}c'_K)}{0.35 + .067c'_{Tl}c''_{Tl} + .001\ c'_Kc''_K + .02(c'_{Tl}c''_K + c''_{Tl}c'_K)} \qquad (1)$$

This behavior is in contrast to that of carriers where P_{Tl}/P_K is independent of ion concentration. It is understandable in terms of a theory derived by Sandblom for a primitive model channel which is postulated to bind a Tl^+ (or K^+) on each of its two sides. It thereby develops another conducting state besides that of the known single-cation-saturable channel. The weights of each term correspond to the contributions of each occupied state (e.g. Tl'Tl", Tl'K") to the permeability of Tl^+ (numerator) or K^+ (denominator). In addition, above 0.5 mM Tl^+ and 50 mM K^+ the gramicidin channel becomes significantly permeable to anions (Cl^-, Ac^-, NO_3^-) as evidenced by P_{Tl}/P_K no longer being the same when measured with a small gradient of Tl^+ as with a small gradient of K^+. Lineweaver-Burke plots of the conductance-concentration dependence for single channels in pure K^+ or Tl^+ (from .0005-1.0M) show two linear regions of differing slopes and intercepts from which Michaelis-Menten parameters have been estimated. For Tl^+, the K_m are 1.0×10^{-3} and 4.5×10^{-2}M for the 1st and 2nd binding sites with G_{max} of 2.0 pmho and 44 pmho, respectively. For K^+, the corresponding K_m are 5.0×10^{-3} and 3.5×10^{-1}M with G_{max} 3.85 pmho and 59 pmho. Sup. by GB 30835 (NSF), NS 09931 (USPHS).

TH-AM-C5 CYCLIC OCTAPEPTIDES ARE SELECTIVE CARRIERS OF CATIONS ACROSS LIPID BILAYERS. G. Eisenman, C. Deber,* and E. R. Blout, UCLA and Harvard Medical Schools.

The membrane effects of the family of ion binding cyclic peptides of glycine (G) and L-proline (P) of the type cyclo$(PG)_n$, where n = 3,4,5, indicate that the cyclic octapeptides (n = 4) are by far the most effective carriers of the group Ia cations in this series. Cyclic octapeptides of D-phenylalanine (DΦ) of the type c$(D\Phi PGP)_2$ are also effective carriers, and we here report that c$(PG)_4$ and c$(D\Phi PGP)_2$ produce selective permeability to monovalent cations in glycerol monooleate (GMO) or glycerol dioleate (GDO)/decane bilayers. Both of these octapeptides act as valinomycin-like carriers, albeit less effective when added via the aqueous solutions, in obeying 1:1 stoichiometry (as judged by aqueous concentration-conductance behavior) and exhibiting "equilibrium domain" properties with the least well carried cations (Na^+, Li^+) and "kinetic domain" behavior with those most effectively carried (K^+, Rb^+) (as judged from conductance-voltage behavior). The selectivities of these molecules, as assessed by membrane potential measurements, are altered systematically by replacement of 2 Gly's by 2 Phenylala's in going from c$(PG)_4$ to c$(D\Phi PGP)_2$, which changes the ionic permeability sequence from RB>Cs>K>Na>Li (Eisenman II) for c$(PG)_4$ to Rb>K>Cs>Na>Li (Eisenman III) for c$(D\Phi PGP)_2$. Low voltage permeability ratios, relative to Cs^+, are: Rb^+, 1.12; Cs^+, 1.0; K^+, 0.42; Tl^+, 0.27; NH_4^+, 0.1; Na^+, <.0002; Li^+, <.0001 as measured with S. Krasne for c$(PG)_4$ vs. Tl^+, 3.32; Rb^+, 2.83; K^+, 1.33; Cs^+, 1.0; NH_4^+, 0.6; Na^+, <.0002; Li^+, <.0001 for c$(D\Phi PGP)_2$. Replacement of 2 Gly's by 2 Phenylala's thus changes the apparent Tl^+ selectivity from "sub Ia" in c$(PG)_4$ to "supra Ia" in c$(D\Phi PGP)_2$; while NH_4^+ remains "sub Ia" in both molecules. The incorporation of an aromatic phenylalanine residue in c$(D\Phi PGP)_2$ offers the possibility of using this well-behaved carrier as a spectroscopic probe. Supported by NSF (GB 30835) and USPHS (NS 09931, AM 07300, AM 10794).

TH-AM-C6 MONOVALENT AND DIVALENT CATION COMPLEXES OF THE IONOPHOROUS ANTIBIOTICS NONACTIN, MONACTIN AND DINACTIN. G.D.J. Phillies,# I.M. Asher,+ H.E. Stanley, Harvard-MIT Program in Health Sciences and Technology, MIT, Cambridge, Mass. 02139

Laser Raman spectroscopic studies of the K^+, Rb^+, Cs^+, NH_3OH^+ and $C(NH_2)_3^+$ complexes of monactin and dinactin in CH_3OH:$CHCl_3$ (4:1 v/v) solution confirm our previous results with nonactin, namely: (i) these complexes are isosteric, (ii) the ester carbonyl stretch frequency is proportional to the cation-carbonyl electrostatic interaction energy. These results further support the applicability of the Krasne-Eisenman model of ion complexation to the nactins. In contrast, spectra of the Na^+ and Ba^{++} complexes display doublets (1709, 1727 cm^{-1} and 1695, 1714 cm^{-1} respectively) in this region; and the NH_4^+ complex shows the effects of intramolecular hydrogen bonding. Polarization studies show that the Tl^+ complex is not isosteric with the other complexes; in particular, the arrangement of the carbonyl groups about the central ion may well not be tetrahedrally symmetric. Spectra of crystalline samples differ in a variety of ways, reflecting the effects of crystalline forces.

Present Address: #Department of Chemistry, UCLA, Los Angeles, Ca. 90024, and +Office of Science, FDA, HEW, Rockville, Md. 20852

TH-AM-C7 CONFORMATIONAL CHANGES OF CA^{2+}-ATPASE OF SARCOPLASMIC RETICULUM LINKED WITH CA^{2+} TRANSPORT. N. Ikemoto, Dept. Muscle Research, Boston Biomedical Research Institute; and Dept. of Neurology, Harvard Medical School, Boston, Mass., 02114

An -SH specific fluorescent probe, S-mercuric N-dansylcysteine (Leavis and Lehrer, Biochemistry 13, 3042, 1974) reacts stoichiometrically with 6-7 SH/10^5 dalton of the ATPase of the sarcoplasmic reticulum accompanied by inhibition of the Ca^{2+}-dependent ATPase activity. With about half of the reactive thiols blocked, upon addition of ATP in the presence of 5 mM Ca^{2+}, the fluorescence at 498 nm of the enzyme-bound probe decreases concomitantly with phosphorylation of the enzyme. Upon addition of ADP the fluorescence increases in parallel with reversal of the phosphorylation reaction. Stopped-flow fluorometry shows that in the initial 400 ms fluorescence changes take place in two steps: a rapid decrease ($t_{1/2}$ = 10 ms) (Step 1) followed by a slow decrease ($t_{1/2}$ = 150 ms) (Step 2). Chemical quenching studies by means of rapid mixing have shown that the time course of the phosphoenzyme formation of the dansylated enzyme corresponds well with that of the fluorescence changes. Previously we have suggested that a key event in Ca^{2+} transport mechanism is the transconformation of the enzyme molecule between two forms of acid stable phosphoenzyme, viz. EPCa and E*PCa in which the transport site has high affinity and low affinity, respectively (Ikemoto, J. Biol. Chem. 250, 7219, 1975). Conformation steps 1 and 2 are tentatively identified with EPCa and E*PCa, respectively.
(Supported by grants from the NIH (AM 16944) and the American Heart Association)

TH-AM-C8 MOLECULAR CHARACTERIZATION OF ENZYMATICALLY ACTIVE, DETERGENT-SOLUBILIZED Ca^{++} ATPase FROM SARCOPLASMIC RETICULUM. Marc le Maire, C.Tanford, Duke University, Dept. of Biochemistry, Durham, N.C. 27710.

Using an appropriate non-ionic detergent, it has been possible to obtain enzymatically active Ca^{++} - ATPase from sarcoplasmic reticulum in true solution as a detergent-lipid-protein complex of low molecular weight. Purified vesicular ATPase was prepared by standard methods using deoxycholate. Dodecyl octaethylene glycol ($C_{12}E_8$) was used at a level of between 3 and 4 g $C_{12}E_8$ per g of protein, at a concentration above its critical micelle concentration, to solubilize the vesicles. This detergent was then exchanged for Tween 80 by chromatography on a Sepharose 4B column saturated with Tween 80. Ca^{++}-stimulated ATPase activity comparable to that of the original vesicles (and measured without dilution of the detergent) was maintained for several days. The size of the Tween-containing particles was somewhat variable, depending on the $C_{12}E_8$/protein ratio used for solubilization, but the specific activity dropped sharply for the smallest particles obtained. Molecular weight measurements by analytical ultracentrifugation showed that the smallest fully active particles contain 3 to 4 ATPase polypeptide chains and only about 30% Tween 80 by weight. All active preparations contain about 30 moles of relatively tightly bound phospholipid per polypeptide chain, confirming the minimal lipid requirement for retention of full activity previously reported by other laboratories. The results suggest that the ATPase is oligomeric in the native state, a suggestion supported by existing electron microscopic data (supported by NIH grant AM-4576).

TH-AM-C9 TRANSIENT STATE KINETICS OF ATPASE ACTIVITY AND Ca^{2+} UPTAKE IN SARCOPLASMIC RETICULUM (SR). Mark Kurzmack* and Giuseppe Inesi, University of the Pacific, San Francisco, California 94115

We were able to measure production of inorganic phosphate and Ca^{2+} transients, with a time delay of ~ 20 msec. following the addition of ATP to reaction mixtures containing SR vesicles and other required cofactors. ATPase activity was initiated and quenched with the aid of an apparatus equipped with two mixing chambers in series and reaction time control. The quenched material was then analyzed for ^{32}P-phosphate hydrolyzed or incorporated into the SR protein from (γ-^{32}P)-ATP.

ATP dependent Ca^{2+} uptake by SR was initiated in a stopped flow apparatus and the reaction mixture conveyed into an optical path. Ca^{2+} transients were then detected by dual wavelength differential photometry, measuring the absorption changes undergone by the metallochromic indicator Arsenazo III. The transients were recorded by an oscilloscope.

The initial rates of inorganic phosphate production and Ca^{2+} uptake were 38.5 ± 5 nmoles/mg protein/sec. and 85 ± 10 nmoles/mg protein/sec, respectively. Therefore, in the transient state, production of inorganic phosphate and Ca^{2+} uptake exhibit a parallel behavior, with a Ca^{2+}: Pi ratio of approximately 2. On the contrary, incorporation of ATP γ-phosphate into the protein is much faster and steady state levels ($2.8 \pm .2$ nmoles/mg protein) of phosphorylated enzyme intermediate are reached within 20 msec. of reaction. This intermediate step is Ca^{2+} and Mg^{2+} dependent.

This work was supported by the NIH (HL 16607) and the Muscular Dystrophy Association.

TH-AM-C10 HIGH AND LOW AFFINITY Ca^{2+} BINDING TO SKELETAL AND CARDIAC SARCOPLASMIC RETICULUM: USE OF A HIGH AFFINITY FLUORESCENT CALCIUM INDICATOR. Vincent C.K. Chiu and Duncan Haynes, Department of Pharmacology, Univ. of Miami Medical School, Miami, Fla. 33152

High and low affinity Ca^{2+} and Mg^{2+} binding to sarcoplasmic reticulum (SR) was studied using calcein as a high-affinity fluorescent indicator of divalent cations in the aqueous phase. Quantitative studies of Ca^{2+} binding to the skeletal SR have revealed two classes of binding sites: One with high capacity and low affinity (ca. 820 nmole/mg protein, K_d = 1.9 mM) and another with low capacity and higher affinity (ca 35 nmole/mg protein, K_d = 17.5 μM). The divalent cation specificity of the low affinity site is low and the Ca^{2+}/Mg^{2+} specificity of the high affinity site is high. Quantitative considerations of the binding indicate that the high affinity site resides in the Ca^{2+} ATPase (carrier) protein and represents the active site of the carrier, and that the low affinity site resides in the nonspecific acidic binding proteins. Stopped-flow kinetic studies of Ca^{2+} passive binding have demonstrated that the binding to the high affinity site is very fast and that the overall binding reaction with the low affinity site is slow, with a time course of about 4 sec. Analysis of the rate constants shows that at least part of the low affinity binding proteins are within the SR matrix and that Ca^{2+} can reach them only by traversing the membrane via the Ca^{2+} carrier (Ca^{2+} ATPase). A model of the SR is proposed which accounts for the maximal active Ca^{2+} uptake and several other functional properties of the organelle in terms of its known protein composition and topological organization. Cardiac SR has been separated into three fractions by a sucrose gradient technique in the presence of hypertonic KCl. Quantitative comparisons of the binding equilibria and kinetics for cardiac and skeletal SR will be given. Supported by Grant 1 P01 HL 16117-01 (NIH).

TH-AM-C11 EVIDENCE FOR A REDOX PUMP IN GASTRIC MICROSOMES. M.C. Goodall. Laboratory of Membrane Biology, University of Alabama in Birmingham, Birmingham, Alabama 35294.

Gastric microsomes (Sachs et al. these abstracts), which show a K^+-stimulated proton uptake on the addition of Mg-ATP, incorporate into a bilayer of (bovine) phosphatidyl serine. Conductance increases from 10^{-9} Ω^{-1} cm^{-2} to 10^{-7} Ω^{-1} cm^{-2} with microsomes (to 2.5 μg protein/ml at 25°C) one side (cis) in symmetrical solutions of $NaKSO_4$ (20 mM) buffered to pH 6.3. Addition of Mg-ATP (0.75 mM, cis) gives -20 mV (cis) which is first increased to -30 mV and then abolished by dicyclohexyl carboimide, 1 mM. This might be interpreted as non-stoichiometric pumping with predominantly H^+-K^+ exchange. However, since there is doubt whether acid secretion is primarily ATP driven (vide: W.S. Rehm, Metabolic Pathways IV, ed. L.E. Hokin, p. 187-241, 1972) an alternative redox pump was sought. Unphysiological redox systems (Ascorbic acid, cis; $FeCl_3$, KIO_4, trans) gave -50 -60 mV cis. NADH-FAD, 0.25 mM wholly cis, gave -25 mV which was abolished by amytal (1 mM). These results were lipid dependent: dioleyl phosphatidyl choline at 36°C gave -4 mV (ATP), -45 -75 mV (NADH-FAD); on the other hand (ATP + NADH-FAD) gave -13 mV, showing apparently two pumps acting in parallel. Increasing the $[K^+]$ in this case causes a further shift to the ATP potential, confirming H^+-K^+ exchange. Since the microsomes were heterogeneous (but free from mitochondrial contamination) on free flow electrophoresis (Sachs et al, ibid.), the possibility exists of separating these activities by this method. Another approach is via a hexane extract which when introduced into the phospholipid yielded results similar to the above for both systems. (NIH, NSF support).

TH-AM-C12 THE MOVEMENT OF ION PAIRS ACROSS BILAYER LIPID MEMBRANES. M.S. Mangel, University of British Columbia, Vancouver, British Columbia, Canada, and G.L. Jendrasiak*, Biophysics Division, University of Illinois, Urbana, Illinois. (Intr. by William Sleator)

If a polyhalide concentration gradient exists across a bilayer lipid membrane (BLM), ion pair movement occurs across the membrane. The term ion pair indicates a lipid soluble complex of cation and anion with stoichiometry dicated by the respective charges. In a mixture of metal halide (MX_n, X = I,Cl,Br) and iodine, the ion pair is of the form $M(I_2X)_n$. The flux of ion pairs was monitored by measuring both the flow of metal ion and polyhalide ion across the BLM. The flux of ion pairs across the BLM increased with the cation crystal radius, the fluidity of the membrane, and the strength of the ion pair complex and decreased with increasing osmotic gradient. In addition the flux was a strong function of alamethicin concentration in the membrane. A technique which isolates the flux of ion pairs across one membrane - water interface is described. The relationship between ion pairing and the electrical conductivity of BLM is briefly discussed. Many of the results found in this work can be explained in terms of the ideas developed from solvent extraction studies.

TH-AM-C13 Ca^{2+}-UPTAKE BY PLASMA MEMBRANE VESICLES AS MEASURED BY FLOW DIALYSIS SYSTEM. Y. Shami, Dept. of Cell Biology, Research Institute, The Hospital for Sick Children, Toronto, Ontario M5G 1X8, Canada.

Calcium transport across the placenta is asymmetrical and is believed to be an energy-requiring process. An essential step in such transport in translocation of the ion across a single plasma membrane. Plasma membrane vesicles derived from Guinea pig placenta are capable of accumulating up to 190 mM Ca^{2+}, 24 times the concentration in the external medium. This process is dependent on ATP hydrolysis by the placental Ca^{2+}-ATPase. The Pi/Ca ratio is dependent on the external Ca^{2+} concentration, and reaches the value of 2 at 10 mM Ca^{2+}. The Ca^{2+}-uptake (in 5 mM Ca^{2+}) is doubled in the presence of phosphate (5 mM), but is affected by Mg^{2+} only at low Ca^{2+} concentration(below 0.01 mM). In this study, uptake can be defined and distinguished from binding using a flow dialysis method. Bound calcium is accessible for immediate exchange and can be displaced by a competitor. It is measured by labelling the membrane with $^{45}Ca^{2+}$ (in the absence of ATP) and displacing it with increasing concentrations of "cold" calcium. Uptake is represented by the fraction of $^{45}Ca^{2+}$ which cannot be rapidly displaced by a large excess of "cold" calcium. The definition allows the binding and uptake to be distinguished throughout the incubation period and overestimation of Ca^{2+}-uptake is avoided. The advantage of using this definition is evident, especially in cases when the Ca^{2+} accumulating system is not as efficient and fast as the sarcoplasmic reticulum.

TH-AM-C14 CALCIUM EFFLUX FROM RAT VASCULAR SMOOTH MUSCLE. V. Palatý and M. Mar*, Dept. of Anatomy, The University of British Columbia, Vancouver, B.C. V6T 1W5

Ca^{2+} efflux from the title cells was evaluated from measurement of the residual cell ^{45}Ca after exposure of the tissue to an isotope-free solution for a given period of time. The extracellular ^{45}Ca was washed out into a La^{3+}-containing, 2 °C warm solution. Efflux of ^{45}Ca from metabolically active cells follows first-order kinetics with a rate constant of 2.7 ± 0.1 hr^{-1} at 37 °C. In contrast to ^{45}Ca influx, ^{45}Ca efflux is much more dependent on temperature exhibiting a Q_{10} of about 3.2 between 37 and 22 °C. There seems to be a break in the Arrhenius plot of the rate constant at about 18 °C. The value of the rate constant is not affected significantly by abolition of the transmembrane concentration gradient of Na^+ brought about by inactivation of the Na pump. Even under these conditions, ^{45}Ca efflux remains highly temperature-dependent. In the presence of external Ca-EGTA, the rate of ^{45}Ca efflux does not seem to be affected even by large variations in $[Ca^{2+}]_o$, which indicates the absence of a Ca_i- Ca_o exchange. External La^{3+} inhibits ^{45}Ca efflux. The rate constant is reduced by 50 % at $[La^{3+}]_o$ equal to 0.2 mM. After depletion of the cell ATP, there is an insignificant decrease in the rate constant of ^{45}Ca efflux. Several observations, particularly that of a low Q_{10} of the efflux, indicate that the relatively fast rate of ^{45}Ca efflux from ATP-depleted cells can be attributed to unspecific leakiness of the plasma membrane. These findings do not support the hypothesis that extrusion of Ca from vascular smooth muscle is coupled to spontaneous influx of Na^+. The rate of ^{45}Ca efflux can be enhanced by as much as 40 % by theophylline or stimulation of β-adrenergic receptors.

(This research was supported by a grant from the Medical Research Council of Canada.)

TH-AM-D1 THE EFFECT OF ANIONS ON OXIDATION AND REDUCTION OF CYTOCHROME C. B.F. Peterman* and R.A. Morton, Department of Biology, McMaster University, Hamilton, Ont., Canada.

Electrophoretic measurements (Margoliash et al, Nature 228, 723, 1970) showed that phosphate ions bind to both oxidation states of mammalian-type cytochrome c while chloride ions were bound predominantly to the ferricytochrome molecule. Tris and cacodylate ions did not bind appreciably to either form. We have used a stopped-flow apparatus, to study the effects of anions on the rates of oxidation and reduction of electrodialyzed horse heart cytochrome c by hexacyanides. Experiments were done at constant ionic strength, replacing the cacodylate ions of Tris buffers with the anion to be studied. Results showed quite different behaviour of phosphate and chloride. Phosphate decreased both oxidation and reduction rates about equally, leaving the redox potential unchanged. Chloride on the other hand, decreased the rate constant for reduction much more than it did that for oxidation, and thus therefore the redox potential was increased. A variety of organic anions are currently under study.

TH-AM-D2 THE DENATURATION OF FERRICYTOCHROME C' BY GUANIDINE HYDROCHLORIDE AND UREA. B.R. Kiggins* and C.P.S. Taylor, Dept. of Biophysics, Univ. of West. Ont., London, Canada.

Unlike mammalian cytochrome c, cytochrome c' did not quickly reach an equilibrium state upon being mixed with a denaturing solution. Instead, the reaction proceeded slowly enough to allow spectrophotometric measurement. The first-order rate constant for urea obeyed the relation $\ell n\ k = \ell n(0.13 \times 10^{-6}) + 0.60\ m$ where m is the molal urea concentration in the range of 2 to 10 molal. The relation for guanidine hydrochloride (GdHCℓ) was found to be $\ell n\ k = \ell n(0.33 \times 10^{-6}) + 1.40\ m$ over the range of 1 to 5 molal GdHCℓ. We have been unable to find a similar relation in the literature. The rates for GdHCℓ were about one hundred times faster than for urea. Regardless of the denaturant concentration, the protein reached the same final spectral state. The rate constant was independent of the protein concentration over a 4-fold range. The effect of temperature was studied at 3 different concentrations of urea and GdHCℓ. From the Arrhenius plots and the absolute theory of rates, we find that the changes in enthalpy, entropy and free energy all decrease linearly as the denaturant concentration is increased. For urea, the slope, $d(\Delta H^{\ddagger})/dm$, is -5500 ± 1500 cal mole^{-1} molal^{-1} and $d(\Delta G^{\ddagger})/dm$ is -320 ± 30 cal mole^{-1} molal^{-1}, from which we obtain $d(T\Delta S^{\ddagger})/dm$ as -5600 ± 600 cal mole^{-1} molal^{-1}. Similar trends were found for GdHCℓ but with slightly higher values. The effect of pH was studied in 3.75 molal GdHCℓ. The rate constant was the same at pH 6 and 7 but lower at pH 8. This is consistent with the existence of multiple forms of c' in the alkaline region.

(Supported by the Medical Research Council of Canada.)

TH-AM-D3 EFFECT OF RESIDUAL STRUCTURES ON THE KINETICS OF FERRICYTOCHROME c CHAIN FOLDING. Tian Yow Tsong, Department of Physiological Chemistry, The Johns Hopkins University School of Medicine, Maryland 21205

Whether some residual structures can exist in a polypeptide chain under strongly denaturing conditions is a question of both theoretical and experimental interest. For example, it is important to examine the effect of these structural elements on the kinetics of protein chain folding. We have found a sensitive way of monitoring the effective volume of cytochrome c in solution by measuring the efficiency of the energy transfer between trp-59 and the heme group. By means of such measurements we have shown that at neutral pH ferricytochrome c retains certain residual structures in concentrated solutions of urea and guanidine-HCl. Cooperative unfolding of these residual structures can be achieved by acidification of the protein in 9 M urea. The acidic titration also reveals a spin-state transformation of the heme at pH 5.1. Kinetics of the spin-state transformation, as measured by the heme absorption changes, occurs in the millisecond time range. In contrast, the unfolding of the residual structures, as reflected in the fluorescence changes, is much slower (in the decisecond time range). Comparison of the kinetics of chain folding when the protein is transferred from 9 M urea, pH 4, to 1.5 M urea, pH 7, with that of transferring from 9 M urea, pH 7, to 1.5 M urea, pH 7, indicates that the residual structures have little effect on the kinetics of the overall reaction. Based on these observations and the presently available kinetic data it is concluded that 1) local structural elements of cytochrome c can exist under strongly denaturing solvents, 2) the formation of the residual structures precedes the major chain folding reaction which may be rate-limited by a nucleation step. (This work was supported by NSF Grant BMS75-08690)

TH-AM-D4 VISIBLE ABSORPTION SPECTRA OF QUANTUM MIXED-SPIN FERRIC HEMES. M.M. Maltempo, Department of Biochemistry and Biophysics, University of Pennsylvania, Philadelphia, PA. 19174 (Intro. by J.S. Leigh).

Recently, it has been shown that the heme in the bacterial ferricytochromes c' has magnetic properties (paramagnetic susceptibility intermediate between high spin and low spin values; a single EPR species with $g_{\perp} \approx 5$ and $g_{\parallel}=2$ consistent with a quantum mechanical mixture of intermediate spin (S=3/2) and high spin (S=5/2) states (Maltempo, M.M., J. Chem. Phys. 61, 2540, 1974). The heme of purified (Leigh, J.S., Maltempo, M.M., Ohlsson, P.I. and Paul, K.G., FEBS Lett. 51, 304, 1975) and in situ horseradish peroxidase can also exist in the quantum mixed spin state, as well as in more common high and low spin states (Tamura, M. and Hori, H., Biochim. Biophys. Acta 284, 20, 1972). The visible absorption spectrum of Chromatium ferricytochrome c' has been recorded at pH 7 and 77°K, where magnetic data show the protein to have quantum mixed spin properties. The spectrum has absorption bands at about 490 and 635 nm (A(490)/A(635)=2.9). This result, in conjunction with previous optical and magnetic data (1.4-300°K) for the two proteins (Ehrenberg, A. and Kamen, M.D., Biochim. Biophys. Acta 102, 333, 1965; Tasaki, A., Otsuka, J. and Kotani, M., Biochim. Biophys. Acta 140, 284, 1967; Schonbaum, G.R., J. Biol. Chem. 248, 502, 1973; Maltempo, M.M., Moss, T.H. and Cusanovich, M.A., Biochim. Biophys. Acta 342, 290, 1974), show that the visible spectrum of quantum mixed spin heme is quite similar to that of typical high spin heme. Moreover, the visible spectrum of quantum mixed spin heme is consistent with the electronic properties and iron-ligand structure inferred from magnetic data, and the current assignment of ferric heme visible bands. More generally, data for these two proteins suggests caution in the interpretation of ferric heme spectral data in terms of only high and low spin components. Supported by GM 55064.

TH-AM-D5 RESONANCE RAMAN ENHANCEMENT OF AXIAL LIGAND MODES IN Mn (III) ETIOPORPHYRIN I: THE USE OF CHARGE TRANSFER BANDS TO MONITOR THE COMPLEXATION STATE OF METALLOPORPHYRINS. S. A. Asher* and K. Sauer, Department of Chemistry and Laboratory of Chemical Biodynamics, University of California, Berkeley, Calif. 94720.

Resonance Raman spectroscopy was used to observe the axial halide vibrations of the F^-, Cl^-, Br^- and I^- complexes of Mn (III) etioporphyrin I by exciting in a charge transfer transition. Resonance Raman spectra obtained by exciting the visible absorption bands of Mn (III) etioporphyrin I between 530 and 600 nm are comparable to spectra obtained in the α and β bands of metalloporphyrins and heme proteins. Resonance Raman spectra obtained by excitation in the charge transfer absorption band between 450 and 500 nm are radically different from spectra previously obtained from metalloporphyrins and heme proteins. Low frequency metal dependent vibrations and axial ligand vibrations are selectively enhanced. The implications of this work for heme proteins using excitation in charge transfer and $n \rightarrow \pi^*$ transitions will be discussed.

TH-AM-D6 MODEL OF CYTOCHROME OXIDASE CO-BINDING SITE DERIVED FROM LOW-TEMPERATURE KINETICS. M. Sharrock and T. Yonetani, Department of Biochemistry and Biophysics, University of Pennsylvania, Philadelphia, Pa. 19174

Flash photolysis has been used to study the reassociation of cyt a_3-CO in cytochrome oxidase isolated from beef heart mitochondria. Experiments were done using an aqueous medium with various concentrations of CO; temperatures ranged from 185°K to 295°K. In the frozen state, the kinetics deviate markedly from the simple Arrhenius law. The slope of a log(rate) vs. 1/T plot changes drastically with temperature. The temperature dependence of the rate can be explained theoretically if the cyt a_3 site is considered to contain three regions in which CO not bound to the heme iron can exist. The model requires that the outer two regions contain mobile CO in concentrations proportional to that in the medium, even at temperatures well below freezing. The innermost region, from which binding to the heme iron can take place, can accommodate only one CO molecule. Enthalpy and entropy values for CO in each of the three regions have been calculated. The parameters that govern the kinetics are sensitive to environmental conditions, in particular, to the concentration of potassium phosphate buffer. Low temperature photolysis reveals pronounced differences between the heme sites of cyt a_3 and myoglobin (1). We speculate that this may be due in part to a lipid character, suggested earlier (2), of the cytochrome oxidase site. Support by HL 14508 and HL 03335 (NIH), and by BMS 73-00970 (NSF).

(1) R. H. Austin, K. W. Beeson, L. Eisenstein, H. Frauenfelder, and I. C. Gunsalus (1975) Biochemistry, in press.
(2) B. Chance, B. Schoener, and T. Yonetani (1965) Oxidases and Related Redox Systems I, Vol. 2, pp. 609-621.

TH-AM-D7 HEME A IRON SPIN STATES IN CYTOCHROME OXIDASE DETECTED BY MAGNETIC CIRCULAR DICHROISM SPECTROSCOPY. G. T. Babcock, L. E. Vickery, and G. Palmer, Department of Biochemistry, Rice University, Houston, Texas 77001; and Laboratory of Chemical Biodynamics, University of California, Berkeley, California 94720

Magnetic circular dichroism (MCD) spectra have been recorded for beef heart cytochrome oxidase and a number of its inhibitor complexes. For the oxidized enzyme a derivative type C term (peak, 420 nm; trough, 435 nm) characteristic of low spin Fe^{+3} heme is observed. Temperature studies, which show that this feature follows a Boltzmann distribution down to 77° K, confirm this assignment. Comparison of the intensity associated with this term to that exhibited by hemin a-imidazole model compounds indicates that this signal accounts for 30-45% of the heme a in the oxidase. Addition of KCN to the oxidized protein doubles the MCD intensity without altering the position of the extrema. When oxidized cytochrome oxidase is reductively titrated under argon a new MCD maximum develops at 452 nm with the first electrons entering the molecule. This feature persists to approximately 50% reduction whereupon the MCD intensity increases sharply and the peak position shifts to 447 nm. The MCD spectrum of the fully reduced protein (peak, 447 nm; trough, 434 nm; neg. shoulder, 413 nm) resembles that observed for deoxy hemoglobin (Vickery et al, J.A.C.S., in press). The temperature dependence for reduced cytochrome oxidase shows strong paramagnetism for the 447 nm peak with a much weaker contribution at 452 nm indicating the presence of both high and low spin ferrous heme a. Addition of either KCN or CO to the reduced protein decreases the MCD intensity by half and shifts the positive extremum to 452 nm. The results fit a model in which cytochrome a is low spin and cytochrome a_3 is high spin in both oxidized and reduced cytochrome oxidase. (This research was supported, in part, by NIH Grants GM-21337 and HL-02052, and, in part, by the Energy and Resources Development Administration).

TH-AM-D8 ESR - DETECTABLE IRON-SULFUR COMPONENTS IN SUBMITOCHONDRIAL PARTICLES FROM WILD-TYPE AND A RESPIRATORY MUTANT OF Neurospora crassa. Susan Jenesel* and David L. Edwards, Department of Biological Sciences, State University of New York, Albany, N.Y. 12222 and Joseph T. Warden*, Department of Chemistry, Rensselaer Polytechnic Institute, Troy, N.Y. 12181

We have obtained in our laboratory a number of respiratory deficient mutants of Neurospora that have defective mitochondrial electron transfer components. Some of these mutants also have the cyanide- and antimycin A-insensitive (salicyl hydroxamate-sensitive) electron transfer pathway. In order to determine the nature of the components of this alternate pathway and to further study the defects in the normal respiratory chains of these mutants, we have initiated a study of the components of both wild-type and mutant mitochondria that are detectable by electron spin resonance (ESR). Submitochondrial particles from wild-type mitochondria display resonances characteristic of iron-sulfur centers 1-4 of respiratory complex I and also of components assigned to complexes II and III upon reduction with exogenous NADH (Orme-Johnson et. al. Biochem. Biophys. Res. Comm. 44, 446 (1971), Ohnishi et. al. J. Biol. Chem. 246, 5960 (1971)). Experiments with the drug pyrrolnitrin show that iron-sulfur centers 1-4 are reduced by NADH in the presence of the drug but not the components assigned to complexes II and III. Pyrrolnitrin is an inhibitor of the cyanide-insensitive pathway. Submitochondrial particles of the respiratory mutant cni-1, a chromosomal mutant with cyanide-insensitive respiration, do not display the resonances characteristic of iron-sulfur center 2 upon reduction with NADH either in the presence or absence of pyrrolnitrin. These data suggest that the branch point for the cyanide-insensitive pathway occurs before iron-sulfur center 2. (Supported by U.S.P.H.S. grant GM-19410)

TH-AM-D9 ANALYSIS OF ENERGY TRANSDUCTION SITES IN ELECTRON TRANSPORT CHAINS. APPLICATION TO IRON-SULFUR CENTER N-2 IN MITOCHONDRIA. Don DeVault and Tomoko Ohnishi, Johnson Research Foundation, Dept of Biochemistry and Biophysics, Univ. of Penna., Philadelphia, PA 19174.

An energy transduction site in an electron transport chain is characterized by two redox potentials: E_1 at the low potential (entrance) side and E_2 at the high potential (exit) side. Many properties of such a site (redox state, phosphorylating potential, ratio of high to low potential forms, etc.) are conveniently studied by plotting contours on a graph of E_2 vs E_1. The redox data on iron-sulfur center N-2 of mitochondria which, on adding ATP, shows oxidation when poised at E_1 (1,2) and reduction when poised at E_2 (2), are plotted this way. The predictions of several chemical intermediate models and of several chemiosmotic models for center N-2 are also plotted this way and compared with experiment. It is concluded that in chemiosmotic models center N-2 cannot be located exclusively at the inside of the mitochondrial membrane as had been suggested by Mitchell (3). This result follows mainly from the observation (2) of reduction when ATP is added to submitochondrial particles poised with succinate-fumarate with antimycin A present and redox mediators absent. Present data are not sufficient to exclude any of the other models tried.

(1) Gutman, M., Singer, T.P. and Beinert, H. (1972) Biochemistry 11, 556-562.
(2) Ohnishi, T., European J. Biochem., in press.
(3) Mitchell, P. (1972) in Mitochondria/Biomembranes, 8th Mtg F.E.B.S., North Holland Publ. Co., Amsterdam, Vol 28, pp 353-370.

TH-AM-D10 EFFECTS OF ETHANOL AND ACETALDEHYDE ON IRON SULFUR CENTERS IN SUBMITOCHONDRIAL PARTICLES. J.C.Salerno* and Tomoko Ohnishi, Department of Biochemistry and Biophysics, University of Pennsylvania, School of Medicine Philadelphia, Penn. 19174

Submitochondrial particles incubated with ethanol or acetaldehyde at relatively low concentrations show alterations in the EPR spectra of the iron sulfur centers in the NADH and succinate dehydrogenase segments of the respiratory chain. The iron sulfur centers in the NADH dehydrogenase region are more sensitive to both ethanol and acetaldehyde than the iron sulfur centers in succinate dehydrogenase and the cytochrome b-c region. Centers N-3,4 , N-5,6 and N-1b are affected after relatively short incubation periods (3-30 minutes) while center N-2 shows considerable sensitivity over somewhat longer (20-90 minute) incubations. HiPIP type center S-3 is the most ethanol sensitive center in the succinate dehydrogenase region of the respiratory chain. Simple changes in the redox state can be ruled out as an explanation for these findings by potentiometric analysis. Decreased rates of oxidation of NADH, and to a lesser extent succinate, in both ethanol and acetaldehyde treated submitochondrial particles were observed.

TH-AM-D11 SPIN-SPIN INTERACTIONS IN THE EIGHT-IRON FERREDOXIN FROM MICROCCUS LACTILYTICUS. K.L. Schepler, W.R. Dunham, and R.H. Sands, Biophysics Research Division, Institute of Science and Technology, University of Michigan, Ann Arbor, Michigan 48105.

Previous investigations in this laboratory by Mathews, et al.[1] indicated that the reduced eight-iron ferredoxin of Micrococcus lactilyticus has two paramagnetic four-iron clusters which interact via an exchange or dipole interaction. Additional experiments and calculations have now been done to learn more about the nature of the spin-spin interactions. Successful computer simulations of the experimental electron paramagnetic resonance (EPR) spectra were obtained by using the following model: The two four-iron clusters are described by identical g-tensors which are not colinear. These two clusters also interact via an exchange interaction (J=350 MHz) and a small dipole interaction (r=8 Å). Electron-electron double resonance (ELDOR) experiments have been done to confirm this spin-spin interaction model.

1. R. Mathews, et al., J. Biol. Chem. 249, 4326 (1974).

TH-AM-D12 PERTURBATION STUDIES OF THE HEME PROTEIN P-450 FROM THE ADRENAL CORTEX. Heinz Schleyer, David Y. Cooper*, and Otto Rosenthal* (with the technical assistance of Pamela Cheung). Harrison Dept. Surg. Res. and Johnson Res. Fdn., Univ. of Pennsylvania, School of Medicine, Philadelphia, Pa. 19104.

We have previously shown that substrates, inhibitors, and many other agents bind to the heme protein P-450 but do not enter the coordination sphere of Fe. To gain a better understanding of these perturbation effects we have investigated the interaction of P-450(Fe^{3+}) from adrenal cortex (J. Biol. Chem. 247:6103, 1972) with anionic and nonionic detergents and the effects of a variety of buffer systems (pH range 6-13) using optical absorption- and EPR spectroscopy. An increase of pH (e.g. to 10.5) leads to large changes in the optical absorption (Fe^{3+} 416 → 420 nm). The typical EPR signature of P-450 (Fe^{3+}), s = 1/2, is maintained while the ability to form P-450 (Fe^{2+})·CO with its characteristic absorption maximum near 450 nm is lost; instead, a different CO-complex (~420 nm) is formed (50% conversion at pH 9.3). Detergents, in low concentration at neutral pH, affect strongly the optical absorption spectra (e.g. SDS, 0.033%, Fe^{3+} 413, Fe^{2+} 423, Fe^{2+}·CO 420 nm). Again we find small perturbations of the EPR absorption with no major change of the principal components of the g-tensor (2.428, 2.256, 1.923), but the ability to form P-450(Fe^{2+})·CO (448 nm) is lost. On the other hand, interaction of P-450(Fe^{3+}) with 3,3-dimethyl-2-butanone or metopirone (MP) leads to significant perturbation of the EPR absorption (e.g. MP, 2.471, 2.262, 1.906) accompanied by small effects on the optical absorption; the ability to form the CO-complex with maximum at 448 nm is retained. Examples of these three types of perturbation of the heme group in P-450 are shown. The observations are discussed in terms of the proposed (hypothetical) structure of the heme protein P-450 in its Fe^{3+} and Fe^{2+} forms.

(Supported by Grants NIH-PHS 5R01 AM-04484-15/16 and NSF BMS 74-01099.)

TH-AM-E1 ELECTRON MICROSCOPY AND CIRCULAR DICHROISM OF ETHANOL-DEHYDRATED DNA. D.M. Gray, T.N. Taylor*, and D. Lang, Molecular Biology Program, University of Texas at Dallas, Box 688, Richardson, Tex. 75080

Supertwisted and relaxed forms of DNA from bacteriophage PM2 and plasmid R6K, dehydrated by ethanol, have been analyzed by electron microscopy. The dehydrated DNA is highly condensed and is concluded to be tightly supercoiled, as described earlier with coliphage T7 DNA, except that the circularity of the DNA impairs the formation of second and third order supercoils to a degree that depends on the molecular weight. Much lower degrees of DNA dehydration in aqueous solvents containing varying amounts of salt and ethanol have been studied by taking circular dichroism spectra in the ultraviolet region. At low salt concentration and 70 - 80% ethanol (w/w), the familiar transition from the B to the A conformation occurs for both supertwisted and linear PM2 DNA. However, at high salt concentration (0.2 M) and below ethanol concentrations at which the DNA obviously precipitates, the CD of both DNA forms have reduced long-wavelength positive CD bands. We propose that the dehydration of DNA in the presence of salt produces an increasing number of bends or kinks in the double helix, that their presence reduces the long-wavelength positive CD bands, and that the DNA segments between the bends or kinks remain essentially in the B conformation. (Supported by USPHS grants GM 34964, GM 20851 and GM 19060; by NSF grant GB 31158XI, and by grant AT-503 from the Robert A. Welch Foundation.)

TH-AM-E2 QUANTITATIVE REQUIREMENTS FOR GENOMIC ANALYSIS BY HIGH RESOLUTION THERMAL DENATURATION. Allen T. Ansevin and Douglas L. Vizard. Department of Physics, The University of Texas System Cancer Center, M. D. Anderson Hospital and Tumor Institute, Houston, Texas 77025.

High resolution analysis of DNA denaturation has maximum usefulness as a method for genomic characterization if the area under peaks in first derivative profiles accurately reflects the length of cooperative segments in the DNA. The requirements for such quantitative interpretation include: the use of a wavelength giving identical hyperchromism for A·T and G·C base pairs, thermal increments appropriately finer than the expected breadth of subtransitions (thermalites), near-equilibrium conditions of denaturation, correction for hyperchromic changes in denatured DNA, minimization of distortions introduced by data smoothing, elimination of ambiguities due to thermalite overlap, and a knowledge of the error level in the final profile. Most of these conditions can be met without extreme difficulty.

Data obtained from quantitatively recorded profiles of small viral DNAs indicate that thermalites correspond to roughly gene-sized segments of DNA. In principle, the techniques of restriction enzyme cleavage and thermal denaturation should complement one another in the genomic analysis of larger DNAs, providing more complete information about deletions, additions, or rearrangements, with greater convenience than when either method is applied separately.

TH-AM-E3 THE MELTING OF DNAS WITH PERIODIC BASE PAIR SEQUENCES; EVALUATION OF PARAMETERS GOVERNING DNA STABILITY. A. L. Oliver and R. M. Wartell, School of Physics, Georgia Institute of Technology, Atlanta, Georgia 30332.

The thermally induced helix coil transitions of three AT DNAs (d(A)·d(T), d(AT)·d(AT), d(ATT)·d(AAT) and two GC DNAs (d(G)·d(C), d(GC)·d(GC) were studied. The aim of this work was to evaluate thermodynamic parameters which govern DNA stability and to test the theoretical model employed in the analysis. The parameters evaluated from d(A)·d(T) and d(AT)·d(AT) should be consistent with those evaluated from d(AAT)·d(ATT). All DNA samples employed were high mole. wt. fractions. Sed. velocity runs indicated they were > 4000 base pairs long. Experimental melting data was obtained by measuring the uv absorbance of the DNAs vs. temperature, T. This data was normalized to give the fraction of broken base pairs, θ, and $\partial\theta/\partial T$. The experimental melting curves were analyzed using the modified Ising model (D.M. Crothers, Acc. Chem. Res. 2, 225, 1969, R. M. Wartell and E. W. Montroll, Adv. Chem. Phys. 22, 175, 1972). In 0.003 M Na^+, a loop entropy exponent of k=1.55 provided an excellent fit to the transition curves of d(A)·d(T) and d(AT)·d(AT). The average stacking free energy for d(A)·d(T) was 6.6 kcal./mole. For d(AT)·d(AT) this value was 5.6 kcal./mole. The parameters evaluated from d(ATT)·d(AAT) were similar to, but not identical with those of the simpler AT DNAs. The source of the differences will be discussed. An analysis of the GC DNA polymers, and the influence of salt concentration on the parameters will also be presented.

TH-AM-E4 MELTING AND PREMELTING OF SHEARED AND UNSHEARED CHROMATIN DURING CELL CYCLE. C. Nicolini, P. Miller*, and F. Kendall, Biophysics Division, Temple University Health Sciences Center, Phila., Pa. 19140

Unsheared "native' chromatin was isolated from synchronized HeLa cell populations, 5 hours (G1 phase) and 12 hours (S phase) after selective mitotic detachment (Nicolini, C. et al. 1975, J.B.C., 250, 3381). Thermal denaturation studies were then conducted on this chromatin by simultaneously measuring the optical density at 260 nm. and the circular dichroism signal at 275 nm. (DNA conformational), as a function of temperature starting at 30°C. These experiments were conducted on our modified J-40 spectropolarimeter equipped with HETO circulating bath and PG-UL thermostat. The temperature was monitored with a thermometer (BAT-4, Bailey) combined with a thermocouple (IT-1 Bailey) at the cell jacket exit. During measurements chromatins were suspended in 0.001 M Tris-HCl, pH8. The molar ellipticity dependence with temperature shows the existence of premelting in both chromatins with a later main helix-coil transition occuring at 81°C for S phase native chromatin and beginning at least 7° higher (>88°C) for G1 native chromatin. The "reconstituted" chromatin (prepared by R.S. Gilmour) from the same HeLa cell population showed in both "reconstituted" G1 and S phase chromatin, a substantial decrease in thermal stability. The same effect on decrease of thermal stability and lack of premelting is obtained by shearing "native" unsheared chromatin by sonication at 50 Watts for 30 seconds or more.

TH-AM-E5 FLUORESCENCE THERMAL DENATURATION PROFILES OF RAT LIVER CHROMATIN. T. R. Hopkins, Department of Biochemistry, University of Otago, Dunedin, New Zealand.

Thermally induced conformation changes of tyrosine-containing proteins in native rat liver chromatin were followed by changes in fluorescence ($\lambda_{excit.}$ 280 nm, $\lambda_{emis.}$ 315 nm). As the temperature increased, subtle changes in fluorescence were seen superimposed upon a general decline in fluorescence due to thermal quenching. Derivative plots of the fluorescence versus temperature curve (dF/dT) revealed reproducible fluorescence transitions at 89°, 74°, 62°, and 53° when in a medium containing 3.6 M urea, 5 mM sodium cacodylate (pH 7) and 0.5 mM EDTA and heated at a rate of 0.5°/min. Changes in the denaturation media or the rate of heating altered the temperatures of the fluorescence transitions. The dF/dT profiles were compared with $dA_{260\ nm}/dT$ profiles obtained from the same chromatin preparations. Not all fluorescence thermal transitions occurred at the four thermal transitions observed following hyperchromicity of DNA. The data suggest that major alterations in the conformation of histones may not lead to an immediate destabilization of the DNA duplex.

TH-AM-E6 CHARACTERIZATION OF THE INTERACTION OF LAC REPRESSOR WITH NON-OPERATOR DNA AND INDUCER. A.P. Butler, A. Revzin, and P.H. von Hippel, Institute of Molecular Biology and Department of Chemistry, University of Oregon, Eugene, Oregon 97403.

We have measured the stoichiometry of binding of lac repressor to non-operator DNA and to the inducer isopropyl-β-D-thiogalactoside. A site size of 12-13 base pairs has been determined for repressor binding to native DNA, by monitoring changes in the circular dichroism spectrum of DNA upon the binding of repressor. (These results also imply that a conformational change takes place in the native DNA on repressor binding). A number of lines of evidence indicate that the overall geometry of repressor binding to operator and non-operator DNA is very similar; thus the above findings suggest either that two repressor molecules bind to the lac operator to protect the 26 nucleotide fragment isolated by Gilbert and coworkers [(PNAS 70, 3581 (1973)], or if one repressor binds to operator, that the actual binding site is smaller than previously assumed. The interaction of inducer with repressor has been studied by equilibrium dialysis, fluorescence, and gel-permeation chromatography. The results indicate a general lack of cooperativity between inducer binding sites on the repressor tetramer. We also find that different preparations of repressor show different numbers of "active" inducer binding sites, in agreement with Oshima et al., [(JMB 89, 127 (1974)]. These findings, together with previous results of Laiken et al., [JMB 66, 143 (1972)] are interpreted in terms of two conformational states of repressor subunits: (i) an "active" inducer binding form which binds weakly to operator; and (ii) a tight operator-binding form with low inducer affinity. To further characterize these conformations, we have studied the kinetics of chemical modification of repressor by various reagents in the presence and absence of inducer and DNA. (Supported by USPHS grants.

TH-AM-E7 FLUORESCENCE OF DNA INDUCED BY PROTEIN BINDING. R.M. Santella* and H.J. Li (Intr. by J.H. Wang), Department of Chemistry, Brooklyn College of the City University of New York, Brooklyn, New York 11210 and Division of Cell and Molecular Biology, State University of New York at Buffalo, Buffalo, New York 14214.

Double helical DNA shows no fluorescence at room temperature. A strong fluorescence of DNA is induced with a peak at 300nm and a shoulder at 360nm when the DNA complexed with poly-L-lysine in 2.5 x 10^{-4}M EDTA, pH 8.0, is excited at 250nm. The fluorescence intensity of the complex is proportional to the input ratio r of polylysine to DNA which is the same as the fraction of DNA base pairs bound by polylysine in the complex. Similar fluorescence results were obtained if DNA was complexed with polyarginine and other model proteins except that the relative intensity depends upon the model protein used. Binding of these model proteins to DNA always stabilizes DNA with one or two melting bands at high temperature depending upon the model protein. Trypsin digestion of the model proteins in the complexes results in a reduction of both the high melting bands and fluorescence intensity of DNA. Presumably the tight binding of protein to DNA, which is responsible for the high melting band, is also responsible for the induced fluorescence. Previously fluorescence has never been used as a major tool to study DNA. Results from this report demonstrate potential applications of fluorescence to the investigations of nucleic acids and their complexes with proteins. (Supported by NIH grant GM21481).

TH-AM-E8 INTERACTIONS BETWEEN α-HELICAL PROTEINS AND DNA. M.F. Pinkston* and H.J. Li, Department of Chemistry, Brooklyn College of the City University of New York, Brooklyn, N.Y. 11210 and the Division of Cell and Molecular Biology, State University of New York at Buffalo, Buffalo, New York 14214.

Interactions between DNA and model proteins, poly (L-lysine^{m} L-alanine^{n}), where m + n = 100%, have been investigated using thermal denaturation and circular dichroism (CD). The melting temperature of model protein-bound DNA regions decreases slightly as the alanine content of the model protein is increased. In the free state, these model proteins possess varying amounts of either α-helix, random coil, or a mixture of these two, depending upon the relative lysine/alanine content. When bound to DNA, the CD of the complex shows a substantial increase in α-helical structure for those model proteins with 40-60% alanine, while there is no significant change in α-helical structure when the percent alanine is either substantially higher or lower (i.e. 81% or 19% alanine). Only those complexes formed with model proteins having 40-60% alanine undergo a drastic transition from a B-type CD to an A-type in the presence of intermediate ionic strength (0.2 M NaCl for example). At the other extreme of lysine-alanine ratio, with high lysine content, poly ($Lys^{81}Ala^{19}$) or polylysine, the presence of NaCl produces B→Ψ transition. Structural transition on DNA complexed with proteins depends greatly upon the α-helical content of the protein and ionic strength. (Supported by NIH grant GM-21481)

TH-AM-E9 FLUORESCENT LABELING OF DNA BY COVALENT BINDING OF ACRIFLAVIN. J. W. Levinson*, A. deSostoa*, L. F. Liebes, and J. J. McCormick, Biology Department, Michigan Cancer Foundation, Detroit, Mich. 48201

We have prepared a fluorescent derivative of DNA based on the acriflavin-Feulgen histological procedure for staining DNA. This procedure involved binding acriflavin to DNA in solution by reacting the acriflavin with aldehydes formed on the deoxyribose of DNA by controlled removal of a few percent of the purine bases of the DNA. Controlled depurination performed by modification of standard methods—incubation at 67° and pH 4.5—released 0.7% of the purines per hr of depurination as determined by measuring the number of released purines from ^{3}H purine labeled DNA. Partially depurinated DNA was reacted with the acriflavin reagent and unbound acriflavin was removed by chromatography on Sephadex G-25 eluded with phosphate buffered guanidine HCl. Such single stranded depurinated DNA bound 0.36 acriflavin molecules per purine base per hr of depurination. With this procedure, one acriflavin bound per 200 bases is the highest ratio we could achieve that still allowed the DNA to hybridize to itself at 85% of the value of control DNA. The acriflavin DNA complex showed new absorption maxima at 465 and 380 nm. The fluorescent product had excitation maxima at 304 and 465 nm and an emission maxima at 500 nm. This labeling procedure can be used in place of radioactive labeling for DNA and may be especially useful for *in situ* hybridization studies when coupled with a laser microfluorometer.

Supported by NCI Contract NOI-CP-33226 and an institutional grant from the United Foundation of Greater Detroit.

TH-AM-E10 ON THE DNA-DISTAMYCIN A COMPLEX. Anne K. Krey and Patrick E. Lorenz‡ Department of Molecular Biology, Walter Reed Army Institute of Research, Washington, DC 20012.

The antibiotic distamycin A (DMC) interacts preferentially with A-T rich DNAs (Zimmer et al., J. Mol. Biol. 58, 329, 1971) but the nature of DMC's binding including parameter(s) for its attachment to DNA has remained difficult to be determined. - Orientation in an electric field of complexes of DMC with calf thymus DNA and with poly d(A-T) yielded a high degree of order of the bound antibiotic and an average inclination of the transition moment of the N-methylpyrrole chromophores of DMC of ∿ 39° relative to the helical axis, assuming a perpendicular base pair orientation in solution for the B-form of DNA. In contrast, electric dichroism of DMC's complex with poly dG·dC, a duplex which prefers the DNA A-form with a 20° tilt of base pairs, suggested a lesser degree of order of bound antibiotic with a 57° orientation of the transition moment of DMC. Titration with calf thymus DNA, monitored spectrophotometrically, indicated > 1 form of bound distamycin; such titration, monitored by electric dichroism, yielded a stoichiometry of 1 antibiotic molecule bound per ∿ 7 base pairs, presumably of A-T rich regions of DNA. A similar stoichiometry is suggested by effects of oligomers on DMC's absorption spectrum: an equimolar mixture of decadeoxyadenylic and decadeoxythymidylic acid produced almost the entire bathochromic shift observed with DNA while either oligomer alone or a mixture of corresponding tetramers failed to significantly alter the absorption of distamycin A. These results agree with a differential interaction of DMC with polydeoxynucleotides according to base composition (Krey et al., FEBS Letters 29, 58, 1973) and we suggest for the binding to DNA a preference, with the above 1:7 stoichiometry, of DMC for regions on which an abundance of A-T pairs imposes the B-form and a 2nd mode of attachment to regions of different conformation (A-form), imposed by G.

TH-AM-E11 QUATERNARY STRUCTURAL ORDERING OF DNA WITHIN EUTHERIAN SPERM NUCLEI. T.E. Wagner and M. L. Sipski, Intr. by J. Langdon Taylor, Jr., Ohio University, Chemistry Dept., Athens, Ohio 45701.

The ordering of DNA molecules in chromosomal fibers of sperm nuclei and the mechanism of their release have been studied. The nucleus of the eutherian spermatozoon is exceptionally resistant to disruption. Laser Raman spectroscopy was utilized to monitor the disulfide → sulfhydryl transition at various stages of decondensation. This process was found to require no other agents in addition to a disulfide reductant. Highly native chromosomal fibers have thus been isolated from the sperm cells of several mammalian species. In the gel state this chromosomal material displays a large anomalous circular dichroism. Clearly, the ψ DNA-like circular dichroism of this chromosomal preparation, which in no way resembles the circular dichroism of purified DNA, arises from the long range ordering of the DNA molecules. The results of linear dichroism and reflectance spectroscopy have been utilized to determine the major geometric parameters of the DNA ordering in these chromosomes. These parameters have, in turn, been used with a simple theoretical development to calculate the circular dichroism of a model of the sperm chromosome. The calculated spectra are compared to the observed circular dichroism of equine sperm chromosomes. In soluble form the same chromosomal preparation exhibits the circular dichroism characteristic of somatic cell chromatin. A model of short- and long-range ordering of the DNA will be discussed.

TH-AM-E12 THE CHROMATIN-LIKE STRUCTURE OF THE ADENOVIRUS CHROMOSOME. Jeff Corden*, Mark Engelking*, and George Pearson. Department of Biochemistry & Biophysics, Oregon State University, Corvallis, Oregon 97331

We have used staphylococcal nuclease to probe the structure of the nucleoprotein core of the adenovirus particle. This nuclease digests 55% of the DNA in disrupted virus particles. The protected DNA is recovered as a series of fragments which are integral multiples of a 200 bp unit. This pattern does not appear when DNA alone is digested. Since virus cores do not contain cellular histones, the regular binding of basic core polypeptides must protect discrete regions of DNA from nuclease attack. We estimate that the 23 x 10^6 dalton DNA molecule is divided into 180 units of roughly 200 bp. The major core protein, polypeptide VII, is present in 1070 copies per virion or 6 copies per repeat unit. An assembly of 6 polypeptides corresponds to a molecular weight of 111,000. By comparison, the complex of 8 histones in the chromatin subunit has a molecular weight of 108,000. Polypeptide V, the minor core protein, has a molecular weight of 48,500 and, remarkably, is present in 180 copies per virion or a single copy per unit. It does not bind to DNA as tightly as polypeptide VII and may cross-link neighboring units as postulated for histone f1 in chromatin. Circular dichroism measurements on adenovirus cores reveal a chromatin-like spectrum in the region of 260-300nm. Since this region represents contributions almost exculsively from DNA, we conclude that the core proteins alter the DNA conformation in a way similar to that of histones. [Supported by the American Cancer Society (NP-67A and B), the National Cancer Institute (CA 17699-01), and the National Science Foundation (BMS73-06819 A02)].

TH-AM-F1 CONFORMATIONAL STUDIES ON ANGIOTENSIN-II AND ANGIOTENSIN-II ANALOGS IN AQUEOUS SOLUTION - A CARBON-13 NMR STUDY. R. Deslauriers*, G.C. Levy‡*, R. Komoroski‡*, A.C.M. Paiva†* and I.C.P. Smith, Div. of Biol. Sci., National Research Council, Ottawa, Canada K1A 0R6 and ‡Dept. of Chem., Florida State University, Tallahassee, Fla. 32306 and †Escola Paulista de Medicina, 04023 São Paulo, Brazil

^{13}C NMR is used to study the conformational flexibility of the peptide hormone [Ile^5]-angiotensin-II (Asp-Arg-Val-Tyr-Ile-His-Pro-Phe) and two analogs in aqueous solution. Angiotensin-II demonstrates a compact, folded conformation as monitored by the ^{13}C spin-lattice relaxation times (T_1) of the individual residues. The N- and C-terminal residues show a greater flexibility than do the remaining residues. In particular the phenylalanyl residue shows greater flexibility in the side-chain than does the central tyrosyl residue. Introduction of two bulky prolyl residues in [Pro^3, Pro^5]-angiotensin-II is associated with increased freedom of the terminal residues when compared with the central residues. The ^{13}C chemical shifts of this peptide indicate conformational heterogeneity - 15% *cis* isomer was detected about each of the Arg-Pro, Tyr-Pro and His-Pro C-N bonds. No *cis* isomer was detected in [Ile^5]-angiotensin-II. The mobility of each amino acid in angiotensin-II is a function of the nature of the side-chain as well as the location of the residue. This is shown by [Phe^4, Tyr^8]-angiotensin-II in which the terminal tyrosyl residue is less mobile than the phenylalanyl residue in angiotensin-II, and the phenylalanyl residue is as restricted as the tyrosyl residue in position 4 of angiotensin-II.

TH-AM-F2 EFFECT OF SALTS ON THE HIGH RESOLUTION NMR PROPERTIES OF POLY-(HYDROXYETHYLGLUTAMINE). H. J. Lader,* R. A. Komoroski, C. C. Wu,* L. Mandelkern, Dept. of Chemistry, Florida State University, Tallahassee, Fla. 32306, and W. L. Mattice, Dept. of Biochemistry, Louisiana State University, Baton Rouge, La. 70803.

Certain classes of salts are known to disrupt the ordered structure of polypeptides and proteins. In aqueous salt solutions of poly-L-proline, new ^1H and ^{13}C NMR resonances, which are attributed to the presence of cis residues, are observed. Aqueous salt solutions of poly(N^5-ω-hydroxyethyl-L-glutamine) (PHEG) exhibit hydrodynamic and circular dichroic properties similar to that of poly-L-proline. However, no additional ^1H or ^{13}C NMR resonances are found for PHEG. The ^{13}C chemical shift change observed for the backbone carbonyl upon addition of $CaCl_2$ to aqueous PHEG is approximately twice that of the side chain carbonyl. These chemical shift changes do not correlate with the corresponding changes in the CD spectrum. Similar ^{13}C chemical shift changes are observed for the model compounds cyclo-(L-Ala)$_2$, N-methyl acetamide, and N,N-dimethyl acetamide. The shifts observed with other salts and other carbon atoms will be presented. Possible explanations of the results will be discussed.

TH-AM-F3 PROTEINS AT HIGH PRESSURES: STUDY BY FLUORESCENCE METHODS. T.M. Li*, J.W. Hook, III*, H.G. Drickamer*, and G. Weber, Departments of Biochemistry and Chemistry, University of Illinois, Urbana, Illinois 61801.

The reversible denaturation of single-chain, globular proteins subjected to pressures in the 1-10 kbar range may be conveniently followed by the changes in fluorescence yield and fluorescence spectrum of the tryptophan residues of the protein. In chymotrypsinogen, the fluorescence yield at high pressure decreases to 55% of the original and virtually all the change takes place in the region of 4 to 7.5 kbars, with midpoint at 5.8 kbars. The maximum of the fluorescence spectrum shifts reversibly from 334 nm (native protein) to 349 nm (at 8 kbars), consistent with the change to a more polar environment upon denaturation. Qualitatively similar results were observed when the riboflavin binding protein (RBP) from hen's egg white was subjected to pressure. The equilibrium of the latter with flavin mononucleotide (FMN) was also followed since the flavin fluorescence is quenched in the complex. A release of the flavin with increase in fluorescence takes place in the denaturation region and the equilibrium of ligand and protein may be poised to obtain a twenty-seven fold enhancement of fluorescence in the critical region. The values of transition midpoint pressure and volume change calculated for the denaturation reaction by FMN fluorescence observations agree well with those calculated from the intrinsic protein fluorescence of the protein. Fluorescence observations at high pressure, on either protein-bound ligands or tryptophan residues of protein, should permit the measurements of the thermodynamic quantities with greater ease and precision than that achieved by absorption spectrophotometry. Moreover, the recognized sensitivity of the emission to the environment, as compared to absorption, should allow a more precise analysis of the stages of the denaturation transition, and of ligand-protein interactions.

TH-AM-F4 VOLUME EFFECTS PRODUCED BY METAL ION:GLOBULAR PROTEIN INTERACTION. S. Katz, and L.C. Roberson* Biochemistry Department, West Virginia University School of Medicine, Morgantown, West Virginia 26506

The primary structure of the protein determines its spatial organization and its ultimate properties; however, the molecular environment, e.g., metal ions, can alter conformation and thus function. For example, metal cations can serve as cofactors, activators and inhibitors of enzymes. The thermodynamics, kinetics and conformational changes produced by protein-ion interaction have been studied extensively but there is no information relevant to volume changes, ΔV, resulting from protein-ion association. Recently, values for the ΔV produced by Cu(II) forming 1:1 coordination compounds with mono-, dicarboxylic acids and with ligand incorporating N-donor atoms (Katz, Donovan and Roberson; J. Phys. Chem., 79, 130, 1975) have been published. This provides a limited frame of reference for estimating the volume effects originating from cation-protein ligand combination. To elucidate the mechanism of specific ion-specific protein interaction a knowledge of the volume effects produced by metal cations reacting with non-specific globular proteins is required. This study deals with the ΔV originating from the addition of 13 cations to four globular proteins. In contrast to the results of anion binding studies, only positive volume effects were observed for these systems. The magnitude of ΔV is determined primarily by the nature of the cation and to a lesser extent by the protein. The values for ΔV varied by two orders of magnitude as function of the ion. Conformational changes and salting-out are parameters which exhibit a large degree of dependency on the nature of the proteins. The volume effects are resolved in terms of the contributions of cation-ligand association, peptide hydrogen displacement and conformational changes. Research supported in part by NIH grant No. HL 12955.

TH-AM-F5 A METHOD OF PHASE DETERMINATION IN OPTICAL TRANSFORMS AND ITS APPLICATION TO THE STRUCTURE OF BACTERIA FLAGELLA. E.H. Thall* and R.S. Morgan, Department of Biochemistry and Biophysics, The Pennsylvania State University, University Park, PA 16802

Optical diffraction is a powerful technique in the analysis of periodicities in electron micrographs. Until recently, however, the utility of this tool has been limited by the difficulty of obtaining phase information. We overcome this problem by a modification of Young's two-slit experiment in which a shift in the fringe pattern is used to calculate the phase relationship. We determine the optical center of our patterns by superimposing a set of coarse fringes produced from two pinholes in the central maximum of the optical transform upon the fine fringes produced by any two maxima of interest. Using these methods, the phase of the first layer line in the diffraction pattern from an electron micrograph of a flagellum from a mutant strain of multi-flagellated Bacilli has been determined. We have found that this line must be caused by a Bessel function of odd order. Our method has the advantages of being much less costly than microdensitometry and more accurate than previous optical methods.

TH-AM-F6 "SALTING-OUT" OF TOBACCO MOSAIC VIRUS BY SERUM ALBUMIN. Max A. Lauffer, Department of Biophysics and Microbiology, University of Pittsburgh, Pittsburgh, Pa. 15260.

The author discovered in 1947 that, while tobacco mosaic virus, TMV, and bovine serum albumin, BSA, form mutual precipitates at low ionic strengths at pH values between the isoelectric points of the two, BSA precipitates TMV at high ionic strengths at pH values above or below both isoelectric points. Dudman apparently rediscovered the precipitating action of BSA and other hydrophyllic macromolecules on TMV and explained it in terms of a variant of excluded volume theory. Current experiments show that, at constant ionic strength, the logarithm of the solubility of TMV decreases linearly as the BSA concentration is increased. This result is analogous to that obtained when proteins are salted-out by simple electrolytes. The amount of BSA required to precipitate TMV depends strongly and inversely on the ionic strength of simple electrolytes. Furthermore, at ionic strength 0.2, the amount of BSA required to precipitate TMV is a minimum near pH 5.5; 50% more is required at pH 5 and 100% more at pH 7. The total positive and negative charge from hydrogen ion binding of BSA is at a maximum near pH 5.5. These findings are contrary to the predictions of excluded volume theory and consistent with salting-out theory. Whatever the explanation, the findings demonstrate that the thermodynamic properties of a protein in solution can be strongly dependent upon the concentration of other proteins present.

TH-AM-F7 HYDROGEN ION BINDING DURING EARLY STAGE POLYMERIZATION OF TOBACCO MOSAIC VIRUS PROTEIN. Ragaa A. Shalaby and Max A. Lauffer, Department of Biophysics and Microbiology, University of Pittsburgh, Pittsburgh, Pa. 15260.

TMVP forms a variety of aggregates on changing pH, ionic strength, temperature and protein concentration. In going from a trimer at pH 7.5 to a helical rod at pH 5.8, the protein is known to bind two protons per monomeric subunit. A study was carried out to attempt to correlate proton binding with the different intermediates formed during this process. Titrations of TMVP from pH 8 to pH 5.2 and back again to pH 8 were performed. The pH readings were taken 20-30 minutes after addition of titrant. This process was undertaken at four different temperatures: 4, 10, 15 and 20°C. Sedimentation velocity was used to study the different aggregation products at these same temperatures and at pH values of 6.05, 6.19, 6.42 and 6.56. Several findings merit consideration.

1. The titration is completely reversible.
2. The results confirmed that two hydrogen ions are bound per protein monomer when material at pH 7.5 is polymerized by reducing the pH to 5.8.
3. At pH 6.05 and 6.19, a substantial fraction of the hydrogen ion is bound at 4° before there is any appreciable polymerization.
4. At pH values where the protein is in the polymerized state at all temperatures studied (below pH 5.8), there is a systematic decrease in the amount of H ion bound on increasing the temperature. This finding can be explained in terms of the enthalpy of dissociation of carboxyl groups.

TH-AM-F8 THE EFFECT OF pH ON THE TRIMERIZATION AND DISC FORMATION OF TOBACCO MOSAIC VIRUS PROTEIN. Charles L. Stevens and Sanda Loga*. Department of Biophysics and Microbiology, University of Pittsburgh, Pittsburgh, Pa. 15260.

The polymerization of TMVP involves a sequence of reactions beginning with the monomer (17,500 MW) and ending with the virus-like rod. For instance, the first reaction is a trimerization. Fortunately, using equilibrium sedimentation measurements, some of these reactions can be observed without interference from others. We have found that over the pH range of 6 to 8, the apparent monomer-trimer equilibrium is virtually independent of pH. This means that fewer than about 1/4 H^+ are bound per trimer. Thus, H^+ binding accompanying overall polymerization occurs at a stage subsequent to trimerization. It is likely that, in velocity sedimentation measurements, material sedimenting at about 4s represents largely trimer with perhaps small amounts of monomer or small aggregates of trimer. Similarly the 20s boundary arises from aggregates of about 34 subunits, the "disc" or "lock-washer". Maintaining temperature constant (8°) we have found a set of values for pH and protein concentration such that about 90% of the protein is present as 4s material and about 10% as 20s material. For 0.1 ionic strength phosphate buffer with pH values of 6.8, 6.7, 6.6 and 6.5, concentration values are 5, 4, 3, and 2 mg/ml respectively. Assuming the above identification of sedimentation boundaries with molecular species, this indicates that about 1.5 H^+ per trimer are bound upon disc formation under these conditions. If assembled discs can bind more H^+ without further aggregation, this method probably would not detect it.

TH-AM-F9 METASTABILITY OF THE DISK AGGREGATE OF TMV PROTEIN. S. J. Shire, J. S. Steckert*, and T. M. Schuster, Biological Sciences Group, University of Connecticut, Storrs, Connecticut 06268

TMV protein at true equilibrium at 20°, pH 6.5, μ=0.1M is composed of short helical rods with sedimentation coefficient >30S (~85%) and small amounts of 20S (~10%) and 4S (~5%) material (Durham and Klug, Nature New Biology 229, 42 (1971)). At 5° under the same conditions all the protein exists as the 4S species. We have found that cooling a sample previously equilibrated at 20° (~12 hours) to 6° yields equal weight fractions of 4S and 20S material but no >30S species. Moreover, the depolymerization of the 20S disk aggregate to the 4S species is slow with a half life of about 11 days. The most likely interpretation of this is that the >30S short helical rods rapidly depolymerize down to a two turn metastable cylindrical disk species. This metastability of the disk species should prove highly useful in studies of the kinetics of recombination of TMV protein with TMV RNA. Previous experiments have been performed under conditions where the disk and A protein species are rapidly equilibrating and hence make difficult an accurate assessment of which species is preferentially incorporated during the propagation of the pre-nucleated rod. We are presently studying the reconstitution kinetics under the conditions of disk metastability where the A protein and the disk species equilibrium is not a rapidly equilibrating system.

Supported by NIH Grant No. AI-11573

TH-AM-F10 CONCENTRATION DEPENDENT HYDROGEN EXCHANGE KINETICS OF THE S-PEPTIDE IN RNASE S: A NEW METHOD FOR MEASURING VERY SMALL DISSOCIATION CONSTANTS. A. A. Schreier*, and R. L. Baldwin, Biochemistry Department, Stanford University School of Medicine, Stanford, Ca. 94305

The hydrogen exchange (HX) kinetics of the S-peptide in RNase S can be measured by first tritiating the S-peptide in the absence of S-protein and then allowing the S-peptide to recombine rapidly with the S-protein to form RNase S. The HX kinetics are concentration dependent owing to the dissociable nature of RNase S. The S-peptide exchanges at its rapid chemical HX rate during the small fraction of time it is dissociated from the RNase S. A simple theory for this concentration dependence can be used to measure the very small dissociation constant (K_D) of the S-peptide in RNase S. K_D values of 10^{-6} to 2×10^{-10}M are measured at 0°C in the pH range 3 to 7, respectively. Concentration dependent HX methods may be a general way to measure very small dissociation constants. Concentration independent breathing equilibria of the S-peptide in RNase S are also measured by HX kinetics. The apparent equilibrium constant for the breathing reaction decreases with pH in a manner parallel to K_D. The simplest interpretation is that this breathing reaction arises from an intermediate in the dissociation process. About five highly protected protons exchange in the breathing reaction, which may involve disruption of the H-bonded α helix formed by residues 7 - 13.

TH-AM-F11 CONFORMATION OF THE PARAMYOSIN MOLECULE AND STRUCTURE OF ITS SMALL AGGREGATES IN LOW IONIC STRENGTH SOLUTION. S. Krause and D. E. DeLaney, Department of Chemistry, Rensselaer Polytechnic Institute, Troy, N.Y. 12181

The data from transient electric birefringence measurements have been used to formulate the following hypotheses about the native form of the paramyosin molecule in solutions of 1 mM ionic strength: 1. At pH 3.2, the molecules have rigid rod conformations but, as the pH increases to 3.8, about 5% of the molecule, at one or both ends, becomes flexible. Possible mechanisms for this change in conformation will be discussed. 2. Between pH 7.4 and 9.6, small aggregates exist in solution; these small aggregates cannot possibly involve end-to-end aggregation of the molecules, but must involve 400-600 Å of overlap in side-to-side aggregation. If one uses an overlap distance of 530 Å [Cohen et al., J. Mol. Biol. 56, 223 (1971)], the observed aggregates are dimers and higher side-to-side aggregates, probably up to heptamers. These aggregates appear to be in equilibrium with monomer in this whole pH range.

TH-AM-F12 EVIDENCE FOR SUBCLASSES OF HUMAN SERUM HIGH DENSITY LIPOPROTEINS BASED ON RATIOS OF CONSTITUENT APOPROTEINS AI AND AII. D. Anderson, T. Forte, A. Nichols, and F. Lindgren (Intr. by J. Forte), Donner Laboratory, University of California, Berkeley, CA. 94720.

The bimodal distribution of flotation coefficients ($F_{1.20}$) observed for human serum high density lipoproteins (HDL) is generally considered to represent the two major lipoprotein subclasses HDL_2 and HDL_3 on the basis on their flotation rates: 3.5-9 and 0-3.5 (-svedbergs), and their hydrated densities: 1.095 and 1.14 g/ml. We have found the wt:wt ratio of apoproteins AI to AII to provide a third important parameter for subclass definition. By subjecting the HDL to equilibrium density gradient ultracentrifugation a fractionation of the total HDL into fifteen subfractions was achieved. Detailed analysis of these subfractions for flotation rate by analytic ultracentrifugation and for size by electron microscopy suggested the presence of three identifiable subclasses in HDL from two non-fasting females. $F_{1.20}$ decreased from 5.6-5.1 for subclass I (banding position on the gradient 1.09-1.10 g/ml) to 4.5-3.2 for subclass II (banding position 1.105-1.115 g/ml) to 3.1-1.4 for subclass III (banding position 1.118-1.145 g/ml). Both the flotation rates and the peak areas and shapes of the schlieren patterns remained essentially the same upon two subsequent reflotations of each subclass in d 1.21 NaBr solutions. Electron microscopy revealed extensive hexagonal packing of particles in I and II and diameter ranges of 105-125 Å for I, 90-115 Å for II, and 75-100 Å for III. A computer monitored scanning densitometer was used to calibrate and to analyse stained polyacrylamide electrophoresis gels for determination of AI:AII wt:wt ratios. The three major subclasses suggested above were clearly distinguished from one another on a molecular basis by their AI:AII ratios as follows: Subclass I: 3.14 ± 0.29, subclass II: 2.23 ± 0.25, and subclass III: 1.75 ± 0.17. These data are consistent with the presence of at least 3 stable subclasses instead of 2 (HDL_2 and HDL_3) in the parent HDL distribution.

TH-AM-F13FORMATION OF A STABLE COMPLEX BETWEEN PROTEIN-POLYSACCARIDE AND HYALURONIC ACID IN THE ABSENCE OF A "LINK" PROTEIN. D.A. Swann, S. Powell, J. B. Broadhurst, and M. Sordillo, Shriners Burns Institute and Harvard Medical School, Boston, Mass., 02114.

It was reported previously (Fed. Proc 34, 564, 1975) that pronase digestion of hyaluronic acid (HA) destroyed the ability of HA to form a complex with cartilage disassociated protein-polysaccaride(s) (DPP). The results suggested that this effect was caused by proteolysis of the aggregating protein associated with the HA. Further studies, however, have shown that when the proteins associated with HA are removed by repeated fractionation in a cesium chloride density gradient the purified HA retains the ability to form a stable complex with DPP as judged by an increase in specific viscosity and the presence of a fast-sedimenting component when analyzed in the analytical ultracentrifuge. Purified HA's always contain a small amount of residual peptide which is different from the aggregating protein removed by density gradient fractionation procedures and this residual peptide material is partially cleaved by pronase treatment. The data suggest that the presence of "Link" protein is not an absolute requirement for the formation of a stable complex between HA and DPP and that the interaction between these substances may involve the residual peptide that remains associated with purified HA's.
(Supported by Grant No.'s AM 15216 and EY-01030 and research funds from the Shriners Burn Institute).

TH-AM-F14 BLOOD PLASMA 180-280 nm ABSORBANCE IN HEALTH AND DISEASE. Germille Colmano, Dept. Vet. Sci., VPI & SU, Blacksburg, VA 24061

On the basis of a 5.72×10^4 molar absorption coefficient for the 280 nm absorbance of protein, with an average molecular weight of 81,500 daltons, from a pooled sample of rat blood plasma, with an average 41.5 mg of protein per milliliter, the 200 nm chromophore had a 7.76×10^6 molar absorption coefficient. From available information on the 200 nm band, the peak is due to a dipeptide bond chromophore, subscribing the concentration of polypeptides in blood plasma. There are obvious clinical implications in a simple practical correlation of the band at 200 nm, indicating the level of dipeptide bonds and consequent protein synthesis, and the band at 280 nm delineating the catabolic breakdown, corresponding to the actual content of aromatic aminoacids (balance of tryptophane and tyrosine) describing the concentration of the total protein in blood plasma. The 200/280 nm correlation could clarify the occurrence of shifts in the homeostatic mechanism controlled by the circulatory system, and would contribute to early clinicopathological detection of some dysproteinemias. So far blood plasma samples from rat, chicken and quail, pig and horse, and also human subjects have shown definite differences between healthy and diseased individuals.

TH-AM-G1 RESONANCE RAMAN SPECTRA OF MANGANESE (III) ETIOPORPHYRIN I. J. A. Shelnutt*, D. C. O'Shea*, School of Physics and R. H. Felton,* N. T. Yu, School of Chemistry, Georgia Institute of Technology, Atlanta, Ga. 30332

Resonance Raman spectra of manganese (III) etioporphyrin I complexes have been obtained with laser excitation in the regions of the Bands III and IV, and Bands V and V_a of the atypical visible absorption spectra of these metalloporphyrins. Excitation profiles in the latter region are interpreted as indicating non-adiabatic coupling between V and V_a as well as vibronic activity of some totally symmetric modes. The Raman data support assignment of Bands III and IV to the 0-0 and 0-1 components of the Q band. Although Bands V and V_a are assigned to a charge transfer transition mixed with the main $\pi \rightarrow \pi^*$ transition, no selective enhancement of low frequency metal-ligand vibrations attributable to the charge transfer contribution of Band V was observed. The Mn (III) porphyrins should be useful as model systems in biological porphyrin studies.

TH-AM-G2THE STORAGE OF LIGHT ENERGY IN THE BATHOPRODUCT OF RHODOPSIN. Barry Honig and Thomas G. Ebrey (Intr. by P. Schmidt), The Hebrew University, Jerusalem, Israel, and University of Illinois, Urbana, Illinois 61801.

The primary photoproduct of rhodopsin is bathorhodopsin (prelumirhodopsin). The action of light appears to be to isomerize the chromophore from the 11-cis to an all-trans configuration. We will show by a simple argument that bathorhodopsin has 15-45 kcal/mol. more free energy than rhodopsin, and that light energy is the source of this "stored" free energy. Batho decays spontaneously (without energy input) through the other intermediates of rhodopsin until the chromophore, as all-trans retinal, becomes detached from the apoprotein opsin. Only one step in this decay sequence, meta I $\rightleftarrows$ meta II has so far been shown to be reversible, suggesting fairly substantial free-energy differences between most of the intermediates. We place a lower limit of 5 kcal/mol. on the sum of the differences, and an upper limit of 30 kcal/mol. (see below). The difference in free energy between all-trans retinal and 11-cis retinal is small, so that the observation that the latter combines with opsin to form rhodopsin with an equilibrium constant of greater than 10^7 (Kropf et al., Exptl. Eye Res. 17, 5a1 (1973) requires that rhodopsin have at least 11 kcal/mol. less free energy than all-trans retinal + opsin. Bathorhodopsin must attain its high energy state (at least 16 kcal/mol. more free energy than rhodopsin) by utilizing the energy of the photon rhodopsin absorbs, which is on the order of 45 kcal/mol. We do not know how the bathoproduct "stores" this energy but it clearly must be through the relationship between the chromophore and opsin. Two simple models of the chromophore-protein interaction in the bathostate which are capable of storing energy as a consequence of cis-trans isomerization and are consistent with the spectroscopic properties of bathorhodopsin will be discussed.

TH-AM-G3 MOLECULAR FLOW RESONANCE RAMAN STUDIES OF RETINALS AND RHODOPSIN*. A. Doukas and R.H. Callender, Physics Dept., City College of N.Y., N.Y.,N.Y. 10031.

We have developed a technique which allows resonance Raman measurements of any photolabile system and have applied it to obtain resonance enhanced spectra arising solely from pure isomeric forms of retinal solutions (all-trans, 11-cis, 9-cis, and 13-cis) and from bovine rhodopsin near physiological temperatures (17°C). The technique involves imposing a molecular velocity transverse to the Raman exciting laser beam sufficient to insure that any given molecule moves through the beam so that it has little probability of absorbing a photon. The rhodopsin spectrum is quite different from that previously published by Lewis et al. (J. Raman Spect. 1 (1973), 465). The data show that each isomer has a distinct and characteristic Raman spectra and that the spectrum of 11-cis-retinal is quite similar but not identical to that of rhodopsin and similarly for 9-cis -retinal compared to isorhodopsin. In agreement with previous work, the Raman data demonstrate that retinal and opsin are joined by a protonated Schiff base linkage. The data suggest that due to the observation of Raman bands near 998 and 1018 cm^{-1} in the spectra of 11-cis retinal solution and rhodopsin, a spectral region previously assigned to C-Me stretching motions, 11-cis retinal in solution is composed of a mixture of 12-s-trans and 12-s-cis comformers and that the conformation of rhodopsin is (perhaps distorted) 12-s-trans.

*Supported by C.U.N.Y. Faculty Award Program, Research Corporation, and N.S.F.

TH-AM-G4 RAPID FLOW RESONANCE RAMAN SPECTROSCOPY OF PHOTOLABILE MOLECULES: RHODOPSIN AND ISORHODOPSIN. R. Mathies, A. Oseroff and L. Stryer, Department of Molecular Biophysics and Biochemistry, Yale University, New Haven, Connecticut 06520.

Resonance Raman spectroscopy can provide detailed information about the conformation of retinal in rhodopsin during the initial stages of visual excitation. However, there is a problem in obtaining the spectrum of a photosensitive molecule. In a typical experiment, all of the rhodopsin in the illuminated volume will be photolyzed within a few milliseconds. We have devised a method for obtaining the resonance Raman spectrum of a photolabile molecule before it is modified by light. The essence of this technique is that the sample is flowed through the light beam at a sufficiently high velocity so that the fraction of photoisomerized (or photodestroyed) molecules in the illuminated volume is very low. This rapid-flow technique has enabled us to measure the resonance Raman spectrum of unphotolyzed bovine rhodopsin in Ammonyx LO detergent solution and in sonicated retinal disc membranes. The major features of these spectra, which are very similar to one another, are the protonated Schiff base line near 1660 cm^{-1}, the ethylenic line at 1545 cm^{-1}, lines due to skeletal modes at 1216, 1240, and 1270 cm^{-1}, and a line due to C-H bending at 971 cm^{-1}. Our rapid-flow spectrum of rhodopsin bears little resemblance to the one reported by Lewis et al. (J. Raman Spect. 1, 465 (1973)) for a stationary sample. The resonance Raman spectrum of unphotolyzed isorhodopsin was also measured and was found to be markedly different from that of rhodopsin; the ethylenic line is shifted to 1550 cm^{-1} and there are six lines between 1153 and 1218 cm^{-1}. Our rapid flow technique makes it feasible to control the extent of interaction between light and any photolabile molecule.

TH-AM-G5 THE OBSERVATION OF RADIATIVE EMISSION FROM A RHODOPSIN. A. Lewis, J.P. Spoonhower* and G.J. Perreault*, School of Applied and Engineering Physics, Cornell Univ., Ithaca, NY

Radiative emission has never been observed from the retinylidene chromophore of any rhodopsin. In addition vibronic structure has not been detected in the absorption spectrum of the chromophore of rhodopsin or, for that matter, in any isomer of retinal. These are some of the principal reasons why little is known about the electronic structure of the retinylidene chromophore of rhodopsin. We would like to report the first observation of radiative emission attributable to the chromophore of a rhodopsin. An emission spectrum has been observed in the near infrared at 12,000cm^{-1} from the retinylidene chromophore of bacteriorhodopsin. A lower bound for the quantum efficiency at room temperature is $(1.1\pm0.9)\times10^{-7}$. The absorption and emission spectra show little overlap and a Stokes shift of ~5000cm^{-1} is observed. The degree of polarization of the room temperature emission is 0.47±0.2. Vibronic structure can be detected in the emission spectra recorded at 77°K and 18°K. The relative intensities of the vibronic components remain constant with excitation wavelength. The emission spectra were recorded on a tunable laser Raman spectrometer designed for visual pigment spectroscopy.[1] A two laser beam technique was used to help assign the emission to either bacteriorhodopsin or to one of its thermal intermediates. Our results indicate that the emission can be attributed to bacteriorhodopsin, is not quenched by O_2 and the lifetime is <10ps. Furthermore, the batho intermediate does not appear to emit light at least in the region where our instrument is sensitive. This suggests that the interaction of a photon with bacteriorhodopsin results in a batho intermediate in which radiative emission may be quenched.

[1]Lewis et al., J. Raman Spectrosc. 1, 465 (1973); PNAS 71, 4462 (1974); in Spectroscopy in Biology and Chemistry, ed. S. Chen and S. Yip (Acad. Press, New York, 1974), p. 347.

TH-AM-G6 FLUORESCENCE FROM THE CHROMOPHORE OF THE PURPLE MEMBRANE PROTEIN OF H. HALOBIUM. T. Ebrey, R. Govindjee*, and B. Becher, Department of Physiology and Biophysics, University of Illinois, Urbana, Illinois 61801; and R. Alfano* and W. Yu*, Department of Physics, City College of the City University of New York, New York, N.Y. 10031

We have recently observed fluorescence from the retinal chromophore of the purple membrane protein of H. halobium. The purple membrane protein has two relatively stable, but interconvertible forms--the dark-adapted, λ_{max}=558 nm and the light-adapted, λ_{max}=568 nm. At room temperature the emission from the light-adapted form consists of a rather broad band at c. 700 nm and has a quantum yield of c. 0.5%. Upon cooling to 77°K, the yield increases considerably, the corrected emission spectrum now shows a triple-peaked structure centered on 710 nm, and the corrected excitation spectrum is close to the absorption spectrum λ_{max} at 77°K (c. 585 nm). The emission spectrum of the dark-adapted form is similar to that of the light-adapted form but distinct differences are seen, and its excitation spectrum is shifted c. 10 nm to shorter wavelengths. The natural fluorescence lifetime, calculated from the main long wavelength absorption band is c. 7 nsec, so the predicted room temperature fluorescence lifetime is c. 30 psec. Direct measurements of the lifetime using psec laser pulses indicate that the lifetime is at least this short. This suggests that for the protonated Schiff base retinal chromophore of the purple membrane protein, the emission is probably from the main absorbing state (^1B_u) and is not from a forbidden transition such as the $^1Ag^- \rightarrow {}^1Ag^+$. This transition has been proposed by Hudson and Kohler [Ann. Rev. Phys. Chem., 1974] as being the source of the emission in other polyene-like molecules.

TH-AM-G7 EVIDENCE FOR CHROMOPHORE-CHROMOPHORE (EXCITON) INTERACTION IN THE PURPLE MEMBRANE OF HALOBACTERIUM HALOBIUM. B. Becher and T.G. Ebrey, Department of Physiology and Biophysics, University of Illinois, Urbana, Illinois 61801.

The visible circular dichroic spectrum (CD) of the purple membrane (PM) of H. halobium includes intense positive and negative bands with cross-over near the wavelength of the absorption maximum. This spectra could result from exciton interaction of the retinal chromophores (Becher and Cassim, Biophys. Soc. Abstr., 1975) which may be close to each other since the protein is found in clusters of three in purple membrane [Henderson and Unwin, Nature 257, 28 (1975)]. Alternatively, the CD spectrum could be due to a combination of positive and negative CD bands arising from both allowed and forbidden electronic transitions as described by Hudson (Amer. Soc. Photobiol. Abstr., 1975) for a conjugated polyene. We report here results that exclude this second possibility and show that the CD spectrum has two contributions: a positive band due to retinal bound to the protein, and positive and negative bands due to the interaction of the chromophores from different proteins. Bleached PM was regenerated by successive additions of retinal. The shape of the CD spectrum was dependent on the percent of the retinal binding sites occupied. For example, when 50% of the membrane is regenerated, the positive CD band is found to be less than 50% of the fully regenerated band and there is no negative CD band. At this percent regeneration, only 10% of the clusters would be expected to contain all three retinals, assuming random binding during regeneration. This dependence of the shape of the CD spectrum on the fraction of sites occupied strongly suggests that the CD spectrum of fully regenerated PM has an important contribution from chromophore-chromophore interactions.

TH-AM-G8 EXCITED STATE DIPOLE MOMENTS OF RETINALS. R. Mathies and L. Stryer, Department of Molecular Biophysics and Biochemistry, Yale University, New Haven, Connecticut 06520.

An electric field perturbation technique has been used to determine the excited state dipole moments of a series of retinals and their derivatives. The chromophore is dissolved in an organic solvent and then subjected to an electric field of 5×10^4 volt/cm. The field-induced changes in the absorption are then measured and analyzed in terms of derivatives of the zero-field absorption spectrum to give both ground and excited state dipole moments. Our device can detect field-induced changes in the extinction coefficient, $\Delta\epsilon/\epsilon$, as small as 10^{-5}. The observed changes in the dipole moments of all-trans retinal and its protonated and unprotonated n-butyl Schiff bases upon excitation are 15.5 D, 12.0 D, and 9.9 D, respectively, implying that these molecules become very dipolar in their excited states. A change in dipole moment of 15 D (all-trans retinal) could result from the movement of 0.25 e^- over the length of the chromophore ($\sim$ 12 Å). This large shift in positive charge toward the ionone ring of these molecules is consistent with the observed solvent-sensitivity of their solution absorption spectra. Furthermore, this light-induced charge movement may critically affect the energetics and kinetics of photoisomerization. The production of charge delocalization in the first excited state of retinal may initiate the formation of prelumirhodopsin, which is known from resonance Raman measurements (Oseroff and Callender, Biochem. 13, 4243 (1974)) to have a delocalized charge distribution.

TH-AM-G9 SPECTRAL AND QUANTUM YIELD STUDIES ON A FLAVOENZYME INTERMEDIATE IN BACTERIAL BIOLUMINESCENCE. J.E. Becvar, S.-C. Tu*, and J.W. Hastings, The Biological Laboratories, Harvard University, Cambridge, Mass. 02138.

We have previously demonstrated that an intermediate in the bacterial bioluminescence reaction can be isolated by chromatography on Sephadex at subzero temperatures in 50% ethylene glycol [Hastings et al. PNAS 70:3468 (1973)]. Although its lifetime is shorter, this intermediate may be similarly isolated at 0° in aqueous buffer. We find that the light emission capability of the intermediate decays exponentially with a half life at 0° of about 11 min (0.02 M phosphate, pH 7.0) in agreement with the results of Murphy et al. [BBRC 58:119 (1974)]. However, in contrast to Murphy et al., we find the chromatographed intermediate to be not an apoprotein but rather a flavoprotein, which initially absorbs maximally at 375 nm and has little absorbance near 440 nm. With kinetics paralleling the decrease in bioluminescence potential, the spectrum of this species changes to one with maxima at both 370 nm and 442 nm. The appearance of well defined isosbestic points (329 nm, 368 nm, 401 nm, for Beneckea harveyi luciferase; 333 nm, 382 nm, 404 nm, for Photobacterium fischeri luciferase) indicates that only two principal flavin species exist during this reaction. The number of photons emitted per flavin in the complex is about 0.2, in good agreement with the bioluminescence quantum yield for enzyme and flavin [Becvar and Hastings PNAS 72:3374 (1975)]. Higher phosphate concentrations slow the rate of intermediate decomposition ($t_{1/2} \sim 40$ min in 0.8 M phosphate, pH 7.0). [Supported by an NSF grant (BMS74-23651) to J.W.H. and by NIH grants to S.C.T. (1 F32 GM00348-01) and to J.E.B. (4 F02 GM55606-03)]

TH-AM-G10 A BIOCHEMICAL COMPARISON BETWEEN LUMINESCENT AND NON-LUMINESCENT GONYAULAX. R. J. Schmidt*, V. D. Gooch, and L. A. Loeblich*. The Biological Laboratories, Harvard University, Cambridge, Mass. 02138.

Ten isolates of the marine dinoflagellate Gonyaulax excavata (formerly G. tamarensis) were studied. All isolates were made from two samples collected at Gloucester, Mass, during the 1972 red tide outbreak. Some of these isolates lack the usual bioluminescent characteristic, but otherwise all isolates appear identical with respect to morphology, growth characteristics, and behavior. Stimulation of the nonbioluminescent clones by means of H^+, Ca^{++} or mechanical means elicited no detectable light (our instruments could have detected one millionth the amount of light produced by the luminescent isolates). The nonluminescent isolates were further investigated to determine if they were lacking any or all of the known components of bioluminescence: the substrate luciferin, the enzyme luciferase, a luciferin-binding protein, and scintillons (luminescent particulate system). The nonbioluminescent clones were deficient with respect to all of the above components. However, these in vitro experiments indicate the presence in extracts of nonluminescent strains of a heat stable bioluminescent inhibitor which is capable of inhibiting the light activity of luminescent extracts on the order of 75%. The fact that similar isolates of the same species may or may not be luminescent again raises the intriguing question of the function or purpose of bioluminescence in dinoflagellates.

TH-AM-G11 INORGANIC PHOSPHORS AS MICROSPECTROFLUORIMETRIC STANDARDS.[1] S.S. West and J.F. Golden*, Dept. of Engineering Biophysics, Univ. of Alabama in Birmingham, Birmingham, AL 35294

Individual dehydrated inorganic phosphor particles, hermetically sealed on microscope slides, are employed as standards for microspectrofluorometric measurements. A particlar phosphor particle has been chosen to establish the unit of measurement. This unit is related to fundamental units by a constant. Other individual phosphor particles on additional microscope slides are calibrated with the unit phosphor particle. The emission spectra are constant in spectral composition. In the microspectrofluorophotometer, the flux from the phosphor particle is a direct measure of excitation flux impinging on the sample. A 3-cavity narrow band interference filter isolates the 436 nm Hg line for excitation. The flux produced by the phosphor particle passes through a rapid-scanning monochromator ($\simeq$ 0.6 s/spectrum) and is then detected by a PMT with known spectral response. Spectroscopic correction is applied on-line. The resulting corrected spectrum is displayed on an oscilloscope and can be calibrated in phosphor particle units (ppu). Constant absolute PMT sensitivity is maintained with a self-luminous phosphor button excited by tritium. The ppu and the radioactively-excited phosphor are easily maintained and could easily be supplied to the public. These standards have been utilized in microspectrofluorophotometry of acridine orange-stained cells to establish quantitative intensity relationships and to analyze fluorescence fading.

*This work was supported in part by U.S.P.H.S. Research Grant GM18252 and NCI Contract NO1-CB-43960

TH-POS-E1 SURFACE LOCALIZATION OF SITES OF REDUCTION OF NITROXIDE SPIN LABELED MOLECULES IN MITOCHONDRIA. A.T. Quintanilha, and L. Packer. Membrane Bioenergetics Group, Energy and Environment Division, LBL, University of California, Berkeley, Calif. 94720

Nitroxide spin labels in their oxidized form act as electron acceptors in the electron transport chain of mitochondria. Rat liver mitochondria were studied using sodium succinate as substrate at concentrations of different spin labeled molecules (R.J. Mehlhorn, collaboration) which did not effect the O_2 uptake rates nor the state of coupling of the mitochondria. We find that the more hydrophobic partitioned spin labeled molecules tempo, tempol, tempamine, tempol-caprate, 2N3 and A12NS get reduced only when the sample becomes anaerobic, while the more hydrophobic partitioned spin labeled molecules 2N11, 7N14, A4NS and the spin labeled cationic detergent CTAB (cetyl-trimethyl ammonium bromide) designated as CDTAB are reduced concurrently with O_2 consumption. Reduction rates relative to the rate of O_2 uptake are as follows: 0.5 for CDTAB; 0.25 for 2N11 and tempo; 0.1 for tempol, tempamine, tempol-caprate, A12NS and A4NS; 0.03 for 2N3 and 0.01 for 7N14. Spin labels that partition closer to the hydrophobic-hydrophilic interface show higher rates of reduction. Spin labels localized deep inside the hydrophobic region, like 7N14, are unable to accept reducing equivalents from the electron transport chain. CDTAB showed the fastest rate of reduction. Using glutamate-malate as substrate in mitochondria and mitoplasts, spin reduction is partially inhibited by rotenone but insensitive to antimycin A and KCN. Using NADH as substrate in submitochondrial preparations, spin reduction is inhibited by rotenone and antimycin A but only partially inhibited by KCN. This suggests that electrons or reducing equivalents are channeled from the respiratory chain to the membrane interface in the region after the rotenone and before the antimycin sensitive site, and more readily so to the outer half of the inner membrane than the inner half.

TH-POS-E2 PROPOSED STRUCTURE AND FUNCTION OF PROTEIN IN MEMBRANE: A. K. Dunker, Program in Biochemistry and Biophysics, Washington State University, Pullman, Wash., 99163; D. A. Marvin and D. J. Zaleske*, Department of Molecular Biophysics and Biochemistry, Yale University, New Haven, Conn. 06520; and T. Jones*, Biology Dept. Mt. Holyoke College, South Hadley, Mass., 01075.

We have extended the packing rules for coiled-coils to the case of tubular α-helical aggregates, which may form the basis of protein structure in membrane. Using these rules and the amino acid sequences from several membrane associated proteins of widely diverse origin, we have constructed trial structures that are remarkably consistent in design, with hydrophobic side chains exterior and hydrophilic side chains interacting along the interfaces. The Pfl and fd coat protein trial structures contain three α-helices. The glycophorin trial structure contains seven to nine α-helices in a tube with a hydrophobic interior and of the size observed for the glycophorin-containing membrane associated particles. The murein-lipoprotein trial structure contains an extended connected set of hydrogen bonds and a hydrophilic interior channel in an aggregate containing four to six α-helices. Based on such structures, we propose a proton jump mechanism for proton transport and a traveling distortion mechanism for other transport. In the proton-jump hypothesis, the extended connected set of hydrogen bonds provide a pathway for rapid proton exchange, analogous to proton jumping in water. In the traveling distortion hypothesis, a slight distortion involving motions of just a few angstroms changes the local character of the interior channel; as the distortion travels through the structure, the altered character comigrates with the distortion, carrying along the molecule or ion being transported.

TH-POS-E3 THERMOTROPIC MESOMORPHISM OF THE CELL MEMBRANE OF *THERMOPLASMA ACIDOPHILUM* ADAPTED TO GROWTH AT 37°, 56°, AND 65°C. Herman G. Weller, Jr. and Alfred Haug*, Department of Biophysics, Michigan State University, and MSU/ERDA Plant Research Laboratory, Michigan State University, East Lansing, Michigan, 48824

The thermophilic acidophilic mycoplasma *Thermoplasma acidophilum* grows at pH2 at temperatures between 37°C and 65°C, with optimum log phase growth rate at about 56°C. As part of its adaptation to growth at different temperatures, this organism apparently adjusts the thermotropic mesomorphic properties of its cell membrane. Cells were adapted from 56°C to growth at 37°C or 65°C for at least 34 generations. The temperature dependence of microfluidity of isolated cell membranes and membranes of intact cells was studied with nitroxyl-stearate spin probes. In the temperature range 0 - 80°C, the microfluidity of isolated or intact cell membranes is similar. Two ESR-determined transitions occur, one below 25°C and one at about 45°C. The membrane microfluidity throughout this temperature range depends on the growth temperature. The lower-temperature transition of vesicles of the isolated membranes increases with increasing Mg^{++} or Ca^{++} concentration of the suspension. This transition is also influenced by the combination of pH and the concentration of the monovalent cation K^+ of the suspension.

(Supported by funds from NIH Training Grant # GM-01422, the College of Osteopathic Medicine of Michigan State University, and U.S.-ERDA Contract No. E(11-1)-1338.)

TH-POS-E4 MEASUREMENT OF THE TRANSLATIONAL MOTION OF CONCANAVALIN A IN GLYCEROL-SALINE SOLUTIONS AND ON THE CELL SURFACE BY FLUORESCENCE RECOVERY AFTER PHOTOBLEACHING. K. Jacobson,[a] E-S. Wu,[*b] and G. Poste,[*a] [a]Dept. of Expt. Pathology, Roswell Park Memorial Institute, Buffalo, N. Y. 14263 and [b]Dept. of Physics, Univ. of Maryland-Baltimore County, Baltimore, Md. 14228

The fluorescence recovery kinetics of succinyl-fluorescein Concanavalin A (S-F-ConA) in glycerol-physiological saline solutions of high viscosity and when bound to the surface of mouse fibroblasts were measured following brief photobleaching using a laser excited fluorescence microscope. In the high viscosity solutions, the recovery kinetics, interpreted on the basis of a simple diffusion model, yielded a diffusion coefficient in close agreement with the values predicted by the Stokes-Einstein equation. Recovery kinetics for S-F-ConA bound to the surface of mouse 3T3 and SV3T3 cells cultured in vitro yielded diffusion coefficients in the range of 5-10 x 10^{-11} cm^2/sec, values considerably lower than those reported previously for membrane proteins. These measurements indicated that a considerable fraction of the S-F-ConA molecules bound to the cell surface are immobilized. These results are discussed in relation to current concepts of lateral motion of protein components within natural membranes.

This work was supported by Grants CA-16743 (K.J.) and CA-13393 (G.P.) from the National Institutes of Health.

TH-POS-E5 PHASE TRANSITIONS IN PURPLE MEMBRANE AND CELL-MEMBRANE VESICLES IN HALOBACTERIUM HALOBIUM. Sharmila S. Gupte, Alfred Haug*, and M. Ashraf El-Bayoumi, Department of Biophysics, Michigan State University, and MSU/ERDA Plant Research Laboratory, Michigan State University, East Lansing, Michigan 48824

Halobacterium Halobium is a halophilic bacterium which requires 4 M NaCl in its growth medium. Under optimum condition of illumination and rate of aeration, it exhibits differentiated purple membrane regions in the cytoplasmic membrane. The temperature dependence of the microfluidity of the purple membrane (PM) and cell-membrane vesicles has been studied using nitroxyl-stearate spin probes for cells grown at 37°C. The microfluidity as indicated by maximum hyperfine splitting ($2T_{//}$) of the PM is lower than that of the vesicles in the temperature range of 5 to 50°C. Reversible bleaching with white light has no effect on the microfluidity of the PM as indicated by 5-nitroxyl-stearate (5-NS) probe. 5-NS labelled PM exhibits a phase transition at about 31°C whereas the cell-membrane vesicles show a phase transition at about 22°C. Cell-membrane vesicles were labelled with a fluorescence probe: 12-(9-anthroyl)stearate. Probe fluorescence lifetime measurements suggest that two lipid populations of different microfluidity exist in the cell membrane. Structural implications of fluorescence and spin label studies will be presented. (Supported by funds from the College of Osteopathic Medicine of Michigan State University)

TH-POS-E6 CORRELATED X-RAY DIFFRACTION AND FREEZE-FRACTURE STUDIES OF MEMBRANE MODEL SYSTEMS: PERTURBATIONS INDUCED BY FREEZE-FRACTURE PREPARATIVE PROCEDURES. M.J. Costello and T. Gulik-Krzywicki*, Department of Anatomy, Duke University Medical Center, Durham, N.C. 27710 and C.N.R.S., Centre de Génétique Moléculaire, 91190 Gif-sur-Yvette, France.

Multilamellar lipid-water and protein-lipid-water phases have been examined by X-ray methods before and after freezing. Frozen samples have been subsequently fractured and replicated, thus permitting an evaluation of the nature of structural perturbations in samples examined by freeze-fracture electron microscopy. Important results are summarized: (1) Freezing low water content (ca.<25%) phases causes perturbations in the packing of hydrocarbon chains. For example, freezing liquid paraffin chains produces a condensed "glass-like" packing and this change is accompanied by an expansion of the thickness of the lipid leaflet. (2) Additional perturbations occur in high water content samples. After freezing, much smaller lamellar repeat distances, intense ice reflections, extensive perturbations of fracture faces, and prominent ice pockets are all consistant with the expulsion of water from between lamellae. The presence of glycerol generally relieves these perturbations but in some cases introduces additional lattice disorder. (3) Complex perturbations occur in phases containing integral membrane proteins and therefore the influence of these proteins cannot be completely evaluated. Preliminary results for cytochrome b_5-lecithin associations show neighboring rough and smooth fracture faces, consistant with the formation of lamellae from precursor vesicles having bilayers with an asymmetric distribution of protein. For these phases, the fracture faces do not display clearly defined particles. (4) Freezing in Freon-22 (-160°C) is not rapid enough to prevent some perturbations which can influence the interpretation of freeze-fracture data. Surprisingly, much slower freezing in a stream of N_2 gas (-140°C) produces similar structural changes.

TH-POS-E7 CHANGES IN E. COLI ENVELOPE STRUCTURE AND THE SITES OF FLUORESCENCE PROBE BINDING CAUSED BY UNCOUPLERS OF ACTIVE TRANSPORT. S.L. Helgerson* and W.A. Cramer, Department of Biological Sciences, Purdue University, West Lafayette, Indiana 47907

In intact E. coli ML-308-225 cells the inhibition of [^{14}C]-proline active transport by carbonyl cyanide-p-trifluoromethoxy-phenylhydrazone (FCCP) increases with uncoupler concentration from ~20% at 2 μM to ~100% at 5 μM. The increase in the rotational relaxation time of the cell-bound fluorescent probe N-phenyl-1-naphthylamine (PhNap) and 8-anilino-1-naphthalene-sulfonate (ANS) under these conditions shows the same dependence on FCCP concentration. The rotational relaxation times of both ANS and PhNap increase 3-3.5X when the cells are treated with 5 μM FCCP. When the cells are pretreated with 0.1 mM ethylenediamine-tetraacetic acid (EDTA) for 1.5 min to remove 30-50% of the outer lipopolysaccharide layer, complete inhibition of [^{14}C]-proline transport is achieved at 0.3 μM FCCP. This treatment removes a permeability barrier to FCCP since active transport of [^{14}C]-proline by ML-308-225 membrane vesicles is also completely inhibited by 0.3 μM FCCP. After EDTA treatment the rotational relaxation time of ANS in the absence of FCCP is unchanged and increases with the same dependence on FCCP concentration as does the inhibition of active transport. However, the rotational relaxation time of cell-bound PhNap is increased in the EDTA treated cells to a value slightly higher than that obtained in fully uncoupled (+5 μM FCCP) intact cells and shows no further increase when FCCP is added. It is concluded that uncoupling by FCCP causes a structural change in the cell envelope which removes a permeability barrier to PhNap and allows increased uptake of the hydrophobic dye. There is no increase in uptake of ANS due to uncoupling, so ANS is monitoring a structural change at dye binding sites within the cell envelope.

TH-POS-E8 TRANSFER OF A FLUORESCENT DYE FROM LIPID VESICLES TO CELLS. J.N. Weinstein (LTB, NCI), S. Yoshikami (NEI), P. Henkart (IB, NCI), R. Blumenthal (LTB, NCI), W. A. Hagins (NIAMDD). National Institutes of Health, Bethesda, Md 20014

We have used the water-soluble fluorescent dye 6-carboxyfluorescein (6-CF) to investigate the interaction between small lipid vesicles and cells of several types. Vesicles of dipalmitoyl phosphatidyl choline (DPPC) were formed in 200 mM 6-CF, either by sonication or by the injection method (Batzri and Korn, Biochim. Biophys. Acta 298, 1015, 1973). Excess fluorophore was then removed from the suspending medium by gel filtration and ion exchange. Within the vesicles, the dye is almost non-fluorescent because of concentration-quenching. Frog retinas, human lymphocytes, and mouse peritoneal macrophages all showed uptake of 6-CF from the vesicles within a few minutes of incubation. The retinas remained functional; the lymphocytes showed no damage in trypan blue exclusion and light-scattering tests. In each case, microscopy revealed all cells to be fluorescent. There was no discernible uptake in control incubations with free 6-CF and vesicles containing only a pH buffer. After incubation with vesicles, dye appeared to be distributed throughout the lymphocytes and rod outer segments, strongly suggesting that it had entered the cytoplasmic compartment and that it had been diluted enough to reduce greatly the concentration-quenching of the dye in the original vesicles. Macrophages stained much more irregularly. Vesicles of dioleyoyl phosphatidyl choline gave qualitatively similar results with each cell type. Uptake of dye by lymphocytes from DPPC vesicles increased with temperature between 5 and 37°C. The mechanism of the interaction of vesicles with rods and lymphocytes is probably membrane fusion. Lymphocytes are known to endocytose only under special circumstances, and we find that azide has little effect on the incorporation of 6-CF. Rods are not known to endocytose at all.

TH-POS-E9 A NUCLEAR MAGNETIC RESONANCE STUDY OF THE INTERACTION OF 1-ANILINO-8-NAPHTHALENE-SULFONATE WITH NATURAL AND ARTIFICIAL MEMBRANES. T.N. Estep and G.L. Jendrasiak,* Department of Physiology and Biophysics, University of Illinois, Urbana, Illinois 61801.

Proton magnetic resonance spectroscopy at 220 MHz was used to study the interaction of the fluorescent dye 1-anilino-8-naphthalenesulfonate (ANS) with aqueous dispersions of egg phosphatidylcholine (EPC), porcine erythrocyte ghosts, and porcine thyroid plasma membranes. When 10^{-3} to 10^{-2}M ANS was added to EPC dispersions, the choline methyl proton resonance was broadened and shifted upfield. Resonances arising from choline methylene protons, as well as hydrocarbon chain methylene protons near the glycerol backbone, were also shifted upfield. Other resonances were unaffected. In this concentration range ANS appeared to be interacting primarily with the polar head group of the phospholipid. At higher concentrations (up to .12M) there were further upfield shifts of the specific resonances mentioned above along with a narrowing of the choline methyl proton peak. In addition, the hydrocarbon chain methyl proton resonance was split into a doublet. These spectral changes were accompanied by a marked reduction in sample turbidity. Such results are consistent with the hypothesis that high concentrations of ANS disrupt EPC liposomes. Similar effects were obtained when ANS was added to suspensions of natural membranes. Dye concentrations up to 10^{-2}M affected the choline methyl proton resonance exclusively, while higher concentrations intensified all membrane peaks. These results provide direct evidence that a significant amount of ANS is being bound by membrane lipids. 10^{-3}M ANS was found to inhibit iodide uptake in thyroid tissue slices more than 50%, indicating that the dye-phospholipid interaction may be of physiological significance.

TH-POS-E10 MEMBRANE FLUIDITY AND DISCONTINUOUS ARRHENIUS PLOTS. J.N.Finkelstein* and S. Ghosh, Department of Biochemistry, Northwestern University Medical and Dental Schools, Chicago, Illinois, 60611

Discontinuities in Arrhenius plots for membrane enzyme or transport systems have been attributed to phase changes in membrane phospholipids and the concomitant changes in membrane fluidity. The precise mechanism for such effects is however not known. We propose the following as a possible explanation for the effects of membrane fluidity on enzymatic reaction rates. Classical enzyme kinetics is based on enzyme-substrate binding which is akin to adsorption on fixed sites as described by the Langmuir adsorption isotherm. Theories of carrier-mediated transport are based on similar considerations. At temperatures above the phase transition, because of the possibility of lateral movement, binding behavior will differ as described by the Volmer isotherm. On this basis it can be shown that at the onset of surface mobility the concentration required for half-maximal saturation will increase, such that at finite concentrations a step-wise increase in apparent Km will be observed, independent of possible changes in Vmax. In the limited number of cases where the effects of temperature on Km have been reported for membrane systems, the predicted effects have been seen.

TH-POS-E11 LOCAL ANESTHETIC - MEMBRANE INTERACTION. H.H. Wang and D.D. Koblin, Division of Natural Sciences, University of California at Santa Cruz and Division of Biology, California Institute of Technology, Pasadena, California

The interaction of local anesthetics with membrane lipids and phospholipid model systems have been well studied previously. The present study is concerned with the detection of membrane protein-local anesthetic interaction. In the first series of experiments, a spin-labeled local anesthetic was used to detect the binding of the anesthetic to membrane proteins. The rotational mobility of the spin-labeled local anesthetic in erythrocyte membranes was found to decrease upon addition of chemical modifiers that react covalently with free amino groups of the membrane and decrease the concentration of the membrane's fixed positive charge.Reagents that did not react with free amino groups, or those that did react with amino groups but did not alter the net charge of the membrane, had no effect on the mobility of the spin-labeled local anesthetic. The decrease in the anesthetic's mobility found after reaction with amino directed reagents was shown to be due to the attraction of the positively charged anesthetic to the modified site. In further experiments, the spin-labeled local anesthetic was used as a fluorescene quencher of membrane bound 1-anilinonaphthalene-8-sulfonate (ANS). It is known that ANS in the presence of human erythrocyte ghosts exhibits two fluorescence lifetimes which represent ANS bound to lipid and protein components respectively. By examining the relative quenching of these two fluorescence lifetimes in the presence of the spin-labeled local anesthetic, evidence was provided for membrane protein-local anesthetic interaction.

TH-POS-E12 LASER RAMAN SPECTROSCOPIC INVESTIGATION OF LIPID-PROTEIN SYSTEMS: DIFFERENCES IN THE EFFECT OF INTRINSIC AND EXTRINSIC PROTEINS ON THE PHOSPHATIDYLCHOLINE RAMAN SPECTRUM. L.J. Lis, S.C. Goheen, and J.W. Kauffman, Department of Materials Science and Engineering, and D.F. Shriver‡ Department of Chemistry, Northwestern University, Evanston, Illinois 60201

Laser Raman spectroscopy was used to examine the interaction of intrinsic and extrinsic proteins with the lipid layer structure. The interactions of cytochrome c and cytochrome c oxidase with lipids have been well established by others using a variety of techniques. Cytochrome c is thought to act as an extrinsic membrane protein while cytochrome c oxidase is thought to act as an intrinsic membrane protein. The lipid-cytochrome c and lipid-cytochrome c oxidase systems are used to assist in interpreting the spectral changes due to intrinsic and extrinsic protein interaction. The two types of proteins examined produced differential changes in the lipid hydrocarbon C-H stretch Raman modes for both dimyristoyl and dipalmitoyl phosphatidylcholine. The lipid hydrocarbon C-H stretch modes have been shown to be environment and configuartion dependent and can be used to indicate changes in the hydrocarbon fluidity and environment. Interpretations are made as to the relationship of the effect of the two protein types on the lipid Raman spectrum and their effect on the lipid packing structure. The high signal to noise ratio in the C-H stretch region allows a quantitative analysis of these changes. The above analysis was extended to less well understood lipid model membrane systems containing the plasma proteins fibrinogen or albumin, or the red blood cell glycoprotein glycophorin. Initial studies on these systems will also be reported.

TH-POS-E13 RAMAN SPECTROSCOPY OF NORMAL AND ROUS-TRANSFORMED CELL MEMBRANES. E.B.Carew*, H.W.Kaufman*, P.W.Robbins*, and H.E.Stanley, Harvard-MIT Program in Health Sciences and Technology, Center for Cancer Research, Department of Physics, and Department of Biology, Massachusetts Institute of Technology, Cambridge,Mass. 02139.

Conformational properties of lipids and proteins have been characterized by Raman spectroscopy. Raman spectra of plasma membrane vesicles (PMV) and endoplasmic reticulum vesicles (ERV) obtained from tissue-cultured chick embryo fibroblasts are interpreted in terms of their lipid and protein constituents. A first set of peaks at 1062,1089, and 1128 cm^{-1}, the relative intensities of which have been shown in model lipid vesicles to vary with the temperature-dependent order-disorder transition, are apparent in spectra of all vesicle preparations. The I_{1089}/I_{1130} ratio for PMV is on the order of unity, while it is considerably larger than unity for ERV. PMV obtained from fibroblasts that had been tumorigenically transformed by Rous sarcoma virus or pseudotransformed with trypsin have I_{1089}/I_{1130} ratios similar to ERV of normal cells. A second set of peaks at 1238, 1268,and 1302 cm^{-1} , which are partly or totally shifted on deuteration (NH → ND exchange), are interpreted as amide III modes; two peaks (1268 and 1302 cm^{-1}) fall within the α-helical range, while the third (1238 cm^{-1}) is in the β pleat or "random" coil structure region. The 1302 cm^{-1} peak of PMV of transformed and trypsin-modified cells is compared with ERV and PMV of normal cells. This work was supported by grants from the NIH and the Research Corporation.

TH-POS-E14 DYNAMIC ASPECTS OF THE REACTION OF OPSIN WITH 11-*cis*-RETINAL. M.A. Cusanovich, and R.A. Henselman*, Department of Chemistry, University of Arizona, Tucson, Arizona 85721

The reaction of the apoprotein opsin with 11-*cis* retinal to form the visual pigment rhodopsin is an important aspect of the visual process. This reaction, termed recombination, has been investigated with a view towards obtaining information on its kinetic and chemical properties. Using bleached bovine rod outer segments as a source of opsin, psuedo first-order rate constants for recombination were determined as a function of 11-*cis*-retinal concentration. In the pH range 6.4 to 7.4 plots of $\ln\Delta A_{500}$ vs time were linear for at least three half lives yielding k_{obs}. Graphical analysis of k_{obs} as a function of 11-*cis* retinal concentration indicate a complex process with the rate constants not directly proportional to the ligand concentration. Based on our studies and known properties of opsin and rhodopsin the kinetic data are consistent with the nucleophilic attack of an ε-NH_2 group of opsin on the carbonyl carbon of 11-*cis*-retinal ($k>900 m^{-1}s^{-1}$) to form an intermediate addition compound. The dehydration of the intermediate compound ($k=0.055 s^{-1}$), facilitated by the donation of a proton from some species (BH^+), results in the formation of the protonated aldimine product which is rhodopsin. From these data and the effect of pH on the kinetics of recombination at pH values below 6.4 and above 7.4, opsin appears to be in a pH dependent equilibrium with a conformation of opsin incapable of undergoing recombination. The rate constant for the formation of the active conformer from the inactive conformer is 0.04-0.06 s^{-1}. This research was supported by NIH Research Grant EY 01113-07A2.

TH-POS-E15 CALORIMETRIC STUDIES OF THE BINDING OF APOLIPOPROTEIN TO DIMYRISTOYL PHOSPHATIDYLCHOLINE. H.J. Pownall, F.J. Hsu*, and A.M. Gotto*, Division of Atherosclerosis and Lipoprotein Research, Baylor College of Medicine and The Methodist Hospital, Houston, Texas 77025.

We have studied the enthalpy of binding, ΔH_B, of apoC-III, an apolipoprotein, to dimyristoyl phosphatidylcholine vesicles, DMV, as a function of temperature and protein concentration. At 24° and at a protein to vesicle ratio of 15 or less, the ΔH_B per bound protein is constant suggesting that each protein molecule is binding to equivalent and non-interacting sites on the vesicle. Above a protein to vesicle ratio of 50:1, ΔH_B is unchanged, suggesting that the binding sites on the vesicles are saturated. At the gel → liquid crystalline transition temperature, T_C = 24°, the reaction is highly exothermic, ΔH_B= -313 ± 12 kcal per mole of protein. At higher and lower temperatures, the ΔH_B decreases dramatically; we assign the small ΔH_B below T_C to the low reactivity of the gel state compared to the liquid crystalline state. Above T_C, the ΔH_B decreases gradually to <10 kcal/mole of protein. The large ΔH_B at T_C is unchanged between 0 → 3.0 M NaCl and is assigned to the smaller number of degrees of freedom available in the vesicle at T_C. Although the enthalpy term is usually considered most important in the maintenance of membrane organization, these results suggest that the enthalpy change is important to the formation and stability of this lipid-protein system. This may be particularly important in cell and lipoprotein systems which are viable within the melting range of their membranes and lipids, respectively.

TH-POS-E16 NAP-TAURINE ACTS AS A PHOTO-AFFINITY LABEL FOR THE ANION EXCHANGE SYSTEM IN HUMAN ERYTHROCYTES. P. A. Knauf, W. Breuer, L. Davidson* and A. Rothstein, Research Institute, The Hospital for Sick Children, Toronto, Ontario, M5G 1X8.

In the dark, N-(4-azido-2-nitrophenyl)-2-aminoethyl sulfonate (NAP-taurine) is chemically unreactive, but when exposed to light it forms a short-lived, but highly reactive nitrene capable of indiscriminate reaction with any membrane components in its vicinity. In the dark this agent acts as a substrate for the anion exchange system of human erythrocytes and reversibly inhibits the exchange flux of other substrates such as Cl^- and SO_4^{-2}, with a K_i of less than 40 μM. Plots of the reciprocal of the rate constant for sulfate efflux versus the NAP-taurine concentration are linear, as are plots of the reciprocal of the fractional inhibition against the reciprocal of NAP-taurine concentration. After exposure to light, the inhibition becomes irreversible, and closely matches the reversible inhibition in the dark, except at high hematocrits (>5%) or NAP-taurine concentrations (>100 μM), when screening of the incident light becomes significant. Pre-photolyzed NAP-taurine does not inhibit anion exchange either before or after exposure to light. Addition of scavengers capable of reacting with nitrenes, such as p-aminobenzoic acid, to the medium does not interfere with the ability of NAP-taurine to irreversibly inhibit anion exchange. Thus, according to all of the criteria so far suggested, NAP-taurine behaves as a true photo-affinity label. The binding of NAP-taurine to membrane components after exposure to light can therefore be considered to accurately reflect its reversible interactions with these sites in the dark. In the presence of high Cl^- concentrations, the irreversible binding of NAP-taurine to membrane components is substantially reduced. It can therefore be concluded that Cl^- and NAP-taurine compete for common sites and that some fraction of these may be transport sites. (Supported by Medical Research Council (Canada) Grants No. MA 5149 and MA 4665.)

TH-POS-E17 MICROVISCOSITY OF THE HYDROCARBON REGION OF THE BOVINE RETINAL ROD OUTER SEGMENT DISC MEMBRANE DETERMINED BY FLOURESCENT PROBE MEASUREMENTS. Gene W. Stubbs*, Burton J. Litman, and Yechezkel Barenholz*, Department of Biochemistry, University of Virginia School of Medicine, Charlottesville, Virginia 22901.

The microviscosity of the hydrocarbon region of the bovine retinal rod outer segment disc membrane was determined by measuring the anisotropy of fluorescence from the probe 1,6-diphenyl-1,3,5,-hexatriene (DPH). The microviscosity ranged from 1.4 poise at 40° to 15 poise at 0°, and no phase transition was observed in this temperature range. Bleaching of rhodopsin in the disc membrane produced no change in the microviscosity with the limits of error of our measurement (+5%). The presence of retinal in the disc membrane caused strong quenching of DPH fluorescence. Removal of retinal produced a three-fold increase in total fluorescent intensity, but less than 10% reduction in fluorescence anisotropy. Bilayers prepared from extracted disc lipids had a microviscosity which was 3 to 4 times lower than that of the intact disc membrane, indicating that rhodopsin hinders the hydrocarbon chain mobility of the disc phospholipids. (Supported by U.S.P.H.S. Grant EY000548 and NSF Grant GB-41313.)

TH-POS-E18 RESTRICTIONS ON ROTATIONAL AND TRANSLATIONAL DIFFUSION OF PIGMENT IN THE MEMBRANES OF A RHABDOMERIC PHOTORECEPTOR. T.H. Goldsmith and R. Wehner,* Department of Biology, Yale University, New Haven, Conn. 06520, University of Zurich, Zurich, Switzerland, and Marine Biological Laboratory, Woods Hole, Mass.

Recent evidence indicates that rhodopsin molecules not only undergo translational diffusion but are also free to rotate in the planes of the disk membranes of rod outer segments. Both polarization sensitivity of arthropod retinular cells and measurements of dichroic absorption of isolated crustacean rhabdoms, on the other hand, indicate some preferential alignment of the chromophores with the axes of the microvilli, implying restrictions on the orientations that the pigment molecules can assume. In order to ascertain whether translational diffusion is restricted, isolated, dark-adapted crayfish rhabdoms were examined from the side by microspectrophotometry. Local photobleaching of crayfish metarhodopsin (λ_{max} 515nm) was accomplished in 2 min at pH 9 in the presence of 0.25 M formaldehyde or glutaraldehyde. The remaining metarhodopsin did not redistribute in the dark, but underwent a first-order dark decay, with the same rate constant at the bleaching and reference spots. There is therefore no evidence for translational diffusion of pigment. Photo-induced dichroism is also observed. A quantitative theoretical description of photo-induced dichroism in microvilli has been developed for comparison. The magnitude of the observed photo-induced dichroism is less than theory predicts for random orientation of chromophores, consistent with the hypothesis that not all rotational positions are allowed. The photodichroism is greater in the presence of the cross-linking reagent glutaraldehyde than it is in formaldehyde, however, indicating that the molecules are normally free to wobble within some limiting angle with the microvillar axis.

TH-POS-E19 POLARIZED-LIGHT DETECTION IN THE BEE RETINA. Gary D. Bernard, Yale Univ., Dept. of Ophthalmology and Visual Science, 333 Cedar St., New Haven, Ct. 06510, and Rüdiger Wehner*, University of Zürich, Dept. of Zoology, Switzerland; and the Marine Biological Laboratory, Woods Hole, Mass.

The worker bee can see the polarization pattern of ultraviolet (UV) sky-light. The part of her retina that mediates polarization vision contains four types of UV receptors embedded in twisted rhabdoms of two types (clockwise and counter-clockwise). Each rhabdom contains two long UV rhabdomeres and one short, basal, UV rhabdomere.

We created a waveguide-theoretical model of a twisted, dichroic, birefringent, bee rhabdom for the purpose of predicting the responses of UV cells to polarized light. The analysis suggests that a) long UV cells have a "luminosity" response that depends on total intensity of illumination but not on either degree or angle of polarization; b) a basal UV cell has an "opponent" response in which the ratio- (response to polarized light)/(response to unpolarized light of the same total intensity) - is greater than unity for half of the possible polarizational angles and less than unity for the remainder; c) basal cells of different twist types have polarizational responses that are linearly independent because their rhabdomeres twist in opposite directions. These three types of responses are sufficient for analysis of both angle and degree of partially polarized light.

The polarization-vision system of the bee has much in common with a trichromatic color-vision system; angle and degree of polarization are analogous to hue and saturation, respectively. Neural circuitry involved in polarization vision may be very similar to that involved in color vision. (This research is supported in part by NIH grant EY01140, RCDA EY48264, and center grant EY00785, and by Swiss NSF grant 3.814.72 .

TH-POS-F1 LOCALIZATION OF IONOPHORE ACTIVITY IN A 20,000 MOLECULAR WEIGHT FRAGMENT OF THE SARCOPLASMIC RETICULUM ATPase. A.E. Shamoo, T.E. Ryan*, P.S. Stewart*, and D.H. MacLennan*. Univ. Rochester School of Medicine & Dentistry, Rochester, N.Y. 14642. Banting & Best Dept. Medical Research, Charles H. Best. Inst., Univ. Toronto, Toronto, Ontario M5G 1L6, Canada.

The Ca^{++} + Mg^{++}-Dependent ATPase of sarcoplasmic reticulum has been shown to act as a Ca^{++}-dependent and -selective ionophore in artificial bilayers. Tryptic digestion leads to a 55,000, 45,000, 30,000 and 20,000 fragments of the ATPase. A 55,000 molecular weight fragment was shown to be facing the cytoplasm and a 45,000 molecular fragment was shown to be embedded in the membrane. The 55,000 and 20,000 mol. wt. fragments have ionophore activity inhibited by Ruthenium red and by mercuric chloride but not by methyl mercuric chloride, an inhibitor of the hydrolytic site of the enzyme. The 55,000 and 30,000 mol. wt. fragments have been shown to contain the site of phosphorylation and ^{3}H-NEM binding indicative of the hydrolytic site in the enzyme and this site is absent from the 20,000 mol. wt. fragment. Therefore, the ionophoric and hydrolytic sites are located in separate regions of the ATPase and they have now been physically separated.

The further degradation of the 20,000 fragment with cyanogen bromide indicate that the ionophoric activity is associated with a fragment less than 2000 mol. wt. The Ca^{++}-dependency and selectivity of the 20,000 and the 2,000 fragments are the same. But the dependency and selectivity of the 55,000 and the intact enzyme are stronger than those of the 20,000 and 2,000 fragments.

Supported by U.S. ERDA Contract and assigned Report No. UR-3490-850. Also supported in part by NIH.

TH-POS-F2 MECHANISM OF INHIBITION OF THE CA^{2+}-ATPASE ACTIVITY OF SARCOPLASMIC RETICULUM BY A SATURATED PHOSPHOLIPID. C. Hidalgo* (Intr. by J. Gergely), Dept. Muscle Research, Boston Biomedical Research Institute, Boston, Massachusetts, 02114.

Replacement of the endogenous phospholipids of the Ca^{2+}-ATPase enzyme of fragmented sarcoplasmic reticulum by dipalmitoyl lecithin (DPL) results in a partially purified enzyme preparation (DPL enzyme) which at low temperature has a strongly inhibited ATPase activity. This inhibition takes place at the level of the decomposition of the phosphorylated intermediate during the ATPase reaction, since neither the phosphorylation reaction nor its reversal is affected by DPL replacement. Raising the temperature decreases this inhibitory effect. The Arrhenius plot of the ATPase activity of DPL-enzyme revealed a sharp break at 29°. Below this temperature there is a large increase in entropy of activation from 20.1 e.u. to 86.4 e.u., which is compensated by an increase in activation enthalpy from 22.6 Kcal/mol to 42.9 Kcal/mol. The large increase in activation entropy indicates that DPL replacement leads to a more ordered structure in the enzyme below the transition temperature. Treatment of DPL-enzyme with either a non-ionic detergent (Triton X-100) or hydrophobic molecules which perturb the axial order of the phospholipid alkyl chains in the membrane (viz. adamantane) produces a complete reversal of the strong inhibitory effect of DPL replacement at 0°, further supporting the view that a fluid phospholipid environment is a stringent requirement for the proper functioning of the Ca^{2+}-ATPase enzyme.
(Work carried out during the tenure of a Postgraduate Fellowship from the American Heart Association, Mass. Affiliate; supported by grants from the NIH, NSF, AHA and MDAA)

TH-POS-F3 DIVALENT CATION BINDING TO POLYANIONIC SURFACES. J. S. Puskin, Department of Radiation Biology and Biophysics, University of Rochester Medical Center, Rochester, N.Y. 14642.

EPR has been employed to investigate the interaction between the Ca^{2+}/Mg^{2+} analog Mn^{2+} with anionic surfaces. A spectral method is discussed for distinguishing between cations which are complexed to a surface and those loosely associated in a diffuse layer. The method has been applied to ion exchange resins as a model system. The spectra indicate that Mn^{2+} associated with Cellex-SE and -CM resins is mobile and fully hydrated while the association to Chelex-100 is found, as expected, to be a tight complex. Evidence for diffuse association of Mn^{2+} with yeast cell surfaces has also been found.

The spectral characteristics of Mn^{2+} in phosphatidyl serine and cardiolipin vesicle suspensions has been studied. The variation of Mn^{2+} binding with ionic strength has been measured and the results compared with calculations made from the Gouy-Chapman Theory of diffuse double layers. Binding of Mn^{2+} to mixed PS/PC vesicles decreased only very slowly with increasing PC. This result is in disagreement with the Gouy-Chapman Theory unless extensive clustering of PS is assumed.

This work was supported by ERDA and has been assigned Report No. UR-3490-857.

TH-POS-F4 Ca^{2+} SELF-LIMITS ITS DIFFUSION THROUGH JUNCTIONAL MEMBRANE. B. Rose, Department of Physiology and Biophysics, University of Miami School of Medicine, Miami, Florida 33152

Two contiguous Chironomus salivary gland cells were loaded with the Ca^{2+}-sensitive luminescent protein aequorin to determine the spatial distribution of free ionized Ca on either side of the cell junction with the aid of an image intensifier TV system.[1] Ca^{2+} was injected by iontophoresis into one cell while electrical coupling was monitored across the junction. When Ca^{2+} visibly reached the region of the junction, the junction became electrically uncoupled. At no time was Ca^{2+} detectable on the other side of the junction (sensitivity, 1×10^{-6} M) even when the Ca^{2+} concentration on the injected side was of the order of 10^{-4} M. Thus, the change in junctional permeability produced by Ca^{2+} seems fast enough to limit significant transjunctional flux of this ion, as one would expect if Ca^{2+} acted directly on the junctional membrane channels.

[1] Rose, B., Loewenstein, W.R. 1975. Nature 254, 250-252.

TH-POS-F5 GRADIENTS OF CALCIUM ION CONCENTRATION WITHIN PELVETIA FASTIGIATA EMBRYOS. J. C. Gilkey* and L. F. Jaffe, Department of Biological Sciences, Purdue University, Lafayette IN 47907.

Before germination, Pelvetia embryos exhibit a net influx of calcium-45 at the future rhizoid pole and a net efflux of calcium-45 at the future thallus pole; these assymetric fluxes persist for some time after germination [Robinson, K.R. and L.F. Jaffe, Science, 187, pp 70-72 (1975)]. If calcium ion is tightly bound within the cell by anionic species of low mobility, these calcium fluxes should give rise to a thallus-to-rhizoid gradient of calcium concentration, the higher calcium concentration being at the rhizoid pole.

We have been investigating the distribution of calcium-45 in Pelvetia embryos using low-temperature (-78°C) autoradiography of 5 μm sections cut at -60°C. Sections from 16-hr-old (post-germination) embryos which had been exposed to 1 mCi/ml calcium-45 in natural sea water (NSW) for a 12 hr period beginning 6 hr after fertilization consistently revealed substantial gradients of grain density in the expected direction. Because 1 mCi/ml calcium-45 was found to delay cell division (with no other obvious effects on growth), the experiments with 16-hr-old embryos were repeated using 0.1 mCi/ml calcium-45 in NSW (which did not affect cell division); preliminary observations indicated that the gradients of grain density were smaller on the average than when the higher label concentration was used, for reasons which are not yet clear.

Preliminary results of experiments performed using 9-hr-old embryos (pre-germination) which had been exposed to 1 mCi/ml calcium-45 in NSW for a 3 hr period beginning 6 hr after fertilization suggest the presence of a small gradient of grain density in the expected direction.

TH-POS-F6 CALCIUM-INDUCED VOLUME CHANGES IN CELL SUSPENSIONS PREPARED FROM HYDRA LITTORALIS. Daniel C. Koblick, Department of Biology, Illinios Institute of Technology, Chicago, Ill. 60616.

Changes in light scattering from suspensions of hydra cells, which occurred on addition of chlorides to the suspending medium, were measured using a Coleman Model 9 Nepho-colorimeter and a Sargent Model SR Recorder. These changes were interpreted as resulting from changes in average cell volume. It was observed that increases in the range 0.6 to 6.0 mM $(Ca^{++})_o$ produced decreases in cell volume, which were only partially reversed by addition of EDTA. Mg^{++} was much less effective than Ca^{++}, while K^+ had no effect. An increase in $(Na^+)_o$ produced an apparent increase in cell volume. The Ca^{++}-induced changes were markedly pH dependent, exhibiting an optimum between pH 7.0 and 7.5 and falling off rapidly in both directions. These results are consistent with the suggestion that these cells oppose osmotic water influx from the hypotonic media in which they are normally bathed, by development of a hydrostatic gradient in opposition to the osmotic one.

TH-POS-F7 Ca^{2+} INTERACTIONS IN INTACT ELD ASCITES TUMOR CELLS. R. Resch*, R. Hines*, J. Hackney* and C. Wenner, Expt. Biol. Dept., Roswell Park Mem. Inst., Buffalo, N. Y. 14263

Two aspects of Ca^{2+} interactions in intact mammalian cells were examined: (1) The mechanism by which extracellular Ca^{2+} maintains high intracellular K^+ and (2) The principal factors contributing to cellular Ca^{2+} homeostasis.

The mechanism of the protective effect of Ca^{2+} on cellular K^+ content was studied by examination of the effect of Ca^{2+} on efflux of the K^+ analog, $^{86}Rb^+$, from preloaded cells with the use of compounds which interfere with monovalent cation movements. Ca^{2+} decreased $^{86}Rb^+$ efflux to the same extent in the presence and absence of ouabain, suggestive that Ca^{2+} did not alter the activity of the (Na^+-K^+)-ATPase pump. Ca^{2+} exerted a similar protective effect in the presence of furosemide, an inhibitor of K^+-K^+ exchange, indicative that Ca^{2+} was not inhibiting this pathway. Since Ca^{2+} did not influence these pathways, it is concluded that Ca^{2+} exerts its primary effects by slowing passive diffusion. In support of this, Ca^{2+} also slowed $^{22}Na^+$ efflux. In addition, ethanol-induced leakage of $^{86}Rb^+$ was reversed by extracellular Ca^{2+} suggestive of a Ca^{2+}-membrane phospholipid interaction.

The two principal factors involved in $^{45}Ca^{2+}$ uptake are the mitochondrial energy state and availability of permeant anions such as Pi. Uncoupler-sensitive $^{45}Ca^{2+}$ uptake @ 37° was observed with endogenous respiration, or with succinate plus rotenone, or in the presence of rotenone when ascorbate and TMPD were present indicative that each energy-conserving site is capable of supporting Ca^{2+} uptake. In each case, enhancement of net Ca^{2+} uptake was observed when extracellular phosphate (5-30 mM) was also included. Conceivably Pi may act by slowing Ca^{2+} efflux. The failure to maintain optimal Ca^{2+} uptake with glucose as substrate was circumvented by Pi addition suggestive that previously reported experiments of glucose inhibition of Ca^{2+} uptake may be due to glycolytic sequestering of available Pi.

TH-POS-F8 KINETIC STUDIES ON BLACK LIPID MEMBRANES WITH UNCOUPLERS OF OXIDATIVE PHOSPHORYLATION. F. Cohen, M. Eisenberg*, and S. McLaughlin. Dept. of Physiology and Biophysics and Dept. of Pharmacology, SUNY, Health Science Center, Stony Brook, N.Y.

For the substituted benzimidazole, DTFB, which is an uncoupler of oxidative phosphorylation, the charged membrane permeant species is a HA_2^- complex formed from the neutral acid HA and its anion A^-. To elucidate the processes occurring at the membrane-solution interfaces we studied the relaxation of the current under voltage clamp conditions. The simplest model consistent with our measurements is shown below. This scheme, which leads to a system of non-linear differential equations, was analyzed by a computer simulation technique. When appropriate rate constants and partition coefficients were chosen, the model described the observed relaxation times and amplitudes as a function of the applied voltage and the aqueous pH. From independent electrophoretic mobility and equilibrium dialysis measurements the interfacial adsorption of A^- and HA were determined. The membrane permeability of HA was deduced by measuring the membrane potential at zero current with different $[H^+]$ but the same uncoupler concentrations on each side of the membrane. These measurements agreed with the parameters deduced from the relaxation measurements. Supported by NIH grant NS10485.

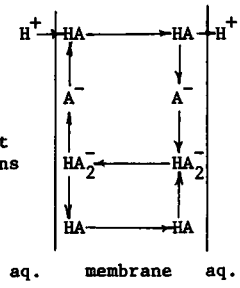

TH-POS-F9 PROTON FLUX ACROSS LIPOSOME MEMBRANES. D.W. Deamer, M.W. Hill* and A.D.Bangham*, Department of Zoology, University of California, Davis 95616, and Animal Physiology Institute, Babraham, Cambridge, England.

Past studies have shown that liposome systems trap monovalent cations and that efflux may be measured with appropriate isotopes. It would be useful to have similar information for proton flux, and we have used an indirect method for estimating decay of proton gradients across liposome membranes. Liposomes were prepared from egg lecithin - phosphatidic acid mixtures by injecting ether-lipid solutions into 0.1 M potassium phosphate (pH 5) at 60°. This novel ether vaporization method produces relatively large liposomes with high volume trapping capacity (10-20 µl µmole^{-1} lipid). The liposomes were placed in equimolar phosphate buffers ranging from pH 7-9, and decay of the pH gradient was estimated by a fluorescent amine method (Deamer et al. BBA 274:323, 1972). In a typical experiment with an initial pH gradient of 3, we found the following initial rates, given as pH units min^{-1}: control = .03, + valinomycin (1 µg ml^{-1}) = .08, + FCCP (25 ng ml^{-1}) = .09. If both valinomycin and FCCP were present the gradient decayed within seconds. From knowledge of the buffer capacity of 0.1 M phosphate at pH 5 it was possible to derive proton flux from the rate at which the pH gradients decayed. This flux was approximately ten times that of sodium when compared under similar conditions. We conclude that the flux of protons across liposome membranes resembles that of other hydrated monovalent cations, and that there are no intrinsic properties of lipid bilayers which permit rapid proton flux. The greater flux measured for protons is probably related to the greater mobility of protons in aqueous solutions.

TH-POS-F10 INTERNAL pH AND ION PERMEABILITY OF ISOLATED CHROMAFFIN VESICLES. R.G. Johnson * and A. Scarpa, Dept. Biochemistry and Biophysics, U. Penna., Philadelphia, Pa. 19174.

The passive ion permeability and the regulation of internal pH of chromaffin granules were studied with radiochemical, potentiometric and spectrophotometric techniques. Bovine chromaffin vesicles were isolated on a sucrose-Ficoll-D_2O gradient in order to preserve isotonicity. The vesicles behave as perfect osmometers between 340 and 1000 mOsm KCl or NaCl, as determined from the changes in absorbance at 430 nm or from intravesicular water measurements using ^3H_2O and ^{14}C polydextran. The vesicular water amounts to 8 µl/mg membrane protein at 350 mOsm decreases to 4 µl at 1000 mOsm, 2.2 µl water/mg membrane protein being osmotically inactive. Potentiometric measurements of H^+ and K^+ movements across the vesicles suspended in choline chloride show little or no leakage of intravesicular K^+ in exchange with extravesicular H^+. This exchange is only slightly increased by the addition of either an uncoupler or valinomycin, while the combination of both ion carriers produces a dramatic K^+ release from the vesicles and H^+ uptake under the same conditions. Nigericin alone produces a comparable 1:1 K^+:H^+ exchange. Externally added Ca^{++} or Mg^{++} do not penetrate the vesicles, but these divalent cations are taken up after addition of A-23187. Two H^+ are released per Ca^{++} accumulated in the presence of the ionophore. Internal pH under various conditions was measured by the extra-intravesicular distribution of ^{14}C methylamine. The intravesicular pH was about one unit more acidic than the surrounding medium. Increase in acidity resulted from the addition of nigericin, whereas a significant decrease in acidity was shown after the addition of nigericin and K^+ or A-23187 and Ca^{++}. These results indicate that the chromaffin granule membrane is impermeable to K^+, Na^+, Ca^{++}, Mg^{++} and H^+ and that a significant ΔpH exists across the vesicles. Supported by GM 02046 and HL 15835.

TH-POS-F11 DOPAMINE-β-HYDROXYLASE INDUCES CONDUCTANCE CHANGES IN BIMOLECULAR LIPID MEMBRANES IN THE PRESENCE OF DOPAMINE AND CALCIUM. M.S. Kafka, R. Blumenthal, and G.A. Walker‡ Adult Psychiatry Branch, NIMH; Laboratory of Theoretical Biology, NCI, and Hypertension-Endocrine Branch, NHLI, NIH, Bethesda, Maryland 20014

Dopamine-β-hydroxylase (DBH), an enzyme which catalyzes the conversion of dopamine to norepinephrine, is a component of adrenal medullary cell chromaffin granule membranes. DBH was reported previously (Blumenthal and Pollard, Biophys. J. 15: 13a [1975]) to increase the conductance of bimolecular lipid membranes (BLM). The data were not reproducible under the experimental conditions reported when a different source and method of preparation of DBH was used. In the current experiments DBH was prepared from bovine adrenal medullae by Walker's modification of the method of Wallace et al. (Proc. Natl. Acad. Sci., USA 70: 2253 [1973]). DBH and dopamine HCl (DA) were added sequentially to both sides of an oxidized cholesterol BLM formed in Hepes-Tris buffer (5 mM, pH 6.0) containing KCl (100 mM) and $CaCl_2$ (4 mM). In 9 of 10 experiments the BLM conductance increased in the presence of DBH (3.4-5 µg/ml) and DA (3.3-8.7 mM), the increase beginning in 0-5 min and reaching 10x the initial value within 7-15 min. The conductance increase occurred in discrete steps of 0.3-0.7 mmho. In the absence of DA, $CaCl_2$, or both, a 10x increase in conductance in 15 min occurred in only 1 of 8 experiments. The conductance increased as the square of the DBH concentration, suggesting that 2 molecules of DBH are required for each unit of conductance increase, and was non-selective with transference numbers $t^- = 0.6$ and $t^+ = 0.4$. The current-voltage curve was symmetrical ± 100 mV. When DBH (17-60 µg/ml) and DA (1-12.5 mM) were added on only one side of the BLM the conductance increased 10x in a 4-min period in 3 of 9 experiments, while DBH alone (6-60 µg/ml) added to one side of the BLM increased the conductance in only 2 of 30 experiments.

TH-POS-F12 DIMERIZATION vs. CONFORMATIONAL CHANGE IN THE BIOLOGICAL ACTIVITY OF GRAMICIDIN A. M. Derechin, Biochemistry Department, SUNYAB, 4248 Ridge Lea Road, Amherst, New York 14226.

Gramicidin A (GA) undergoes (1) a conformational transition with volume change shown by densitometry (Derechin,Hayashi & Jordan,Life Sci.1974,15,403) and refractometry (Derechin & Jordan,Mol.Biol.Reports 1975,2,107) and (2) dimerization shown (Derechin,Biophys.J.1975,15, 316a) by sedimentation equilibrium experiments(SEE).Since a popular theory of transport "by" GA (i.e., channel theory) assumes the passage of cations through a GA dimer, a study of the relative importance of (1) and (2) on GA function was made.The progress in refractive changes (not due to GA sedimentation) in the ultracentrifuge showed for 4 cations (all iodides) that the folded state of GA was favored in the sequence $Li^+ < Na^+ < K^+ < NH_4^+$ which is the sequence (Myers & Haydon,Biochim.Biophys.Acta,1972,274,313) of their increasing rate of transmembrane passage in the presence of GA. SEE in ethanol-water showed moderate (temperature-dependent) dimerization. Whereas in this medium 0.1 M cation strongly enhanced dimerization of 0.003 M GA, the complete dissociation into monomers occurred with 0.01 M salt. However, in any particular medium or cation concentration, all cations dimerized GA equally. These results suggest that (3) the conformational change is the rate limiting step of GA function and (4) dimerization may not be essential for GA activity. These conclusions are in line with the suggestion (Derechin,Physiol.Chem.Phys.,1975,7,283) that GA behavior acting as an "on-off" switch triggers a solvent-propagated chemical-into-mechanical energy transformation. Accordingly, GA folding (unfolding) acts by removing (exposing) the peptide bonds from (to) the solvent which in turn must arrange its molecules (structure) as required by the apolar (polar) nature of the exposed GA surface. Thus, the mechanism of cation transport through membranes outlined on the basis of these principles (Derechin,Physiol.Chem.Phys.,1975,7,283) can be described as a propagated "flipping-over" mechanism of transport.

TH-POS-F13 GRAMICIDIN-A AS A PROBE OF MICROSOME INTERACTIONS WITH PLANAR BILAYER LIPID MEMBRANES. J.A. Cohen and M.M. Moronne*, Laboratory of Physiology and Biophysics, University of the Pacific, San Francisco, California 94115.

The interaction of vesicles of fragmented rabbit skeletal sarcoplasmic reticulum (SR) with planar bilayer lipid membranes (BLM) has been detected by use of the highly water-insoluble antibiotic channel-former Gramicidin A. An SR vesicular solution is pre-treated by addition of 10^{-8} M Gramicidin, corresponding to one Gramicidin molecule per 10 SR vesicles. Subsequent 1:500 (v/v) additions of Gramicidin-treated SR solution to the aqueous phase of egg phosphatidylcholine BLM under 50 mV voltage clamp in 0.1 M KCl and MOPS/TRIS buffer at pH 7 produce BLM conductance increases which achieve steady-state values in 15-20 minutes. The steady-state conductances vary quadratically with the total amount of Gramicidin-SR solution added, reaching $6x10^{-5}$ mho/cm^2 for 100 μg/ml added SR protein. The Gramicidin content of the BLM (molecules/cm^2) is calculated from the measured conductance and found to be linearly related to the total concentration of Gramicidin-treated SR in the aqueous phase, with an effective Gramicidin distribution coefficient of $1.5x10^{-3}$ cm. Transfer of Gramicidin to BLM via the aqueous phase is ruled out as follows: Protein precipitation of the Gramicidin-SR solution with 1% perchloric acid yields a supernatant with negligible Gramicidin activity, as measured by its lack of conductance-producing effect on BLM. Aqueous Gramicidin solutions are not significantly inactivated by similar perchloric acid treatment. It is concluded that the observed increases of BLM conductance occur via direct interaction of the Gramicidin-treated SR vesicles with the BLM. This technique provides a new tool for controlled studies of microsome-BLM interactions.

Supported by NSF (GB-41600) and NIH (HL-16607).

TH-POS-F14 SOLUBILIZATION OF THE GLYCOPROTEINS OF RAT LIVER MITOCHONDRIAL OUTER MEMBRANES. H.M. Tinberg, Physiology Research Laboratory, V.A. Hospital, Martinez, CA 94553.

Outer membrane preparations obtained from rat liver mitochondria using either the osmotic lysis or digitonin method were analyzed by SDS-polyacrylamide gel electrophoresis. Electrophorograms contained a component staining poorly with coomassie brilliant blue but reacting strongly with the periodic acid-Schiff (PAS) stain. This component (PAS_{om}), which possesses an apparent molecular weight of approximately 90000 was sensitive to neuraminidase indicating the presence of sialic acid. The PAS_{om} could be released from the membranes by treatment with 0.3M lithium diiodosalicylate and 50% phenol (Marchesi and Andrews; Science (1971) 174, 1247). This procedure resulted in a water soluble preparation containing 6-7 polypeptides, three of which are PAS positive. The PAS_{om} accounted for 70-80% of the PAS positive material of the preparation.

TH-POS-F15 RETENTION OF ENERGY COUPLING CAPACITY IN BEEF HEART SUBMITOCHONDRIAL MEMBRANES DEPLETED IN ATPase AND ENRICHED IN CARDIOLIPIN. C. P. Lee, C. H. Huang* and B. Cierkosz†
Department of Biochemistry, Wayne State University Medical School, Detroit, Michigan 48201 and The Johnson Research Foundation, University of Pennsylvania, Philadelphia, Penn. 19174.

Cardiolipin micelles in combination with ATP induce the dissociation of mitochondrial ATPase from beef heart submitochondrial membranes (Toson, G. et al, Biochem. Biophys. Res. Commun., 48, 341, 1972; and Lee, C. P. et al, in: Proc. Internatl. Sym. on Membrane Proteins in Transport and Phosphorylation, p.161, 1974) and expose binding sites for cardiolipin in the membrane. The amount of ATPase released from EDTA submitochondrial membranes (ESM) is a function of the concentrations of cardiolipin and ATP; with cardiolipin at 0.3 to 0.4 mg per mg membrane protein and ATP at 5 mM as the optimal condition. Similar results can also be obtained with oligomycin-pretreated ESM. Up to 0.2 mg cardiolipin/mg membrane protein can be tightly bound. Addition of 1 mM EDTA in the incubation mixture appears to enhance the action of cardiolipin and ATP in releasing ATPase from the membrane. Mg^{++}, Mn^{++}, & Ca^{++} induce an aggregation of cardiolipin and prevent the release of ATPase from the membrane.

The ATPase-depleted and cardiolipin-enriched ESM prepared at optimal conditions retain virtually all the NADH oxidase activity and its associated energy coupling capacity, as judged from the oligomycin-induced respiratory control index (8 to 10) and the extent of the energy-linked fluorescence responses of 8-anilinonaphthalene sulfonate (ANS) and quinacrine (QA). The cardiolipin enriched membranes exhibit a higher affinity toward QA and a lower affinity toward ANS as compared with the controls.

Supported by grants from the National Institute of Health (GM 19636 and GM 22751) and the Muscular Dystrophy Association of America.

TH-POS-F16 MONOVALENT CATION PERMEABILITY AND EXCHANGE IN ISOLATED MITOCHONDRIA. G.P. Brierley Dept. of Physiol. Chem., Ohio State University, Columbus, Ohio 43210 and Dept. Biochem., Medical University of South Carolina, Charleston, South Carolina 29401.

The electrophoretic movement of K^+ and Na^+ across the inner membrane of isolated beef heart (BHM) and rat liver mitochondria (RLM) has been compared with cation$^+$/H^+ exchange activity in these organelles. Exchange was measured by the initial rate of swelling in 100 mM acetate salts and electrophoretic cation permeability by the initial rate of swelling in nitrate salts. Exchange has a pH optimum at 7.2 and shows the selectivity sequence $Na^+ > Li^+ > K^+$. Electrophoretic permeability increases with increasing pH showing a selectivity sequence of $Na^+ > K^+ > Li^+$ in BHM at pH 8.2. Exchange shows a triphasic Arrhenius plot with T_t at about 18° and 27° whereas electrophoretic permeability becomes measurable only above 27°. Mg^{+2} and other divalent cations inhibit electrophoretic permeability to a greater extent than exchange. BHM swollen in nitrate salts at 37°, pH 8.2, contract in an energy-dependent reaction ($Na^+ > K^+$). The efficiency of contraction (change in absorbance per O_2 consumed with succinate) decreases when electrophoretic permeability is increased by either elevated pH or addition of gramicidin. Efficiency is increased by Mg^{+2} which reduces permeability. This inverse relationship between electrophoretic cation permeability and the efficiency of energy-dependent contraction of BHM is compatible with an osmotic mechanism which depends on the action of the Na^+/H^+ exchange of the mitochondrial membrane.

Supported by USPHS grant HL09364 and by a grant from the State of South Carolina.

TH-POS-F17 RESOLUTION OF SEVEN POLYPEPTIDE SUBUNITS OF BEEF HEART CYTOCHROME c OXIDASE Nancy W. Downer, Neal C. Robinson,* and Roderick A. Capaldi, Institute of Molecular Biology, University of Oregon, Eugene 97403.

A simple means was needed to completely separate the polypeptide subunits of cytochrome oxidase in order to evaluate protein modification experiments. By applying a method of sodium dodecyl sulfate (SDS) gel electrophoresis (Swank and Munkres, Anal. Biochem. 39: 462, 1971) that utlizes highly cross-linked gels in the presence of 8 M urea, it was possible to resolve the enzyme into seven major polypeptide components with the following apparent molecular weights: I, 35,500; II, 25,000; III, 21,000; IV 16,200; V, 12,000; VI, 6,700; VII, 3,400. Previously the beef heart enzyme has been reported to consist of 6 subunits. We have shown by two-dimensional gel electrophoresis that components II and III reported here can have almost identical mobilities in a standard gel system (e.g. 12% acrylamide in Tris-acetate buffer) and appear as a single component with an apparent molecular weight around 22,500 daltons (Briggs et al., Biochem, in press, 1975). Component III could be further characterized after it was isolated by gel filtration chromatography on Sephadex G-100 in SDS-urea-phosphate buffer. On the basis of its amino acid composition, this component is very similar to subunit III of cytochrome oxidase from n. Crassa and is clearly distinquished from subunit II of beef heart enzyme. Beef heart cytochrome oxidase therefore appears to be quite comparable to the enzymes isolated from several other species in that it contains at least seven major polypeptide subunits of which the three largest are relatively more hydrophobic than subunits IV-VII. Reaction of isolated, intact cytochrome oxidase with ^{35}S-diazobenzene sulfonate labelled all seven subunits. However, the reactivity of potential sites on subunits I-III was generally about 5-fold lower than that of residues on subunits V-VII. Sites on subunit IV were labelled to an intermediate extent.

TH-POS-F18 POLYPEPTIDE STRUCTURE OF UBIQUINONE CYTOCHROME c REDUCTASE. Randy L. Bell,* and Roderick A. Capaldi,* (Intr. by A. Revzin) Institute of Molecular Biology and Biology Department, University of Oregon, Eugene, Oregon 97403.

The polypeptide composition of ubiquinone-cytochrome c reductase has been examined. The complex contains eight different polypeptides. The apparent molecular weights averaged from determinations using gel electrophoresis in SDS and in SDS-8 M urea and column chromatography is SDS and in 6 M guanidine are as follows: Polypeptide I, 50,000; II 46,000; III 32,000; IV 27,800; V 24,800; VI 13,500; VII 11,100; VIII 8,700. The complex has been subfractionated, individual polypeptides have been isolated and their amino acid compositions have been determined. In addition, the functional identity of several polypeptides have been established. I and II are the so called core protein; III is an apoprotein of cytochrome b; IV is the hemoprotein of cytochrome c_1; V is the Rieske non-heme iron protein; VI is a polypeptide bound tightly to the hemoprotein of cytochrome c_1; VII is a component found in fractions enriched in cytochrome b; VIII is the antimycin binding protein.

Labelling with [^{35}S] diazobenzenesulfonate has been used to determine the extent to which different polypeptides are exposed at the surface of the complex. These studies will be discussed with reference to the way multipeptide complexes are organized with respect to the lipid bilayer in biological membranes.